

Improving Settleability and Enhancing Biological Phosphorus Removal through the  
Implementation of Hydrocyclones

Claire M. Welling

Thesis submitted to the faculty of the Virginia Polytechnic Institute and State University  
in partial fulfillment of the requirements for the degree of

Master of Science  
In  
Environmental Engineering

Charles B. Bott, Chair  
Gregory D. Boardman, Co-chair  
John T. Novak

November 17<sup>th</sup> 2015  
Blacksburg, VA

Keywords: settleability, biological phosphorus removal, external selector, hydrocyclone

Copyright 2015, Claire M. Welling

# Improving Settleability and Enhancing Biological Phosphorus Removal through the Implementation of Hydrocyclones

Claire M. Welling

## ABSTRACT

For many wastewater treatment plants, mixed liquor settling is a limiting factor for treatment capacity. However, by creating a balance of granules and flocs, higher settling rates may be achieved. Granules can be defined as discrete particles that do not need bio-flocculation to settle. Through the use of a hydraulic external selector, it is possible to select for dense granules within an existing process which leads to increased settleability. The dense granules are recycled and have the characteristics to achieve not only high settling rates, but also provide a means for biological nutrient removal (Morgenroth and Sherden, 1997). Biological phosphorus removal occurs within the granules without the need for a formal anaerobic selector. Phosphorus accumulating organisms (PAO) and denitrifying PAO (DPAO) are dense and become contained within the granules. PAO and DPAO also have the advantageous characteristic of being more dense than glycogen accumulating organisms (GAO), resulting in selective pressure against GAO (Morgenroth and Sherden, 1997). The granules form stratified layers; ordinary aerobic heterotrophic growth and nitrification occurring in the aerobic outer layer, denitrification in the anoxic layer below, and phosphate removal occurring periodically in the anaerobic core, allowing for not only phosphorus removal, but also nitrogen consumption.

This technology utilizes hydrocyclones for the purpose of improving sludge settling and has been successfully implemented at the Strass wastewater treatment plant in Austria. Hydrocyclones receive mixed liquor tangentially and separate light solids from more dense solids through their tapered shape, increasing the velocity of liquid as it moves downward and allowing for selection of a certain solids fraction. The hydrocyclones select for dense granules through the underflow which are recycled back to the process. The lighter solids are sent to the overflow which represents the waste activated sludge (WAS). Filaments often occur in lighter solids and can exacerbate settleability issues. By wasting lighter solids, filaments will be wasted as well resulting in increased settleability. The Hampton Roads Sanitation District's (HRSD) James River Wastewater Treatment Plant (JR) located in Newport News, VA utilizes an IFAS system. JR achieves some unreliable biological phosphorus removal in warmer temperatures as PAO exist in the bulk liquid but cannot proliferate without a formal anaerobic zone. Chemical phosphorus

removal using ferric chloride addition is used to achieve low effluent phosphorus concentrations. The plant routinely experiences moderate settleability issues with a 4.5 year average SVI of 141 mL/g and a 90th percentile SVI of 179 mL/g. JR is rated at 20 MGD and utilizes a 4-stage Bardenpho configured in an IFAS system. This project includes a full scale implementation of hydrocyclones for improving settleability and stabilizing biological phosphorus removal (reduction in ferric chloride demand) without installation of a formal anaerobic zone.

Plant data collected for James River indicate a reduction in ferric chloride usage as biological phosphorus removal remained constant during the last 2 months of data collection. A reduction in Ferric addition was noticed approximately 3 months after the cyclones were under full operation. 2015 SVI data shows a slight decrease in the average SVI5 decreasing from 292 mL/g to 248 mL/g after cyclones were installed, while the SVI30 value remained fairly constant at an average of  $138 \pm 70$  mL/g. The floc density of the aeration effluent mixed liquor increased steadily over time from 1.050 to 1.071 g/mL. The average density of the cyclone overflow and underflow was  $1.078 \pm .005$  g/mL and  $1.033 \pm .002$  g/mL respectively, indicating that the denser sludge was being selectively retained while wasting the lighter sludge. Classification of settling rate data indicated that granule percentage increased from 0% during the pre-cyclone period to up to 24-40% during the cyclone operation period. Biological phosphorus activity was present in the ML at similar rates when comparing pre-cyclone and post-cyclone periods, indicating that the hydrocyclones may not have had a large effect on the biological phosphorus activity. AOB and NOB activity measurements in the cyclone overflow, underflow, and feed confirm that nitrifiers were not being selectively wasted from the system. Filament data taken from the plant and microscopic analysis showed that some filaments were present in the system but not at levels that would hinder settleability or cause foaming. It was also shown through staining and microscopy that PAO were present while the GAO population was minimal throughout the study.

## Acknowledgements

First and foremost I would like to thank my amazing advisor Dr. Charles Bott for all of his guidance and knowledge. His contagious enthusiasm effects all around him. I cannot express my gratitude enough for being given this opportunity to receive a higher education and conduct innovative research. I would also like to thank Dr. Gregory Boardman and Dr. John Novak for serving on my committee and for their valuable input. Thank you to Hampton Roads Sanitation District for the funding and support.

I would like to recognize Dr. Mark Miller and Dr. Pusker Regmi for introducing me to the pilot plant at HRSD, which included answering endless questions and training me on all lab procedures. Their breadth of knowledge was a valuable resource and I greatly appreciate the opportunity to work with such gifted people. Ryder Bunce and Dana Fredericks also played an important role in my initial training and were great friends throughout the process. Once arriving at Virginia Tech, my fellow HRSD interns Mike Sadowski and Peerawat Noon Charuwat were in the majority of my classes. Without their optimistic attitudes and our frequent study sessions I would have barely gotten by. They are both incredibly intelligent and on top of that never failed to make me smile.

Upon my return to the Hampton Roads area, Stephanie Klaus introduced me to the James River WWTP. Not only did she thoroughly explain the processes at the plant and answer any questions I had, but her support and friendship became crucial to my growth as a student, intern, and person. Her curiosity and drive are inspiring and she will always be a role model to me. I would also like to thank Arba Williamson, Amanda Kennedy, Jon DeArmond, Johnnie Godwin, and Matthew Elliot for always helping when I needed it and being great friends.

Lastly, I would like to thank my family, especially my siblings; Katherine, Sam, Grace, Charlie, Max, Rachel, and Tess, for being my main supporters and molding me into the person I am today.

## Table of Contents

1. Introduction and Project Objectives .....	1
1.1 Project Background .....	1
1.2 Hydrocyclone Installation .....	2
1.3 Project Objectives .....	3
2. Literature Review .....	5
2.1 Settleability .....	5
2.1.1 Overview .....	5
2.1.1.1 Density of Sludge.....	5
2.1.1.2 Clarifier Design.....	6
2.1.2 Types of Settleability Issues.....	6
2.1.2.1 Filamentous Bulking.....	6
2.1.2.2 Pinpoint Floc.....	7
2.1.2.3 Viscous Bulking.....	7
2.1.2.4 Dispersed Growth .....	7
2.1.2.5 Blanket Rising.....	7
2.1.2.6 Foam or Scum Formation .....	8
2.1.3 Filaments .....	8
2.1.3.1 Filament Proliferation .....	10
2.1.3.2 DO.....	11
2.1.3.3 Filament Counting Methods and Characterization .....	11
2.1.4 Bulking Control.....	11
2.1.4.1 Kinetic and Metabolic Selection .....	12
2.1.4.2 Chemical Addition .....	13
2.1.5 Selectors .....	13
2.1.5.1 Aerobic.....	14
2.1.5.2 Anoxic.....	14
2.1.5.3 Anaerobic.....	15
2.1.6 Classifying Selectors .....	15
2.2 Biological Phosphorus Removal.....	16
2.2.1 Background .....	16
2.2.2 PAO, DPAO, and GAO metabolism .....	18
2.2.2.1 PAO .....	18
2.2.2.2 GAO.....	20
2.2.2.3 PAO/GAO competition.....	21
2.2.2.4 DPAO .....	23
2.2.3 Conditions Favoring EBPR .....	23
2.2.3.1 Low Organic Loading.....	25
2.2.3.2 DO.....	25
2.2.4 Processes .....	26
2.3 Granular Sludge .....	26
2.3.1 Background .....	26
2.3.2 Settleability.....	27
2.3.3 Formation .....	28
2.3.4 Biological Nutrient Removal.....	29
2.3.5 Microbiology .....	30
2.4 Hydrocyclones .....	31
2.5 Measurements for Settleability Characterization.....	32
2.5.1 Sludge Volume Index .....	33
2.5.2 Zone Settling Velocity.....	34

2.5.3 Solids Flux.....	34
2.5.3.1 Vesilind.....	36
2.5.4 Classification of Settling Rates Tests.....	39
2.5.4.1 Limit of Stokian Settling.....	39
2.5.4.2 Surface Overflow Rate.....	40
2.5.4.3 Threshold of Flocculation.....	40
3. Methods and Materials.....	42
3.1 Plant Setup.....	42
3.2 Cyclone Data.....	44
3.3 Plant Data.....	45
3.4 Sludge Volume Index (SVI).....	45
3.5 Zone Settling Velocity.....	46
3.6 Solids Flux.....	46
3.7 Classification of Settling Rates.....	47
3.7.1 Limit of Stokian Settling (LOSS).....	47
3.7.2 Threshold of Flocculation (TOF).....	47
3.7.3 Surface Overflow Rate (SOR).....	48
3.8 Floc Density.....	49
3.9 Filament Quantification and Identification.....	50
3.10 PAO Activity Tests.....	50
3.11 AOB and NOB Activity Tests.....	51
3.12 Tank Profiling.....	52
4. Results and Discussion.....	53
4.1 Cyclone Data.....	53
4.2 SVI.....	53
4.3 Solids Flux.....	54
4.4 Settleability.....	57
4.5 Classification of Settling Rates.....	58
4.6 Floc Density.....	59
4.7 Filaments.....	61
4.7.1 Microscopic Analysis.....	61
4.7.2 Plant Data.....	62
4.8 PAO Activity Tests.....	62
4.9 Phosphorus and Ferric Plant Data.....	67
4.10 AOB and NOB Activity Tests.....	68
4.11 Tank Profiling.....	69
5. Conclusions and Engineering Significance.....	71
References.....	73
Appendices.....	75
A. Phosphorus Activity.....	76
B. Phosphorus Uptake and Release Rates in Cyclone Sampling Points.....	78
C. AOB and NOB Activity in Cyclone Sampling Points.....	79
D. Microscopic Analysis.....	80
E. Floc Density of Aeration Effluent and Cyclone Sampling Points.....	86
F. Floc Density SIP Calculation.....	87
G. Cyclone Data.....	89
H. Plant Data.....	92
I. Settleability.....	99
J. Solids Flux Data.....	100
K. Classification of Settling Rates.....	103

L. James River IFAS Tank Profiles.....	104
M. Supplemental Information .....	109

## List of Tables

Table 2.1 Filamentous Organism Characterization and Control .....	8
Table 2.2 Filamentous bacteria found in activated sludge and associated process conditions.....	10
Table 2.3 Selector design guidelines recommended for aerobic, anoxic and anaerobic selectors.	14
Table 2.4 Results of Phosphorus Uptake and Release Tests from 2005 WERF EBPR Study .....	17
Table 2.5 Comparison of PAO/GAO Observations and Uptake and Release Test Results .....	21
Table 2.6 Proposed metabolic features of the most known PAOs and GAOs .....	22
Table 4.1 Flow and Mass Split of Cyclone Underflow and Overflow for different nozzle sizes...	53

## List of Figures

Figure 1.1 Historical SVI30 values of James River WWTP .....	2
Figure 2.1 PAO Metabolism Under Anaerobic and Aerobic/Anoxic Conditions .....	20
Figure 2.2 A Schematic of an Aerobic Granule with Stratified Layers.....	30
Figure 2.3 Strass WWTP SVI over 3 year period, hydrocyclones installed beginning of year 2 ..	32
Figure 2.4 Relationship Between Solids Characteristics and Sedimentation Processes.....	33
Figure 2.5 State Point Analysis of Solids Flux Curve.....	36
Figure 2.6 Settling function of Takács et al. (1991) incorporating the settling characteristics of both dispersed and flocculated suspended solids .....	39
Figure 2.7 (A) Determination of CSV working area as a region whereby no bio-flocculation occurs (No significant decrease in TSS in the supernatant) Percentage TSS in effluent versus ranging TSS of mixed liquor concentrations at an SOR of 1.5 m <sup>3</sup> /m <sup>2</sup> /h, and the grey area exhibits discrete region. Discrete settling is defined as the initial region that is independent of the MLSS, (B) Conceptual SOR curve with indication of the different solids fractions.....	41
Figure 3.1 James River IFAS Process Flow Diagram.....	43
Figure 3.2 Hydrocyclone Process and Instrumentation Diagram.....	44
Figure 3.3 James River IFAS Tank Design.....	52
Figure 4.1 2015 SVI5 and SVI30 of JR .....	54
Figure 4.2 Pre and Post-Cyclone Settling Velocity determined by SFA and the best fit Vesilind Curve .....	55
Figure 4.3 SFg curves pre and post cyclone installation. Calculated SFg curves using the Vesilind settling velocity are shown as curves, actual data shown as points.....	56
Figure 4.4 ISV of Cyclone Points adjusted to 2500 mg/L.....	57
Figure 4.5 Classification of Settling Rates of JR ML, SVI, and MLSS .....	59
Figure 4.6 An example of the floc density analysis using Isopycnic centrifugation from 6/22/15	60
Figure 4.7 James River ML floc density of Aeration effluent and Cyclone Sampling Points .....	61
Figure 4.8 Phosphorus Release and Uptake of Aeration Effluent.....	64
Figure 4.9 Phosphorus Uptake and Release Rate of Cyclone Sample Points and Aeration Effluent .....	66
Figure 4.10 Ratio of Ferric Addition to Raw Influent Phosphorus and Phosphorus Removed.....	67
Figure 4.11 Influent and Effluent Phosphorus concentrations .....	68
Figure 4.12 AOB and NOB activity in cyclone sampling points .....	69
Figure 4.13 NO <sub>2</sub> , NO <sub>x</sub> , and NH <sub>4</sub> of aeration effluent of JR ML.....	70

# 1. Introduction and Project Objectives

## 1.1 Project Background

James River Wastewater Treatment Plant (JR) located in Newport News, Virginia is one of the 9 major wastewater treatment plants operating under the Hampton Roads Sanitation District (HRSD). The plant was initially placed on-line in 1968. After undergoing expansion in the 1970's the plant has an average daily treatment capacity of 20 MGD. After receiving new nitrogen limits of 12 mg/L, JR implemented a study in which an integrated fixed-film activated sludge (IFAS) basin was installed in late 2007 in order to meet these requirements. After optimizing the IFAS system design and achieving effluent TN of 8-12 mg/L, it became fully implemented in June 2009 (Rutherford, 2010). JR utilizes a 4-stage Bardenpho system.

James River currently has some settleability problems with an average SVI of 135 mL/g and a 90<sup>th</sup> percentile of 169 mL/g. Recent SVI data is seen in Figure 1.1. Poor settleability at JR is exacerbated by relatively shallow, peripheral feed secondary clarifiers. It is unclear why JR has such poor settleability as filament levels are low. James River also experiences some unreliable biological phosphorus removal, with ferric addition added before the primary clarifiers and secondary clarifiers to achieve a low total phosphorus (TP) effluent. JR's TP effluent permit is 2 mg/L, but the plant aims to stay under 1 mg/L to make sure the total TP pounds limit for the James River basin is met. Conventionally, enhanced biological phosphorus removal is achieved through a separate anaerobic selector at the beginning of the biological reactors. This process uses a large amount of carbon without much being used by phosphorus accumulating organisms (PAO). The implementation of the hydrocyclones more efficiently utilizes carbon for PAO and denitrifying PAO (DPAO).

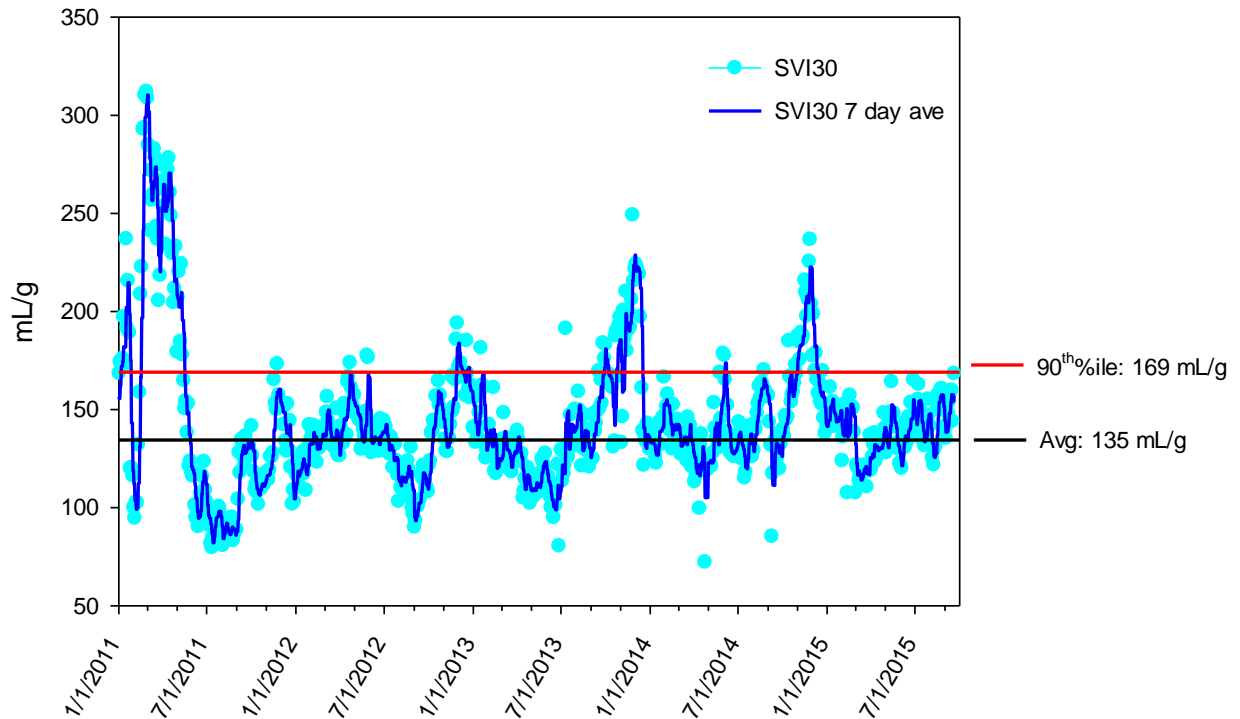


**Figure 1.1 Historical SVI30 values of James River WWTP**

## 1.2 Hydrocyclone Installation

This project utilized hydrocyclones for the improvement of sludge settleability. The Strass wastewater treatment plant in Austria has successfully implemented this technology to improve settleability. In this study hydrocyclones were implemented at a full-scale wastewater treatment plant to select for dense granules for the improvement of settleability and stabilizing biological phosphorus removal. The JR plant was provided 10 ft x 10 ft x 12 ft tank and hydrocyclones by World Water Works. The tank with a bank 8 hydrocyclones attached to one side was installed in the solids handling building. The hydrocyclones received influent from the RAS lines, using two pumps, one feeding each bank of 4 cyclones. The desired hydraulic split of the cyclones was 80% in the overflow and 20% in the underflow with an equal mass of TSS between the overflow and underflow, but it was expected that as the sludge became more granular, the split would become less concentrated in the overflow and more concentrated in the underflow, improving settleability and creating a balance of flocs and granules.

The hydrocyclones came into full operation on March 5<sup>th</sup> 2015. Four nozzle sizes were provided for the cyclone underflow, with the second smallest being already attached to the cyclones upon receipt. These nozzle sizes adjusted the hydraulic split of the overflow and underflow with no clear indication of flowrates, but it was easily calculated once the nozzles were installed. The initial nozzle fitted to the cyclones provided a hydraulic split of about 90% in the overflow and 10% in the underflow. On May 11<sup>th</sup>, 2015 the largest nozzle were installed directing a larger percentage of hydraulic flow to the underflow in hopes of improving performance, as settleability data and granulation were not improving as expected. On May 18<sup>th</sup>, 2015 the cyclones were taken offline and normal wasting to the gravity belt thickeners resumed. The hydrocyclones were restarted June 6<sup>th</sup> 2015 and resumed normal testing.

### 1.3 Project Objectives

The objectives of the hydrocyclone installation at JR were to: 1.) Improve settleability by creating a balance of flocs and granules and 2.) Achieve enhanced biological phosphorus removal by retaining dense granules which contain microorganisms consuming phosphorus.

By wasting lighter flocs to the gravity belt thickener (GBT) while selecting for heavier granules to be returned to the beginning of the IFAS basin, settleability should increase over time. The sludge will become denser and achieve improved settleability characteristics. As the dense solids are retained in the system, PAO will proliferate in the system. PAO are dense and will be retained within the granules, achieving biological phosphorus removal without needing a formal anaerobic selector. Granules may form stratified layers with heterotrophic growth on the outside, an anoxic layer below possibly achieving nitrification with the presence of denitrifying PAO (DPAO), and an anaerobic core where phosphorus is consumed by PAO. Simultaneous nitrification-denitrification (SND) would occur only during higher temperatures as AOB and NOB are retained on the IFAS media during colder temperatures. As the temperature increases AOB and NOB are more centralized in the bulk liquid and may become retained within the granules. As biological phosphorus removal is achieved in the granules, ferric and alkalinity additions to the plant may be reduced, resulting in reduced chemical costs.

Baseline data collection began in June 2014 to provide a comparison of plant performance pre and post-cyclone installation. The success of the hydrocyclones was monitored through multiple settleability tests to characterize the sludge settleability, sludge density, and the amount of granulation within the sludge. Filament identification and abundance was also monitored before and after cyclone installation to give insight into settleability issues and if the hydrocyclones were

successful in reducing the filament count. PAO activity was monitored before and after cyclone installation to observe the rates of biological phosphorus removal in the sludge. Plant data were monitored to track settling characteristics and reduction in ferric and alkalinity.

## 2. Literature Review

### 2.1 Settleability

#### 2.1.1 Overview

Activated sludge (AS) is the most common biological treatment system used today. In an AS process, clarifiers are used to allow solids to settle gravimetrically, producing a clear effluent and a thickened sludge for recycling to the aeration basin called return activated sludge (RAS). Coagulants, such as ferric chloride or alum, may be added in conjunction with a polymer to increase TSS removal by increasing floc size and settling velocities (WEF, 2005). The rate of settling is often a limiting factor in the efficiency of a wastewater treatment plant. Poor settling solids is a common problem in wastewater treatment plants around the world and can lead to loss of solids from the clarifier during peak flow events and then poor treatment following. This results in increased solids treatment costs, increased effluent solids concentrations, decreased disinfection efficiencies, and increased risks to downstream ecosystems and public health (Kim et al, 2010). It is critical for biological solids being produced in biological reactors to be removed through settling. Many actions can be taken to improve sludge settling characteristics including; clarifier design, controlling excessive filamentous bacteria, chemical dosing, etc.

##### 2.1.1.1 Density of Sludge

The gravitational force that drives sedimentation is a linear function of the difference between biomass density and the density of surrounding fluid according to Stokes law (Kim et al, 2010). As biomass is only slightly more dense than water, slight changes in biomass density will have large effects on the buoyant force which corresponds to a change in the settling rate (Jones & Schuler, 2010). Biomass densities have been shown to vary from about 1.015 to 1.06 g/mL, but the ranges were found to vary in different plants (Kim et al, 2010). The variability of these density ranges were shown to significantly affect the settleability of the sludge, especially with a moderate filament presence. Major factors shown to effect density include polyphosphate content, which varies with enhanced biological phosphorus removal activity, non-volatile suspended solids, and SRT (Kim et al, 2010). A 2007 study by Schuler found that biomass density varied with polyphosphate content associated with EBPR, and as biomass density increased SVI did as well.

Jones and Schuler found that mixed liquor biomass density increases with warmer temperatures in 4 different full-scale plants with various configurations, with an average increase of 147%

from smallest biomass buoyant density to largest (Jones and Schuler, 2010). In studies with no change in filament content, a strong correlation between biomass density and SVI values and seasonal variations in settleability may be explained by density change (Jones and Schuler, 2010).

In 2009, a pilot-scale and full-scale study was conducted to test the effects of IFAS installation on biomass density and biomass settling characteristics. Integrated fixed-film activated sludge (IFAS) utilizes solid media to provide surface area for the growth of biofilms, increasing microbial concentrations, which increases biological activity without the addition of new reactors. There is no well-accepted consensus on the effect of IFAS media on settleability, as varied results have come from the minimal testing done on these parameters. It was found that the control system showed a significantly larger biomass density than the biomass in the IFAS system, and that the SVI decreased linearly as the biomass density increased (Kim et al, 2010).

#### ***2.1.1.2 Clarifier Design***

The secondary clarifier serves as a thickener for sludge, a clarifier for effluent, and a storage tank for sludge during peak flows. If one of these functions is compromised, consequences may include excessive loss of solids resulting in the sludge age decreasing and high effluent TSS, which may prevent further nitrification from occurring. Many factors affect the design of the clarifier including; flow rate, inlet, sludge collection, site conditions such as wind and temperature, and sludge characteristics such as settleability and thickenability. If there are excessive solids in the clarifier it is usually due to hydraulic short circuiting or resuspension of solids by high velocity currents, thickening over-loads resulting in loss of solids over the effluent weir, denitrification which causes solids to float to the top of the clarifier, flocculation problems, and insufficient capacity of the sludge collection system. Aeration plays a large factor in clarification. Underaeration can lead to filaments, resulting in bulking. Overaeration causing shear can result in poor flocculation and pin flocs (Ekama, 2006).

#### ***2.1.2 Types of Settleability Issues***

Many settleability issues are caused by filamentous organisms. The most common problems caused by filaments include; filamentous bulking sludge, viscous bulking sludge, nocardioform foaming, and rising sludge (Metcalf, 2014).

##### ***2.1.2.1 Filamentous Bulking***

Filamentous bulking is caused by large amounts of filamentous organisms, which creates diffused flocs and large web-like structures. This interferes with compaction, settling, and thickening and will produce a high SVI with clear supernatant and low RAS and WAS solids concentrations. The

sludge blanket can overflow in the secondary clarifier and solids handling becomes hydraulically overloaded (Jenkins, 2003). Common filaments contributing to bulking in AS systems include Type 0041 and Type 0675 (Martins et al, 2004). Beggiatoa and Thiothrix bulking are found in septic wastewaters. Beggiatoa grows well on hydrogen sulfide and Thiothrix grows well on reduced substrates, such as when the influent has fermentation products such as VFAs and reduced sulfur compounds (Metcalf, 2014). Filamentous bulking proliferates when filaments are competitive at low substrate concentrations, being organic substrates, DO below 0.5 mg/L, or limited nutrients (Metcalf, 2014).

#### ***2.1.2.2 Pinpoint Floc***

An opposing issue to filamentous bulking is the presence of pinpoint floc. Pinpoint floc is characterized by small, weak floc caused by a macrostructure failure when bioflocculation is not well developed. It will produce a low SVI and turbid, high solids in the effluent (Ekama, 2006). Long SRTs can lead to limited growth of filamentous bacteria leading to pinpoint floc (Metcalf, 2014).

#### ***2.1.2.3 Viscous bulking***

Viscous bulking, also known as slime or zooglear bulking is characterized by slimy and jelly-like sludge. Viscous bulking is when the sludge retains water and is low density causing reduced settling velocities, poor compaction, no solids separation, and an overflow of the sludge blanket in the secondary clarifier. It is caused by a presence of excess extracellular biopolymer, which is hydrophilic and imparts a slimy consistency (Metcalf, 2014; Jenkins, 2003). This type of bulking proliferates in nutrient-limited systems or high F/M loading conditions with wastewater having high amounts of rbCOD (Metcalf, 2014). Activated sludge typically has 15-20% carbohydrate in its VSS, but when suffering from viscous bulking it can reach up to 90% (Jenkins, 2003).

#### ***2.1.2.4 Dispersed Growth***

Dispersed growth is caused by floc forming bacteria that have been lysed or their flocculation has been prevented. Flocculation may be prevented by absence or disruption of exopolymer bridging. This can be caused by nonflocculating bacteria at high growth rates, a high concentration of monovalent cations relative to divalent cations, and deflocculation by poorly biodegradable surfactants and toxic materials (Metcalf, 2014).

#### ***2.1.2.5 Blanket rising***

Blanket rising or floating sludge is caused by denitrification in the secondary clarifier which releases soluble N<sub>2</sub> gas. This gas attaches to activated sludge flocs and floats to the secondary

clarifier surface producing a scum layer of activated sludge on the surface of the secondary clarifier and on the aeration basin anoxic zones (Jenkins, 2003).

**2.1.2.6 Foam or scum formation**

Foam formation is caused by surfactants and nocardioforms, *M. parvicella* (both hydrophobic and attach to air bubbles), or type 1863 (produces white foam). Foams cause issues by floating large amounts of SS to surfaces of treatment units, they can putrefy, and may elevate secondary effluent SS.

Foam formation typically occurs in the aeration basin and is transferred to the secondary clarifiers with the mixed liquor. Foam accumulation on the liquid surface can negatively affect effluent quality. In addition, it is unsightly and a nuisance to operating and maintenance staff. Foam control methods, described in detail by Jenkins et al. (2003), include: selectors, selective surface wasting from activated sludge basins, surface chlorine spray, cationic polymer addition to activated sludge basins, and automatic mean cell residence time control using online MLSS and RAS solids concentrations.

**2.1.3 Filaments**

Filaments contribute significantly to settleability issues in wastewater treatment plants. Table 2.1 provides characteristics of the most common filamentous organisms causing settleability issues. Some filament presence is necessary for the formation of sludge flocs. There are two particle bonding mechanisms in the formation of flocs; through polymer bridging or through a filamentous network. In polymer bridging exocellular polymers produced by bacteria known as floc formers to form bridges between neighboring cells. Exocellular biopolymers contribute to 15-20% of MLSS and carry a net negative charge at a neutral pH. Divalent cations interact with negatively charges particles to form bridges that allow cells to adhere. A microstructure is formed which is spherical, small, and compact and may be sheared easily. Flocs may also be formed through a network of filaments with attached floc-formers. This forms the backbone of sludge flocs creating a larger macrostructure which is irregularly shaped and strong (Ekama, 2006).

**Table 2.1 Filamentous Organism Characterization and Control**

<b>Filamentous Organisms</b>	<b>Bridging</b>	<b>Open Floc Structure</b>	<b>Features*</b>	<b>Control*</b>
Type 0041	Yes	Yes	Abundant in	Still uncertainty but the most

Type 0675	No	Yes	anaerobic-anoxic-aerobic systems; present at high SRTs; and possible growth on hydrolysis of particulate substrates.	recommended solutions are: install a skimmer to remove particulate substrate; maintain a plug-flow regime in all the system; the several stages (anaerobic/anoxic/aerobic) should be well defined; maintain a relatively high oxygen concentration in the aerobic phase (1.5 mg O <sub>2</sub> /L) and a low ammonium concentration (<1 mgN/L).
Type 0803	Yes	No		
Type 021N	Yes	No	Use readily biodegradable substrates, especially low molecular weight organic acids; present at moderate to high SRT; capable of sulphide oxidizing to stored sulphur granules; and rapid nutrients uptake rates under nutrient deficiency.	Aerobic, anoxic or anaerobic plug flow selectors; nutrient addition; eliminate sulphide and/or high organic acid concentrations (eliminate septic conditions).
<i>Thiothrix</i> I and II	Yes	No		
<i>Haliscomenobacter hydrossis</i>	Yes	Yes	Use readily biodegradable substrates; grow well at low DO concentrations; grow over wide range of SRTs.	Aerobic, anoxic or anaerobic plugflow selectors, and increase SRT; increase D concentration in the aeration basin (>1.5 mg O <sub>2</sub> /L)

Extracted from (Jenkins, 2003; Martins et al., 2004)

### 2.1.3.1 Filament proliferation

Filament growth is exacerbated by many factors including nutrients in the ML, DO concentration, SRT, pH, etc. Table 2.2 provides common filament types in AS and causes of growth. Some of the most common filaments found in the US in order of most common include; *Nocardia* spp., type 1701, 021N, 0041, and *Thiothrix* spp (Jenkins, 2003).

The proliferation of filaments is strongly affected by the nutrients present in the wastewater. Without sufficient nutrients, filamentous bacteria may thrive over floc formers, with severe nutrient deficiency resulting in production on exocellular slime which causes sludge to settle poorly. The DO concentration also affects the growth of filamentous bacteria. The optimal DO value depends on process loading and specific oxygen uptake rate (OUR). Many sources recommend 2 mg/L, but it is possible to operate at lower concentrations resulting in energy savings. Equations may be used to calculate DO necessary to keep ML suspended without shearing. Floc shearing is not an issue for diffused air systems utilizing membranes as small floc can still be filtered. However, mechanical aerators have high localized velocity gradients (Metcalf, 2014). Filaments are also affected by SRT. Long SRTs can lead to limited growth of filamentous bacteria leading to pinpoint floc (Metcalf, 2014). A low pH encourages the growth of filamentous fungi. Some studies have shown an effect on filament abundance with seasonal variation, while others showed that there was no effect on filament abundance even as SVI varied as temperatures changed (Jones and Schuler, 2010).

**Table 2.2 Filamentous bacteria found in activated sludge and associated process conditions**

<b>Filament Type Identified</b>	<b>Cause of Filament Growth</b>
<i>Sphaerotilus natans</i> , <i>Halsicomenobacter hydrossis</i> , <i>Microthrix parvicella</i> , type 1701	Low dissolved oxygen concentration
<i>M. parvicella</i> , types 0041, 0092, 0675, 1851	Low F/M
<i>H. hydrossis</i> , <i>Nocardia</i> spp., <i>Nostocoida limicola</i> , <i>S. natans</i> , <i>Thiothrix</i> spp., types 021N, 0914	Complete mix reactor conditions
<i>Beggiatoa</i> , <i>Thiothrix</i> spp., types 021N, 0914	Septic wastewater/sulfide available
<i>S. natans</i> , <i>Thiothrix</i> spp., type 021N, possible <i>H. hydrossis</i> , types 0041, 0675	Nutrient deficiency
<b>Fungi</b>	Low pH

Extracted from (Metcalf, 2014)

### **2.1.3.2 DO**

Low dissolved oxygen levels may lead to the growth of bulking organisms. Achieving the oxygen demand profile needed is often done by tapered aeration or step-feed operation (WEF, 2005).

Because filamentous bacteria have the capability of growing outside the floc structure, they have an advantage over floc-forming bacteria in diffusion-resistant environments. This allows filaments to exist outside of the floc, giving them preferential access to the bulk liquid substrate (Martins et al., 2004). Martins et al. (2004) compared floc growth with biofilm growth, finding that low substrate or low oxygen concentrations lead to open, filamentous flocs resulting in poor settling. Palm et al. (1980) found that the DO concentration required was a function of the F/M ratio; as F/M increased, the DO required also increased. This could be remedied by manipulating F/M and DO ratios, but this would take longer than the onset of bulking. A quick fix such as chemical addition could be used if a rapid fix was necessary.

### **2.1.3.3 Filament Counting Methods and Characterization**

Filaments may be counted by observing the amount of filament extending from a floc, by counting the number of filaments intersecting a hairline on a slide cover, or may be counted through Nocardioform filament organism counting where gram positive filaments are visible in a gram stained ML sample (Jenkins, 2003). Floc and filamentous microorganism characterization is useful in determining settling and compaction characteristics of AS. Floc characteristics worth noting include; floc size, shape (round, irregular, compact, diffuse), protozoa and other microorganisms, nonbiological organic and inorganic particles, bacterial colonies, cells dispersed in bulk solution, and effects of filamentous organisms on floc structure. A scale from 0-6 is used for filamentous organism abundance in a floc. In order to identify the filamentous organisms present, a dichotomous key can be used by viewing the filament's characteristics such as; branching, motility, filament shape, location, attached bacteria, sheath, cross-walls, filament width, filament length, cell shape, cell size, sulfur deposits, other granules, and staining reactions (Jenkins, 2003). Once the filamentous organism has been identified, it is necessary to pinpoint relationships between the filaments and the operational conditions present when they occur to control for their growth.

### **2.1.4 Bulking Control**

Care must be taken to control for excessive growth of filaments. It is important to understand the cause of bulking in order to control it. Parameters to take into consideration are wastewater characteristics, DO content, process loading as N and P in industrial wastes may lead to bulking, internal plant overloading, and analyzing ML under a microscope for microbial growth or change in floc structure (Grady, 2011). Filaments can be controlled permanently through types of

selectors, DO concentration, SRT, and nutrient addition. For temporary filament control, which is generally cheaper than permanent solutions, chemical additions such as chlorine or hydrogen peroxide may be used (Ekama, 2006).

#### **2.1.4.1 Kinetic and Metabolic Selection**

Filaments may be controlled through kinetic selection as filamentous bacteria and floc-forming bacteria have separate growth strategies. Chudoba et al (1985) developed the kinetic selection theory based on Monod kinetics to describe filamentous growth in AS. Filamentous bacteria can be described as slow-growing *k* strategists, such as *Sphaerotilus* and *Leucothrix coharens*, while floc-forming bacteria are described as *r* strategist where floc-formers grow faster when the substrate concentration is high and filamentous bacteria grow faster when substrate concentration is low (Grady, 2011). Filamentous bacteria have maximum growth rates ( $\mu_{max}$ ) and affinity constants ( $K_s$ ) lower than floc-forming bacteria. Floc-formers out compete filamentous bacteria at a certain concentration, so this concentration must be kept below this level so biomass formation occurs (Grady, 2011). When the substrate concentration is low filamentous bacteria have a higher substrate uptake rate than floc formers and consume more of the available substrate. When the substrate concentration is high, the filamentous bacteria are suppressed since their growth rate is below that of floc-forming bacteria. The kinetic selection theory gave rise to the selector reactor to control filamentous bulking. Through kinetic selection, a substrate concentration gradient is present throughout the bioreactor. This substrate gradient may be achieved in plug flow like conditions. The concentration at the inlet will favor floc-formers over filamentous bacteria. Filaments may persist over floc formers when readily biodegradable substrate is consistently supplied at low concentrations. In some cases a substrate concentration gradient will form granular floc particles with high settling rates. Chudoba deemed it necessary to keep a high substrate concentration, *S*, to select for filamentous bacteria suppression. However, it has been shown through application that bench scale experiments using selectors to control filamentous bulking does not always translate to full-scale operation.

Filaments with a high affinity for biodegradable organic matter may also be controlled through metabolic selection. This is done by eliminating DO as a terminal electron acceptor and either adding nitrate to create anoxic conditions, or eliminating both to create anaerobic conditions. Many floc formers can take up biodegradable organic matter under anoxic or anaerobic conditions while many filamentous bacteria cannot (Metcalf, 2014).

#### **2.1.4.2 Chemical Addition**

Chemical addition can be used to enhance excess filaments or induce flocculation (WEF, 2005). Chemical coagulants may induce flocculation, cationic polymers added at a concentration of <1 mg/L has been shown to improve mixed liquor settleability. RAS or sidestream chlorination can reduce bulking sludge, although RAS chlorination may interfere with nitrification. Hydrogen peroxide may be substituted for chlorine in many cases. Selection of inorganic salts, polymers, or other flocculent aids can be used but should be based on laboratory studies (Grady, 2011).

#### **2.1.5 Selectors**

The selector was an activated sludge process first used in 1973 for selectively growing non-filamentous organisms and inhibiting filamentous organisms. Selectors are split into three main categories; aerobic, anoxic, and anaerobic, each providing certain advantages, outlined in Table 2.3.

In 1973 J. Chudoba defined selectors as the part of the aeration system with a substantial concentration gradient of substrate (Chudoba, 1973). Chudoba's 1973 study demonstrated that the growth of filamentous microorganisms was effectively suppressed by means of a selector, with soluble COD removal ranging from 90-95%. Once filamentous organisms were placed into a system with a higher concentration gradient, they gradually decreased, but often at a slow rate. It was found that the period needed to attain steady state composition of the mixed culture depended on the original composition of the mixed culture and the concentration gradient of the substrate along the system.

The authors of a 1997 full-scale evaluation of factors affecting the performance of anoxic selectors concluded that both aerobic and anoxic SRTs have more significance when minimizing the growth of filamentous organisms than does the organic loading (F/M) (Parker, 1998). It is still desirable to maintain a high F/M in the initial contact zone to achieve rapid soluble organic matter uptake rates. Although a single selector tank can be effective in controlling filaments, multiple compartments maintaining plug-flow enhance substrate gradient and improve kinetic selection.

**Table 2.3 Selector design guidelines recommended for aerobic, anoxic and anaerobic selectors**

Selector Type	Compartments	Contact Time	Design Parameter	References
<b>Aerobic</b>	≥3	10-15 min	DO concentration: ≥2 mg O <sub>2</sub> /L	Eikelboom et al., 1998; Martins et al, 2003; Martins et al, 2004; Daigger et al., 2007
<b>Anoxic</b>	≥3	45-60 min	(rbCOD/NO <sub>3</sub> -N)CONSUMED: >79 mg rbCOD/mg NO <sub>3</sub> -N due to storage	Albertson 1987; Jenkins, et al, 2004
<b>Anaerobic</b>	≥3, long channel (l:w larger than 10:1)	1-2 hours	(CODVFA+fermentable/PO <sub>4</sub> -P)inf: 9-20 g COD/g P	Albertson 1987

Extracted from (Martins et al, 2004)

### 2.1.51 Aerobic

Aerobic selectors have oxygen present and are used to control bulking sludge attributed to the excessive growth of Type 021N, *Thiothrix* spp., *S. natans*, and sometimes *M. parvicella* (Martins et al, 2004). It is important for aerobic selectors to have a long retention time as there is a strong correlation between contact time and sludge settleability (Martins et al, 2004). If the contact time is too short, soluble substrate is not consumed and flows into the main aeration basin. If the contact time is too long, too much soluble substrate is consumed which induces substrate limited conditions, favoring filamentous bacteria over floc-forming bacteria (Martins et al, 2004). The DO concentration is also an important parameter, as low DO concentrations may lead to proliferation of bulking organisms.

### 2.1.5.2 Anoxic

Anoxic selectors are absent of oxygen and instead have nitrogen species present as an electron acceptor. Anoxic zones are located at the front of the aeration basin where the influent wastewater

and RAS mix. This is achieved through a RAS line being fed into the anoxic zone, supplying nitrate-rich wastewater. Soluble substrate is consumed in anoxic selectors, selecting against filamentous bacteria before entering the aerobic phase. Too much rbCOD entering the aerobic phase because of limited storage capacity in the anoxic phase may result in bulking sludge. The main design parameter for anoxic selectors is the rbCOD/NO<sub>3</sub>-N (readily biodegradable chemical oxygen demand/nitrate) ratio. It can be difficult to determine this ratio as some denitrification takes place in the secondary clarifier, resulting in periods with lower nitrate concentrations or possibly even anaerobic conditions (Martins et al, 2004).

### **2.1.5.3 Anaerobic**

Anaerobic selectors contain no oxygen or oxidized nitrogen species. In an anaerobic selector, it is desired for the rbCOD to be consumed before the aerobic phase. The main design parameter is the ratio of rbCOD uptake rate to phosphorus release rate. In anaerobic selectors, PAO and GAO are able to store substrate, allowing them to remove the incoming organic load. As the PAOs and GAOs consume more, there is less substrate available in the aerobic stage allowing for improved sludge settleability.

### **2.1.6 Classifying Selectors**

A classifying selector is a physical mechanism by which nuisance organisms (foam-causing) are selected against (Parker, 2003). In 1987 Pretorius and Laubscher proposed a method for wasting foam-causing organisms based on their physical properties by using aeration to waste them at the surface of a “flotation cell” which became the basis for developing classifying selectors (Parker, 2003). The term classifying selector was coined by Brown and Caldwell in the 1990s. Nuisance organisms are an issue for wastewater treatment plants, especially when operating at high SRTs. Foam causing organisms will remain at the surface of a tank remaining in the tank for longer than the ML, or will be wasted into the effluent which is undesired unless continuous surface wasting through an external selector is applied. A classifying selector works by selectively wasting the foam layer accumulating on the surface in an aeration basin. In certain plants *Nocardia* filament trapping is often an issue and it is difficult to control *Nocardia* proliferation through any method, which was the case for an oxygen activated sludge plant in a 1996 study which split the plant in half and applied classifying selectors to the end of the aeration basin on one side and on the RAS line in the other. It was found that the side with the classifying selector applied to the aeration basin was more effective at controlling foam than the one applied to the RAS line and that *Nocardia* levels has been reduced by 30% (Pagilla et al, 1996). The optimum approach to reducing nuisance organisms has been found to be continuous surface wasting regardless of foam

levels. The benefits of a classifying selector allow for not only eliminating nuisance conditions but also reducing foam causing organisms, preventing them from proliferating downstream processes.

## 2.2 Biological Phosphorus Removal

### 2.2.1 Background

Phosphorus can be removed through enhanced biological phosphorus removal (EBPR) in which microorganisms called PAO exist in the solids which consume phosphorus. Phosphorus may also be removed through chemical phosphorus removal to form a precipitate. This is used as an effluent polishing step, to prevent struvite formation, or to supplement EBPR. Ferric is a common chemical often applied before the primary and/or secondary clarifier to bind the phosphorus which can then be settled out. Chemical addition to primary clarifiers is also used to remove phosphorus for nutrient control, heavy metals to meet toxicity requirements, and hydrogen sulfide to lower odor emissions (WEF, 2005).

In both of these methods, phosphorus is contained in a solid form and is then settled in a clarifier and removed in sludge wasting. EBPR has been used for decades and allows for plants to reach effluent standards while minimizing chemical consumption and sludge production (Metcalf, 2014; Neethling et al, 2005). EBPR consists of alternating anaerobic and aerobic zones where organic uptake and P release occur under anaerobic conditions and P uptake occurs under aerobic or anoxic conditions. The initial anaerobic selector allows for the enrichment of the bacteria that take up P in aerobic conditions. Many factors affect the performance of EBPR, such as; influent wastewater characteristics, nitrogen removal requirements, presence of nitrate, management of return flow from anaerobic solids processing steps, chemical addition for phosphorus polishing, and other processes used to enhance EBPR (Neethling, 2005). IFAS installation could also improve EBPR as it allows for a short SRT in the suspended growth which favors biomass phosphorus accumulation (Sriwiriyarat and Randall, 2005). Some issues utilizing IFAS for EBPR include the low biomass MCRTs, and low temperatures resulting in washout and lack of an anaerobic selector in most plants utilizing BNR. A 2005 study implemented IFAS media into anoxic selectors only, aerobic selectors only, and both anoxic and aerobic selectors, finding that each one of these was a viable method for EBPR. However, the control system utilized COD more efficiently than the IFAS systems. EBPR performance was reduced in systems that split the influent flow between aerobic and anoxic zones for enhancing denitrification because the rbCOD present in the anoxic zone caused the biofilms on the media to release phosphorus, which was not

then sent to the aerobic phase to take up the released phosphorus. The performance was found to be similar in the IFAS systems and conventional BNR systems under the same type of operation (Sriwiriyarat and Randall, 2005).

PAO activity test results from a WERF study taken from multiple locations can be found in Table 2.4. The ratio between the uptake and release rates are quite consistent across the five plants; around 3-4, indicating that the aerobic and anoxic period should be about 3-4 times that of the anaerobic period at a full-scale WWTP.

**Table 2.4 Results of Phosphorus Uptake and Release Tests from 2005 WERF EBPR Study**

<b>Test Parameter</b>	<b>Unit</b>	<b>Durham</b>	<b>VIP</b>	<b>Nansemond</b>	<b>McDowell Creek</b>	<b>Lower Reedy</b>
<b>Phosphate Release Rate</b>	mg P/g VSS/hr	7.4	12.0	6.4	11.9	24.6
<b>Phosphate Uptake Rate</b>	mg P/g VSS/hr	2.4	5.3	3.0	3.6	5.9
<b>Release Rate: Uptake Rate</b>	Ratio	3.1	2.7	2.3	3.6	4.0
<b>Acetic Acid/ <math>\Delta</math>P</b>	mg COD/ mg PO <sub>4</sub> -P	3.6	2.9	4.6	3.7	2.0
<b><math>\Delta</math>P/ <math>\Delta</math>Mg-Release</b>	mg PO <sub>4</sub> -P/mg Mg	4	6	14	6	4
<b><math>\Delta</math>P/ <math>\Delta</math>Mg-Uptake</b>	mg PO <sub>4</sub> -P/mg Mg	3.5	4.6	5.7	5.1	3.6
<b>MLVSS</b>	mg/L	2600	2070	2010	2200	1850

Extracted from (Neethling, 2005)

## 2.2.2 PAO, DPAO and GAO metabolism

### 2.2.2.1 PAO

PAO are heterotrophic bacteria that take up phosphorus in aerobic conditions and are critical for EBPR performance. PAO may provide over 80% biological phosphorus removal (Metcalf, 2014). The anaerobic zone provides for the fermentation of the influent rbCOD to acetate. (Metcalf, 2014). PAO are able to outcompete ordinary heterotrophic bacteria, as they have the ability to accumulate volatile fatty acids (VFAs) in their cells in the absence of an electron acceptor. Other heterotrophic bacteria are not able to uptake acetate and starve while the PAO use COD in the anaerobic zone (Metcalf, 2014). Under anaerobic conditions, PAO consume acetic and propionic acid and use stored polyphosphates as energy to assimilate acetate and produce intracellular poly- $\beta$ -hydroxyalkanoate (PHA). The energy for this transport and storage reaction is thought to be supplied by the hydrolysis of the intracellular polyphosphate to phosphate, which is released from the cell to the liquid. Polyphosphate is stored intracellularly as PHA (Metcalf, 2014; Smolders, 1994). A schematic of anaerobic PAO metabolism can be found in Figure 2.1. The most common PHAs are poly- $\beta$ -hydroxybutyrate (PHB) and polyhydroxyvalerate (PHV). Glycogen within the cell is also used for PHA storage. As acetic and propionic acid are consumed, orthophosphate is released, as well as magnesium, potassium, and calcium cations. The PHA content in PAO increases, while the polyphosphate content decreases. (Metcalf, 2014). The uptake and storage of acetate and degradation of polyphosphate are coupled to each other and their ratio should be constant, but ranges from 0.25-0.75 P-mol/C-mol have been found in literature (Smolders, 1994). From a 1994 study developing a model for P metabolism by Smolders, it was found that glycogen metabolism took place during anaerobic conditions and that glycogen as an internal carbon source was used in the P-metabolism. P-release in the anaerobic phase was strongly influenced by the pH, with P-release increasing with an increased pH (pH 5.5-8.5 measured) (Smolders, 1994). An optimum pH range of 7.0-7.5 for PAO proliferation has been found in a 2001 study (Filipe, et al., 2001).

In the aerobic zone, the PHA is metabolized and produces some glycogen. This energy is used for polyphosphate synthesis so that  $O\text{-PO}_4$  is taken up in the cell, cell growth occurs due to PHA utilization, and phosphorus is taken up in the cell. Due to the anaerobic consumption of acetate, the PAO accumulate in the sludge and strictly aerobic organisms decrease in number as they lack the substrate in the aerobic phase (Smolders, 1994). This process may occur in an anoxic zone prior to the anaerobic zone as denitrifying PAO (DPAO) can use nitrate and nitrite as an electron

acceptor for substrate oxidation (Metcalf, 2014). A schematic of PAO metabolism under aerobic/anoxic conditions can be found on the right side of Figure 2.1.

After the aerobic zone, the phosphate is then settled out in the excess sludge or can be stripped from the biomass and regained in crystallized form (Smolders, 1994). It is critical for recirculation of activated sludge to the anaerobic and aerobic zone to occur to obtain phosphorus removal. PAO also form very dense floc which settle well, and in some facilities this advantage has been used to improve settleability even though EBPR was not required (Metcalf, 2014). Although PAO exist in large quantities in totally aerobic suspended growth cultures, they only develop the ability to store large amounts of phosphate when they alternate between anaerobic and aerobic conditions by being recycled between the two (Grady, 2011). The current and most widely accepted model for PAO metabolism, called the Mino model was developed by Arun et al. and has been adapted by many others. Other models have been developed combining activated sludge models (ASM) and EBPR metabolic models, one being the TUD-P model which has been used for wastewater treatment plant optimization (Oehman et al, 2010).

The most common PAO group is *Candidatus Accumulibacter phosphatis* (i.e. *Accumulibacter*), closely related to *Rhodocyclus* in the *Betaproteobacteria*, which are generally abundant in full-scale EBPR systems (5-20% of total Bacteria) and are also commonly enriched in lab-scale EBPR reactors (Oehmen et al, 2007). Through molecular techniques Bond et al. (1995) identified PAOs in the *Rhodocyclus* group in the *Betaprotobacteria*. They were named *Candidatus Accumulibacter Phosphatis*, which were further divided into *Accumulibacter* Type I and Type II (Oehmen et al, 2010). Type I can use nitrate or nitrite as electron acceptors are referred to as DPAO (Nielsen et al, 2010). A 2007 study hypothesized that PAO of the rod morphotype was linked with PAO that were able to use nitrate as an electron acceptor, while coccus morphotypes were associated with PAO that could use nitrite but not nitrate (Carvalho, 2007).

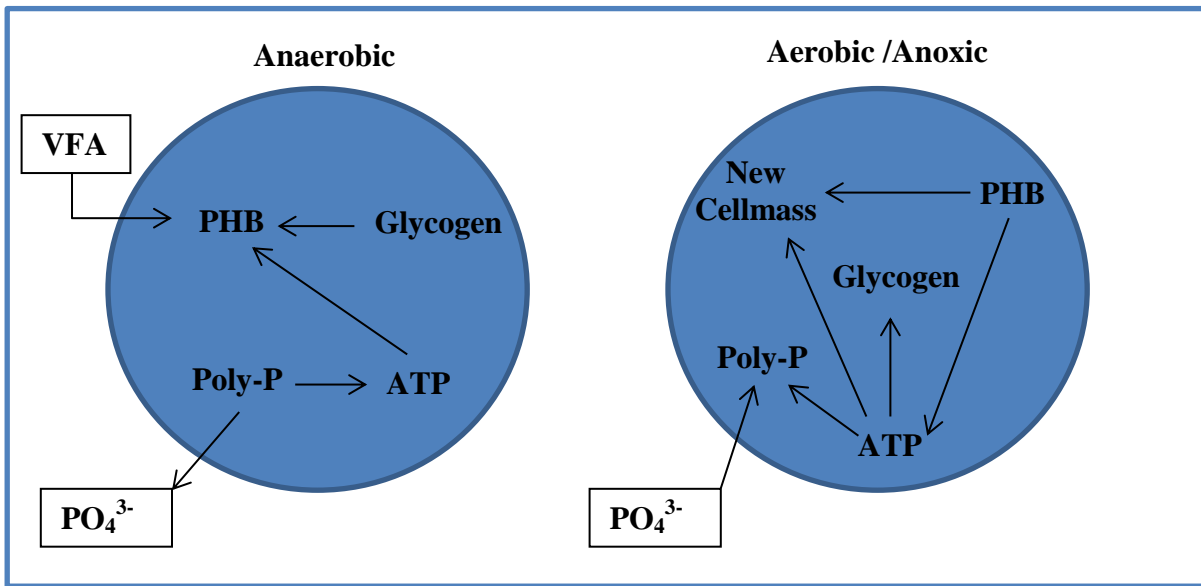


**Figure 2.1 PAO metabolism under anaerobic and aerobic/anoxic conditions.**

#### 2.2.2.2 GAO

GAOs were originally referred to as “G” bacteria because of their growth and glycogen storage with glucose feed. The term GAO (Mino et al, 1995) is based on the organism’s storage of glycogen under aerobic conditions and consumption of glycogen under anaerobic conditions to provide energy for VFA uptake and production of PHA in the anaerobic zone of an EBPR system (Metcalf, 2014). GAO compete with PAO for substrate, and do not remove any phosphorus from the system. In addition to GAO, many other organisms may compete with PAO for substrate. GAOs use glycolysis to obtain energy and reducing equivalents for VFA uptake and PHA storage. Under aerobic conditions, glycogen is regenerated from PHAs (Acevedo et al, 2014). PAO and GAO were thought to be different organisms, but recent studies have shown PAO are able to act like GAO under certain conditions (Acevedo et al, 2014). A 2014 study by Acevedo generated a new model to include PAO which altered their metabolism to act like GAO under low phosphorus concentrations.

GAO belong to the phenotype *Gammaproteobacteria* and were named “Candidatus *Competibacter Phosphatis*” by Crocetti et al (2002). All GAOs identified so far have been able to use nitrate and an electron acceptor in addition to oxygen, but only *Competibacter* Type I can use nitrite as well. (Nielsen et al, 2010.)

### 2.2.2.3 PAO/GAO competition

PAO and GAO competition are affected by many factors including; acetate and propionate composition, pH, temperature, and SRT. PAO are able to proliferate over GAO when pH is above 7.0, with a pH over 7.5 being preferred (Lopez-Vaquez et al, 2009). GAO has a faster anaerobic VFA consumption rate leading to an increased growth rate at lower pH levels. Another study by Zhang et al. found that EBPR performance dramatically declined as pH was reduced from 7.0 to 6.5. Temperature effects also effect PAO and GAO levels, with temperatures of 10°C or less greatly favoring PAO growth. At temperatures between 20 and 30°C GAO proliferated over PAO unless the pH was above 7.5. At temperatures below 15°C or above 30°C GAO have much lower growth rates and require a much higher aerobic SRT than PAO (Metcalf, 2014).

Based on values given in BioWin modeling software, a COD uptake (mg COD/ g MLVSS/hr) to P release (mg OP/ g MLVSS/hr) ratio > 1.96 is indicative of GAO presence in activated sludge (EnviroSim Associates, 2014). In Table 2.4 the Acetate uptake/P release ratio shows that each plant has >1.96 mg COD/ mg PO<sub>4</sub>-P, indicating GAO presence. Table 2.5 provides a comparison of PAO/GAO uptake activity in a study published in 2005 and indicates that all plants had GAO presence except for Nansemond.(Neethling, 2005). Table 2.6 provides the metabolic features of common PAO and GAO, which provides valuable information on the organisms that are able to denitrify using NO<sub>3</sub> and/or NO<sub>2</sub> in addition to taking up P.

**Table 2.5 Comparison of PAO/GAO Observations and Uptake and Release Test Results**

Sample	Summary of Microbial Investigation	Phosphate Release mg P/mg acetic acid	Phosphate Release Rate (mg P/VSS/hr)	Phosphate Uptake Rate (mg P/g VSS/hr)	RR:UR ratio <sup>2</sup>
Durham Side 1	PAOs dominant, some GAOs were easily observed	0.4	10	3.6	2.8
Durham Side 2	PAOs dominant, some GAOs were easily observed	0.14	4.2	1.5	2.8
VIP, July 2003	PAO dominant, both tetrapod-shaped and <i>Competibacter</i> -type GAOs easily observed	0.32	11.6 <sup>1</sup>	3.0 <sup>1</sup>	3.9
VIP, September 3, 2003	PAO dominant, both tetrapod-shaped and <i>Competibacter</i> -type GAOs easily	-	11.1	2.2	5.0

	observed				
<b>VIP, September 12, 2003</b>	Abundant GAOs, almost as abundant as PAOs	-	None	None	-
<b>Nansemond, July 2003</b>	PAO dominant, no tetrapod-shaped, but <i>Competibacter</i> -type GAOs easily observed	-	None	None	-
<b>Nansemond, September 2003</b>	PAO dominant, no GAOs observed	0.30	7.7	2.6	3.0
<b>McDowell</b>	GAO seemed to be dominant, more abundant than PAO	0.28	5.5	1.4	3.9
<b>Lower Reedy</b>	PAOs dominant in big flocs, only a few GAO were found	.78	24.3	4.6	5.2

1. URT run in August 2003

2. RR:UR=Ratio of Release Rate to Uptake Rate

3. Rates are shown normalized to VSS for illustration. PAO/VSS composition will vary from plant to plant

Extracted from

**Table 2.6 Proposed metabolic features of the most known PAOs and GAOs**

Organism	Preferred VFA	Substrate uptake mechanisms	Source of Reducing Power	Denitrification Capacity	
				NO <sub>3</sub>	NO <sub>2</sub>
<i>Accumulibacter</i> Type I	Acetate and propionate	PMF by efflux of protons and P	Glycolysis	yes	yes
<i>Accumulibacter</i> Type II				no	Yes
<i>Competibacter</i>	Acetate	PMF by ATPase and fumarate reductase	Glycolysis		
Sub-groups 1, 4, 5				Yes	No
Sub-groups 3, 7				No	No
Sub-groups 6				Yes	Yes
<i>Defluviococcus vanus</i> Cluster I	Propionate	PMF by methamalonyl-CoA & fumarate reductase	Glycolysis	Yes	No
<i>Defluviococcus vanus</i> Cluster II				no	No

Extracted from (Oehmen et al, 2010)

#### **2.2.2.4 DPAO**

Some PAO species can use nitrate and nitrite as an electron acceptor for substrate oxidation (Metcalf, 2014). These organisms are called Denitrifying PAO, or DPAO, and have the ability to remove nitrogen and phosphorus simultaneously. Some recent studies have focused on the development of simultaneous nitrification, denitrification and P removal processes, sometimes using granular sludge (Oehmen et al, 2007). The results from a 2010 study by Oehmen et al, in combination with previous studies, strongly suggest that DPAOs and PAOs are different microorganisms, whereby *Accumulibacter* Type I are likely to be able to reduce nitrate and *Accumulibacter* Type II are not likely to be able to reduce nitrate (Oehmen et al, 2010). An advantage to having DPAO in a BNR process is that the use of nitrate rather than oxygen as the electron acceptor leads to slightly less sludge production and a more efficient use of COD as it is used for phosphorus uptake and denitrification simultaneously (Ahn, 2002). Kuba et al (1996) developed a two sludge system with nitrifiers in one and DPAO in another where supernatant from the nitrifier system fed nitrate to the DPAO. Conventionally an aerobic step is needed for nitrification to supply nitrate as an electron acceptor for PAO. This results in large amounts of PHB being aerobically oxidized by PAO in long aerobic periods resulting in less COD available for denitrification. By skipping this nitrification step, it was found that 15 mg P/l and 105 mg N/l were removed using only 400 mg COD/l HAc. Calculations proved that the sludge production required COD was 30% and 50% less than conventional phosphorus and nitrogen removal systems, respectively. A study was performed on phosphorus activity in three separate reactors with different electron acceptors; one with only oxygen, one with oxygen and nitrate, and one with only nitrate. The reactor using oxygen and nitrate had the highest phosphorus uptake rates, indicating a presence of DPAO that could utilize nitrate under aerobic conditions, while the reactor with only nitrate had a decreasing phosphorus uptake over time (Ahn, 2002).

#### **2.2.3 Conditions favoring EBPR**

EBPR performance strongly relies on the bacteria population, which varies depending on factors such as pH, temperature, influent characteristics, and SRT. Conditions found to favor EBPR and achieve consistent low effluent phosphate concentrations include: high influent BOD:TP, exclusion of oxidants (nitrate and DO) from anaerobic zone, excluding or minimizing recycle flows and loads fluctuations from solids processing, favorable operation conditions (low SRT, modest temperature, sufficient DO in aeration basin, balanced anaerobic and aerobic HRTs) (Neethling, 2005). A high SRT may lead to a larger portion of the PAO population being lost to endogenous decay, reducing the PAO in the waste sludge (Whang and Park, 2002). EBPR

systems have shown decreased EBPR activity rates and lower temperatures (Brdjanovic, 1998). Some EBPR has achieved good performance at lower temperatures but a higher sludge age is needed as the process kinetics decrease at lower temperatures. Brdyanovic found that as the temperature decreased from 20°C to 10°C, incomplete phosphorus uptake occurred and that only 15% of acetate was consumed in the anaerobic zone and the rest was consumed in the aerobic zone. The result was a high phosphorus concentration in the effluent and a washout of PAO. However, an increase in SRT, the system gradually recovered (Brdjanovic, 1998) Similar trends were seen when the temperature was decreased to 5°C, with the system recovering when the SRT was increased further.

A WERF study conducted in 2010 collecting plant data from 47 facilities through the U.S. found that plants achieving the highest percentage of influent phosphorus removal supplement EBPR by adding volatile fatty acids (VFAs) or by polishing with iron or aluminum containing chemicals (Neethling, 2005). It was also found that two thirds of the facilities meeting effluent TP levels lower than 0.5 mg/L did not have solids recycle streams from the dewatering of anaerobically digested sludge. No correlation was found with TP removal and SRT. The maximum TP removal for facilities with no VFA or chemical addition is 95%, with effluent TP concentrations ranging from 0.2-2.0 mg/L.

Temperature impacts EBPR as it relates to VFA generation in the aerobic zone (Stensel, 1991). The microbiology of the activated sludge is also impacted by temperature, including PAO. Studies at warm-weather BNR plants showed temperatures exceeding 30°C compromised EBPR efficiency, possibly because PAO growth rate was reduced and GAO proliferate at higher temperatures (Neethling, 2005). This results in leftover substrate not consumed by PAO to enter the aerobic zone, resulting in possible filament growth. Temperatures above 20°C have been shown to favor GAO proliferation.

In the Neethling (2005) study, a correlation was found between the ratio of the uptake HRT to release HRT and the observed performance rating, which was based on the conditions listed above. The ratio between the uptake rate and release rate are extremely consistent, typically between three and four based on release rate: uptake rate. This implies that in full scale treatment, the aerobic contact time should be three to four times as long as the release time (anaerobic plus excess-anoxic time) (Neethling, 2005).

### **2.2.3.1 Low Organic Loading**

Under conditions of low total organic loading, the maintenance processes of PAOs and GAOs are pushed to their limit since both organisms are put under conditions of no external carbon sources for extended periods (Carvalheria et al, 2014). This causes them to deplete their internal carbon and energy sources: PHAs and glycogen, as well as polyphosphate in the case of PAOs. This study found that the biomass decay rate of GAOs was about 4 times higher than PAOs, showing that PAOs are better adapted to survive in low carbon loading conditions. In the aerobic phase PAOs tended to maintain a PHA reserve, while GAOs exhausted all of their PHA, which may have contributed to their increased biomass decay rate (Carvalheria et al, 2014). Tu and Schuler (2013) studied the effect of lowering the acetate concentration in an EBPR system through decreasing the feeding rate, while maintaining the total acetate load to the bioreactor (i.e., 200 mg COD/L per cycle). They similarly found that PAOs were able to flourish over GAOs under low loading rates.

### **2.2.3.2 DO**

Narayanan (2006) found that DO concentrations  $>2$  mg/L in the initial aerobic zone resulted in OP effluent values  $<0.05$  mg/L while DO concentrations  $<2$  mg/L led to variable yet increasing effluent OP values. It was also found that EBPR upsets were due to disruption of the aerobic uptake and not due to initial P release in the anaerobic phase, indicating that the initial aerobic uptake phase is critical (Narayanan, 2006). This may be because the P uptake rate is highest when the PHA content is highest. As PHA is constantly being used as an energy source in the aerobic zone, the initial PHA concentration would be highest during the initial aerobic zone, and therefore, this is where the P uptake rate would be highest and would decrease through further aerobic zones. It is critical to maintain a high DO concentration in the initial aerobic zone, ensuring it does not drop below 1.5 mg/L (Narayanan, 2006).

However, Narayanan (2006) did not take into account GAO. In a 2014 study by Carvalho et al. the effect of aeration on the competition between PAOs and GAOs was investigated. Batch tests of enriched PAO and GAO cultures were performed at different DO levels in the aerobic zone, in order to determine how the aerobic kinetics of each population varies as a function of the DO concentration. Long term tests were also administered to observe the microbial population performance on each system at different DO levels. The study found that PAO thrive in low DO levels in the aerobic zone, while high DO levels led to higher growth and activity of GAO. PAO possess a higher affinity for oxygen and show a clear kinetic advantage over GAO at low DO concentrations. The impact of aerobic HRT on the microbial population and EBPR performance

was also investigated, with results indicating a high aerobic HRT promoted the growth of GAO over PAO. Incorporation of the oxygen affinity of PAOs and GAOs into WWTP models could be highly useful to optimize EBPR processes (Carvalheria et al, 2014). A low HRT aerobic period with low DO levels is optimal for PAO proliferation, which is beneficial as estimates of aeration requirements in WWTP correspond to 45-75% of energetic costs (Rosso et al, 2008).

#### 2.2.4 Processes

Reactors need to be designed to provide PAO with a competitive advantage over other bacteria. This is done by utilizing an initial anaerobic selector (Metcalf, 2014). An anaerobic environment allows for PAO to transport and consume influent rbCOD in the form of VFAs by using energy made available from their stored phosphorus and polyphosphates. Other heterotrophic bacteria cannot consume the rbCOD because they need an electron donor such as oxygen, nitrate, or nitrite for oxidation-reduction reactions. PAO can then use their stored energy along with cellular glycogen to direct the substrate uptake to internal carbohydrate storage products for oxidation later in the aerobic zone (Metcalf, 2014).

The contents of the anaerobic tank are thoroughly mixed to provide contact with the return activated sludge (RAS) and influent wastewater, and will have an HRT of 0.5-1.0 hour. SRT values in the aerobic tank may range from 3-40 days (Metcalf, 2014). Conventionally bio-p removal is established at high total SRTs (3-15 days) to retain PAOs. However, longer SRTs allow for GAO to compete with PAO for carbon substrates. Competition between PAO and GAO is also affected by the DO concentration and HRT. At low DO levels, *Accumulibacter* PAO have an advantage over GAO. An increase of the aerobic HRT when the DO is at 2 mg/L promoted proliferation of GAO over PAO as found in a 2014 study by Carvalheria *et al.*

## 2.3 Granular Sludge

### 2.3.1 Background

Granular sludge is well understood in anaerobic processes, while aerobic granular sludge has not yet been well researched. Granular sludge was first found in an upflow anaerobic sludge blanket (UASB) at the end of the 1970s (Lettinga et al, 1980). Since the 1980s, granular sludge has been used extensively in full-scale anaerobic reactors. Aerobic granular sludge was first discovered in an upflow sludge blanket reactor in 1991 (Mishima and Nakamura, 1991). In 1997 a sequencing batch reactor (SBR) was used to develop aerobic granular sludge and has been shown to be the preferred reactor for aerobic granule formation as oppose to a UASB for anaerobic granular

sludge (Gao et al, 2011). Most research on aerobic granules has been done using an SBR and focuses on cultivation conditions, factors influencing granulation, and the microbial community. In 2005, aerobic granules were defined by the International Water Association (IWA) as aggregates of microbial origin, which do not coagulate under reduced hydrodynamic shear, and which settle significantly faster than activated sludge flocs (Gao et al, 2011). Aerobic granular sludge is advantageous over sludge in floc form in that aerobic granules have a high biomass retention when compared to flocculent sludge because of their high density and compact structure; allowing a reactor to treat wastewater at a higher volumetric loading rate. They also have a high settling velocity which can reach 50-90 m/h depending on the size and density (Gao et al, 2011). Various wastewaters and shock loadings are both treatable using aerobic granular sludge (Gao et al, 2011). No sludge bulking has been observed in aerobic granular sludge.

Granular sludge is unique to conventional sludge in that there is no need for separate aerobic and anaerobic selectors; all processes occur in different layers within the granular biomass, there will be segregation of bacteria as a function of depth within the granules. A stratification of layers exists within granules as nitrifiers are located in layers receiving oxygen penetration and denitrifiers and PAO are present in the inner anoxic layers. A 2013 study found that the outer layers are subjected to more shear stress and that high biomass retention selects for slow growing organisms (Winkler et al, 2013).

### 2.3.2 Settleability

Aerobic granules have a high density and a high biomass retention capacity which directly relates to the settleability of sludge and solids liquid separation in the reactor (Gao, et al., 2011). Various studies showed the settling of aerobic granules to vary between 18-90 m/h with some even reaching 130 m/h, which are similar for anaerobic granules, but much higher than activated sludge which range from 7-10 m/h. The SVI of aerobic granules is generally below 80 mL/g and can even get as low as 20 mL/g. A settling model for aerobic granules was developed by Lui et al in 2005 showing that the settling velocity was a function of SVI, average size, and biomass concentration (Liu et al, 2005).

In a 2011 study Gao found that the density of aerobic granules in SBR varied from 1.004 to 1.1 g/m<sup>3</sup> which is much higher than the specific gravity for flocculent sludge (1.002-1.006 g/m<sup>3</sup>). The water content of granules is about 94-97% which is much lower than flocculent sludge at 99% (Gao et al, 2011).

In a 1998 study to achieve aerobic granular sludge in a sequencing batch reactor (SBR), filamentous bacteria were shown to disappear after about 20 days, decreasing the SVI from 250-500 mL/g to 100-150 mL/g (Dangcong, 1998). In this study it took about one month for the floc to become completely granulized, and at this point COD, NH<sub>3</sub>-N and nitrogen removal efficiencies were 95%, 95%, and 60% respectively, some filamentous bacteria were present, and SVI decrease to 80-100 mL/g. These results remained for a 3-month duration. In anaerobic or anoxic reactors, granules can grow to be 2-3 mm, but in this study the aerobic granules were found to reach only 0.3-0.5 mm, and did not increase in size with time (Dangcong, 1998). This may be due to high mixing rates and aeration causing shear in the aerobic SBR. Activity and settleability of the aerobic granules in this study were similar to anoxic and anaerobic granules from previous research.

### **2.3.3 Formation**

In pilot studies, aerobic granulation has been established by applying high substrate gradients, a certain degree of shear stress, and selection of fast-settling particles (Gao et al, 2011). An initial high substrate concentration is desired for granulation because it results in high EPS and internal storage product formation. This allows the substrate to penetrate to the anaerobic core and various layers within the granule. Aerobic granulation is usually achieved in SBRs but can also be achieved in a plug flow configurations. In many studies it has been found that a short settling time that selects for fast settling particles is a significant factor in establishing granular sludge in SBRs (Liu, 2004). The formation of granules may also occur using a selector to continuously retain larger particles. To retain only fast settling particles, a minimum critical settling velocity may be applied to the system, typically > 10 m/hr . Eventually, the particles will become granules under continuous internal selection. This is usually done in SBRs with short settling periods, but this restricts applying this technology to existing infrastructure. It is also necessary for the slow-settling particles to be washed out to maintain granular sludge. Granulation may also be achieved through an external selector such as a hydrocyclones. A balance of flocs and granules within a system may provide superior settling characteristics as flocs will sweep finer particles and granules have superior settling rates. Studies forming aerobic granules in SBRs found that the formation of mature granules did not occur until 75, 49, and 39 days (Figueroa et al, 2008; Adav et al, 2008; Carucci et al, 2009).

#### 2.3.4 Biological Nutrient Removal

As granules are dense particles, they have the capacity to carry dense organisms. PAO and DPAO are dense and exist in these granules, providing phosphorus removal and even simultaneous nitrogen removal within a granule. In a 2006 study, simultaneous nutrient removal was achieved in aerobic granules because of heterotrophic growth inside the granules as DPAO and autotrophic growth existed on the aerobic surface (de Kreuk, 2006). A schematic of one of these granules with stratified layers can be seen in Figure 2.2. This process was coined the Nereda™ process in which biological nutrient removal (BNR) existed in aerobic granules without the need for anoxic or anaerobic selectors (de Kreuk, 2006). Full scale Nereda™ operations exist in Europe and South Africa with footprints up to 4 times smaller than conventional activated sludge processes with excellent reported removal of carbon, nitrogen and phosphorus (de Kreuk et al, 2005). Once stable aerobic granular sludge was achieved in the Nereda™ study, it was found that a 60 minute anaerobic feed period within a full cycle of 3 hours and a low oxygen concentration (20%) led to high simultaneous COD, phosphate and nitrogen removal efficiencies (de Kreuk, 2006). It was shown that nitrogen removal efficiencies greatly depended on the granule diameter, with an optimal size between 1.2-1.4 mm at a DO of 2 mg/L and at a temperature of 20°C. However, aerobic granules were found to range widely from 0.2 up to 16 mm (Gao et al, 2011). Optimum COD loading rate was 1.9 kg COD/m<sup>3</sup>/day. N removal efficiency was also affected by the ratio between aerobic and anoxic volume in the granule. Granules formed with an initial temperature of 8°C were irregular and aggregated as soon as aeration ceased, leading to washout. With an initial temperature of 20°C however, granulation was maintained, even as temperatures lowered to 15°C and 8°C. With this information, it is preferential to initially form granules in warmer temperatures, while maintaining granulation is achievable year round.

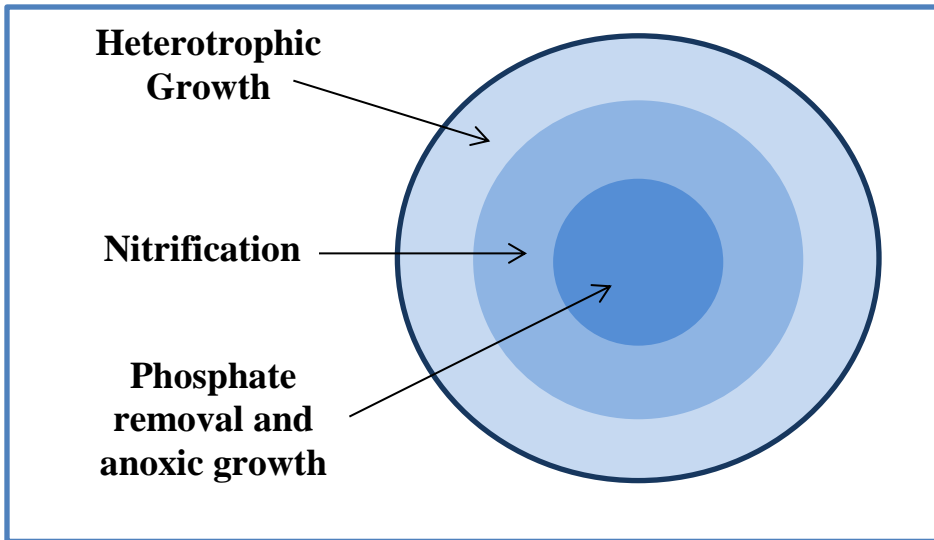


**Figure 2.2 A schematic of an aerobic granule with stratified layers.**

Anaerobic granular sludge mainly consists of methanogenic, syntrophic acetogenic and various hydrolytical-fermentative bacteria while aerobic granular sludge is mainly used for the aerobic degradation of organics and also for nitrogen removal under aerobic and anoxic conditions (Gao et al, 2011). Anaerobic or anoxic granular sludge containing ANAMMOX has also been developed. Aerobic granules are composed of stratified layers, where anoxic zones exist on the inside which allows for multiple biological processes to occur within a granule such as simultaneous nitrification-denitrification (SND) (Gao et al, 2011). However, granules may be at a disadvantage because particulate substrate is not entrapped and then hydrolyzed, causing elevated effluent suspended solids concentrations. A balance of flocs and granules may be desired for superior substrate utilization and effluent quality.

### 2.3.5 Microbiology

The microbial characterization of aerobic granules can vary widely depending on the substrate, wastewater characteristics, granule size, DO concentration, and other environmental factors (Gao et al, 2011). Generally aerobic granules contain organic-degrading, nitrifying, and denitrifying bacteria as well as anaerobic bacteria such as Anammox or methanogens (Gao et al, 2011). An aerobic granular sludge developed with organic carbon compounds and contained species such as *Poteroiochromonas*, *Epistylis*, *Geotrichum*, and *Geotrichum klebahnii* (Williams et al, 2006). It has been found that aerobic granules consist of no filamentous bacteria while anaerobic granules contain filamentous bacteria such as *Methanothrix* (Dangcong, 1998). However, Morgenroth et al, (1997) found that filamentous bacteria may provide a framework, serving as cores or carriers for granule formation. Granule size also affected the microbial makeup as found by Lemaire et al.

(2008). It was reported that *Accumulibacter* spp. was dominant in the outer 200  $\mu\text{m}$  of the granule, while the *Competibacter* spp. dominated in the cores of the granules. DO concentrations influenced the filamentous bacteria population as *Thiothrix* sp. was favored at low DO concentrations (Lee et al, 2003).

## 2.4 Hydrocyclones

Hydrocyclones are external selectors that receive mixed liquor tangentially and separate light solids from dense solids through their tapered shape, increasing the velocity of liquid as it moves downward and allowing for selection of a certain solids fraction. The underflow produces the dense solids while the lighter solids are sent to the overflow. Hydrocyclones have been used in multiple studies including full-scale plants to fulfill various functions. A 2014 patent on a wastewater treatment method describes a gravimetric selector that selects for solids with superior settling characteristics from the underflow and supplying this to the recycle stream. The velocity or hydraulic loading rate of the wastewater into the selector is controlled to select for solids of a predetermined size or density. (Wett et al, 2014).

A patent application was published in 2013 on a deammonification process where hydrocyclones were utilized to separate the sludge into a heavy sludge phase containing ANAMMOX, and a light sludge phase (Nyhuis, 2013). The heavy sludge phase was returned to the aeration tank and the light sludge was fed as surplus sludge to the sludge digestion.

The Strass Wastewater Treatment Plant located in Austria implemented the S-Select® technology to improve settleability. Strass experiences drastic changes in wastewater characteristics due to tourist season in winter. The temperature and load during winter in spring causes the settling behavior to deteriorate, but recovers during the summer and fall. As seen in Figure 2.3, Strass successfully used hydrocyclones to improve sludge settling properties. SVI values below 100 mL/g were maintained year-round after cyclone installation in year 2 and 3, greatly improving from SVI values reaching 180 mL/g in year 1 before the hydrocyclones were installed.

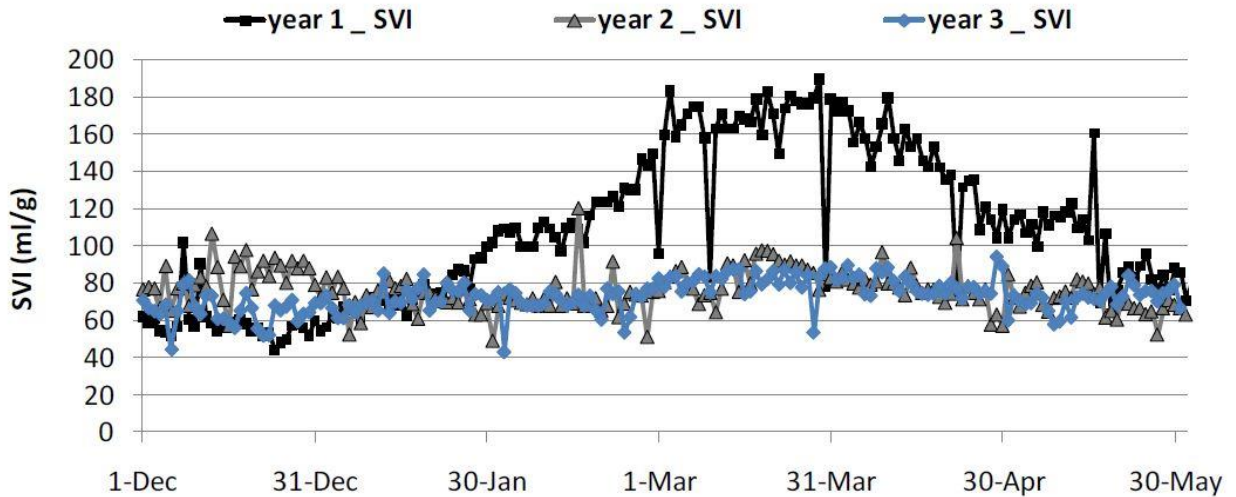


**Figure 2.3 Strass WWTP SVI over 3 year period, hydrocyclones installed beginning of year 2. Extracted from (Wett, 2015). [Strass SVI Update] Used under fair use, 2015.**

VCS Denmark operates the Ejby Mølle Wastewater Treatment Plant (EMWWTP). In April 2014 EMWWTP started passing the WAS stream through hydrocyclones. Diluted sludge volume index (DSVI) for the hydrocyclone underflow had been consistently in the range of 60 to 80 mL/g whereas the DSVI of the overflow had gradually increased from 125 to over 200 mL/g since the implementation of WAS hydrocyclones. During this period, however, the DSVI of the mixed liquor itself has remained constant in the range of 150 to 200 mL/g. It is possible, however, that the hydrocyclones have helped to stabilize the DSVI in the mixed liquor during a period when bulking organisms were otherwise proliferating, as revealed by the increasing DSVI of the overflow (Houweling, 2015).

## 2.5 Measurements for Settleability Characterization

Settling can be classified into four types; type I (discrete settling): particles settling independently at terminal velocity, type II (flocculent settling): dispersed material that with a strong affinity to flocculate, type III (zone settling): particles coalesce and settle together as a matrix at the same settling velocity, and type IV (compressive settling): solids settle at the bottom of the tank, the sludge is thickened and water is squeezed out (Figure 2.4).

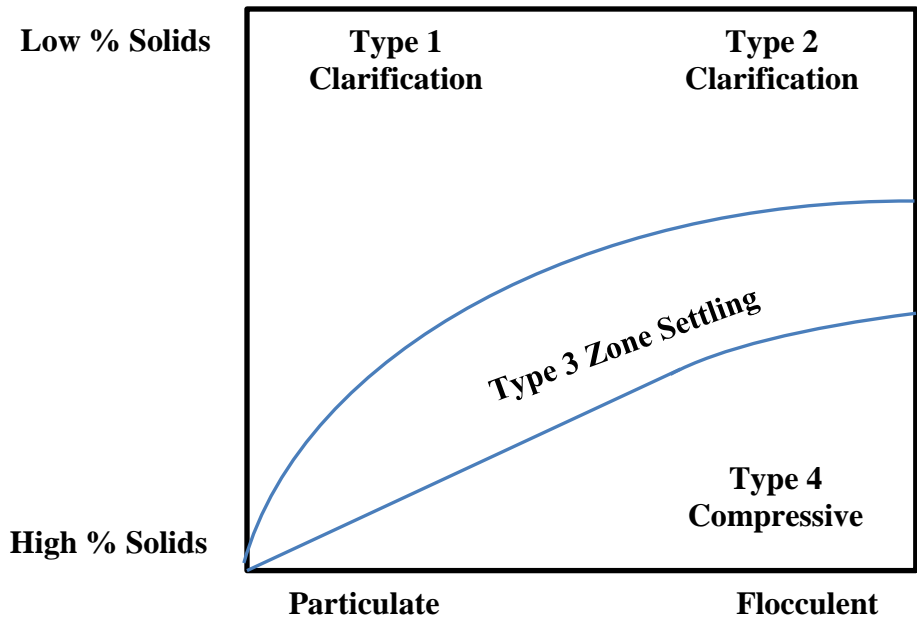


**Figure 2.4 Relationship between solids characteristics and sedimentation processes.**

### 2.5.1 Sludge Volume Index

SVI is frequently used for its simplicity and convenience, but has been criticized for not being a representative of actual settling processes in a secondary clarifier (Schuler, 2007). Seasonal variations have been shown to affect settleability, with multiple studies showing an increase in SVI in the winter than the summer and better settling characteristics in summer (Jones and Schuler, 2010). SVI values over 150 mL/g are considered to represent poor settling sludge. The SVI is the volume in mL occupied by 1 g of a ML after 30 minutes of settling. The SVI is determined by placing a well-mixed ML sample in a 2-L graduated cylinder with volumetric markings. Once 30 minutes has passed the interface between the settled sludge and supernatant is measured using the volumetric markings in mL/L. The SVI may be obtained by dividing this value by the MLSS concentration and multiplying by a conversion factor as seen in Eq.4 (Standard Methods 2710C). The SVI is most commonly used for a 30 (SVI30) minute settling period, but a 5 minute settling time (SSV5) is used as well. SSV5 can characterize the speed at which the sludge is settling before reaching compaction settling.

$$SVI \left( \frac{mL}{g} \right) = \frac{SSV \left( \frac{mL}{L} \right) \times 10^3 \left( \frac{mg}{g} \right)}{SS \left( \frac{mg}{L} \right)} \quad \text{Eq. 4}$$

### 2.5.2 Zone Settling Velocity

The zone settling velocity (ZSV) is another name for the initial settling velocity (ISV). The zone settling curve is generated by plotting the time versus the interface height of the solids-supernatant interface. The resulting zone settling curve is divided into 4 stages; the induction, constant-rate, falling-rate, and compression stages. The zone settling is the slope on the curve at which the interface height is falling at a constant rate, representing type 3 or hindered settling. At high concentrations, sludge settles in the zone-settling regime and is characterized by a distinct interface between the supernatant and the sludge zone. The height of this distinct sludge interface is measured with time. Zone settling data for suspensions that undergo zone settling can be used in the design, operation, and evaluation of settling basins (Rice, 2012).

The method for determining the ZSV can be found in Standard Methods (2710 E). ZSV as a function of the mixed liquor concentration and SVI can be estimated using the following equation:

$$ZSV \left( \frac{m}{hr} \right) = \text{slope of linear portion of ZSV curve} \left( \frac{mm}{min} \right) * \frac{60 \left( \frac{min}{hr} \right)}{100 \left( \frac{mm}{m} \right)}$$

Eq. 5

Unpredictable behavior may exist for sludges with a high concentration or sludges with poor settling characteristics. In a 2007 study Schuler found that as biomass concentration increases in zone settling tests, settling velocities decreased because the increased resistance to water flow through the settling biomass matrix occurs with decreasing volume since zone settling velocity tests are not thought to measure compression phenomena (Schuler, 2007).

### 2.5.3 Solids Flux

The flux theory was originally conceived by Coe and Clevenger in 1916 and has had many contributors to the theory since (Ekama, 2006). This theory is a one-dimensional model providing the value of the limiting concentration ( $X_L$ ) and the limiting solids flux. Solids flux is defined as the rate of the solids mass moving downward across a unit area in the clarifier (Metcalf, 2014). The applied loading rate must not exceed the limiting flux for safe operation of the clarifier (Ekama, 2006). The downward flux of solids in a clarifier is due to gravity (hindered settling) plus the transport of solids being pumped through the RAS. The limiting solids flux is the maximum rate at which solids can reach the bottom of the clarifier. A state point analysis on the solids flux curve may be used for process control, providing useful information for the maximum solids loading rate and settling model parameters when designing a clarifier. The area required for thickening of the solids is dependent on this maximum solids loading rate. The depth of the thickening portion of the clarifier must also be able to provide a thick enough sludge blanket so

that unthickened solids are not recycled (Metcalf, 2014). The underflow velocity may be decreased or increased, shifting the total flux curve. The required cross sectional area of a clarifier may be determined by drawing a horizontal line tangent to the low point on the total flux curve. The intersection of this line with the vertical axis represent the limiting solids flux that can be processed through the basin (WEF, 2005).

A solids flux analysis is determined through creating multiple ZSV curves at varying MLTSS concentrations. The linear portion of the ZSV curves represent type III settling and when plotted against the varying TSS values, it is possible to determine the zone settling velocity for any TSS value desired. The solids flux analysis (SFA) plot, which is used to determine the limiting solids flux, is a plot of the solids flux versus the solids concentration (Figure 2.5). The gravity solids flux  $SF_G$  is a product of settling velocity and the solids concentration (Eq. 6) and represents the mass flow rate at which solids settle out in a clarifier normalized to the surface area of the clarifier. The solids flux due to the underflow ( $SF_U$ ) is the mass flow rate of solids which are removed from the clarifier through the RAS flow rate. The  $SF_U$  is a product of the underflow velocity and solids concentration (Eq. 7). The underflow velocity is a ratio of the RAS flow rate to the clarifier surface area. The total solids flux ( $SF_T$ ) is determined by adding the  $SF_G$  and  $SF_U$  together (Eq. 8). The  $SF_G$ ,  $SF_U$ , and  $SF_T$  are all plotted against solids concentration to determine the limiting solids flux. The limiting solids flux ( $SF_L$ ) occurs at the local minimum or dip in the  $SF_T$  curve (Eq. 9). The corresponding solids concentration is the maximum solids loading rate which may be expected to be completely removed by a clarifier operating at the parameters used to calculate the solids flux values. If the solids loading rate exceed the  $SF_L$  a sludge blanket will accumulate in the clarifier, resulting in eventual solids in the effluent. Operators may use a state point graph to determine whether or not a clarifier is operating within its capacity.

$$SF_G = X_i * V_i * \frac{1 \text{ kg}}{10^3 \text{ g}} \quad \text{Eq. 6}$$

$$SF_U = X_i * U * \frac{1 \text{ kg}}{10^3 \text{ g}} \quad \text{Eq. 7}$$

$$\text{Where: } U = \frac{Q_{RAS}}{A} \quad \text{Eq. 8}$$

$$SF_T = SF_U + SF_G \quad \text{Eq. 9}$$

$$SF_L = X * \left( \frac{Q_{inf} + Q_{RAS}}{A} \right) \quad \text{Eq. 10}$$

$SF_{G/U/L}$  = Solids flux ( $\text{kg}/\text{m}^2\text{hr}$ )

$X$  = Solids concentration ( $\text{g}/\text{L}$ )

$V$  = Unhindered settling velocity found by the linear portion of the zone settling velocity curve ( $\text{m}/\text{hr}$ )

$U$  = Bulk downward velocity caused by recycle ( $\text{m}/\text{hr}$ )

$Q$  = Flow rate ( $\text{m}^3/\text{hr}$ )

$A$  = Clarifier surface area ( $\text{m}^2$ )

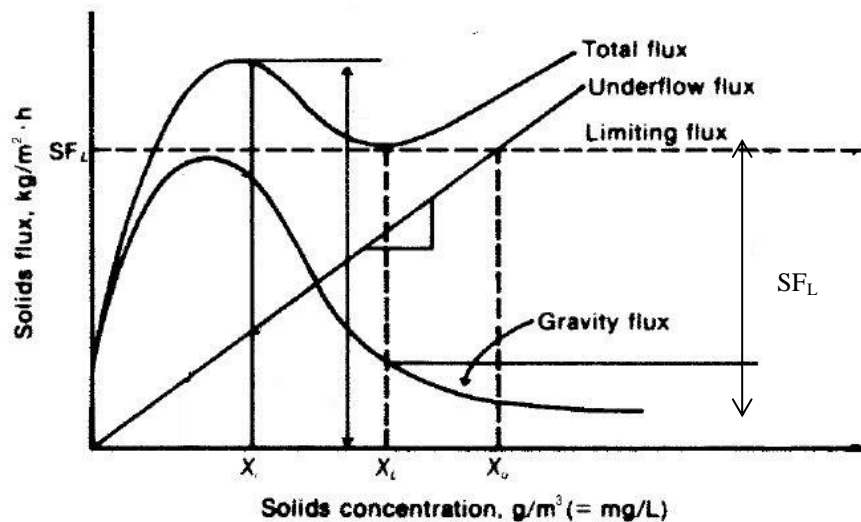


**Figure 2.5 State Point Analysis of Solids Flux Curve.**

The flux theory is not representative of the sludge thickenability and is not often used for design purposes due to being a labor-intensive test (Ekama, 2006). At concentrations below 1000 mg/L the  $SF_G$  is low because the settling velocity of the solids is mostly independent of the concentration. If the velocity remains constant as the solids concentration increases, the  $SFG$  will start to increase as the solids concentration increases. At higher solids concentrations, hindered settling occurs and the ZSV, SVI, and gravity flux decreases. At a very high concentration the flux approaches zero (Metcalf, 2014).

### 2.5.3.1 Vesilind

In 1968 Vesilind developed a semi-logarithmic equation relating the stirred zone settling velocity (SZSV) and the solids concentration, which is commonly used today. The Vesilind model is

based on flux theory. A reference describing the methodology of the Vesilind model may be found in EnviroSim (2014) BioWin wastewater process modelling software. The BioWin software provides default Vesilind parameters of  $k=0.37 \text{ m}^3/\text{kg}$  and  $V_o=7.08 \text{ m/hr}$ . The Vesilind parameters depend on the settleability of activated sludge. Conventionally these parameters are determined using the SVI, diluted SVI (DSVI) or the stirred SVI (SSVI). However, in 1999 Bye and Dold exposed the questionable relationship between these parameters (Yuen, 2002). The SVI is a time efficient tool to estimate performance, but it does not correlate with sludge ZSV or viscosity and can change with the sludge concentration and cylinder geometry. It is much more viable to fit the Vesilind model data obtained in the solids flux analysis. The semi-logarithmic Vesilind equation is seen in Eq. 11.

$$\text{Vesilind Equation:} \quad V = V_o e^{-kX} \quad \text{Eq. 11}$$

The Vesilind parameters may be determined using the sum of least squares method. Experimental solids flux data from this study was used to determine  $V_o$  and  $k$  by estimating values  $V_o$  and  $k$  and using the sum of least squares in Microsoft Excel to obtain velocity values. The error was calculated as the sum of differences between the estimated  $V_o$  and experimental  $V$  squared. The error was then minimized using the solver function in Microsoft Excel to vary the model parameters  $V_o$  and  $k$  to produce the smallest error. Using the determined parameters, the settling velocity was produced using the Vesilind equation and the MLSS concentrations collected during solids flux tests. The sum of least squares method generally provides a more accurate result (smaller error) than the conventional exponential regression method.

The Vesilind parameters may also be determined through linear regression. Eq. 12 may be linearized as seen in Eq. 13 to determine the Vesilind parameters. By plotting the biomass concentration ( $X$ ) versus the natural log of the measured settling velocities ( $V$ ), the negative slope of these lines represent the Vesilind  $k$  values and the y-intercepts are the  $\ln(V_o)$  as seen in Eq. 13 and Eq. 14.

$$\text{Linearized Vesilind:} \quad \ln(V) = -kX + \ln(V_o) \quad \text{Eq. 12}$$

Vesilind parameters from linearized equation:

$$k = (-)\text{slope} = -b \quad \text{Eq. 13}$$

$$V_o = e^{(y\text{-intercept})} \quad \text{Eq. 14}$$

$V$ = Settling velocity (m/s)

$X$ = Biomass Density (g/L)

$V_o$ = constant (m/s)

$k$ = constant ( $\text{m}^3/\text{kg}$ )

Well settling sludges may have max settling velocities ( $V_o$ ) of around 13 m/hr versus 5 m/hr or less for poor settling sludges. The Vesilind constant ( $k$ ) is typically low for well settling sludges: around  $0.25 \text{ m}^3/\text{kg}$  is excellent and  $0.5 \text{ m}^3/\text{kg}$  is poor (Ekama, 2006). It has been suggested that the coefficient  $V_o$  in the Vesilind equation form is related to Stokes-type settling for an individual floc, while  $k$  may represent factors affecting compaction or factors that contribute to resistance of settling (Schuler, 2007). Figure 2.6 represents a model of the semi-logarithmic Vesilind equation. Region 1 represents the non-settleable solids, Region 2 represents the low solids concentration, whereby discrete settling is in effect, Region 3 represents flocculent settling which is assumed to be independent of solids concentration and is a function of the maximum settling velocity, and Region 4 is the non-stokian region that described hindered and compressional settling (Mancell-Egala, In Preparation). The highest settling occurs during flocculent settling and as it transitions into non-stokian settling, velocity decreases.

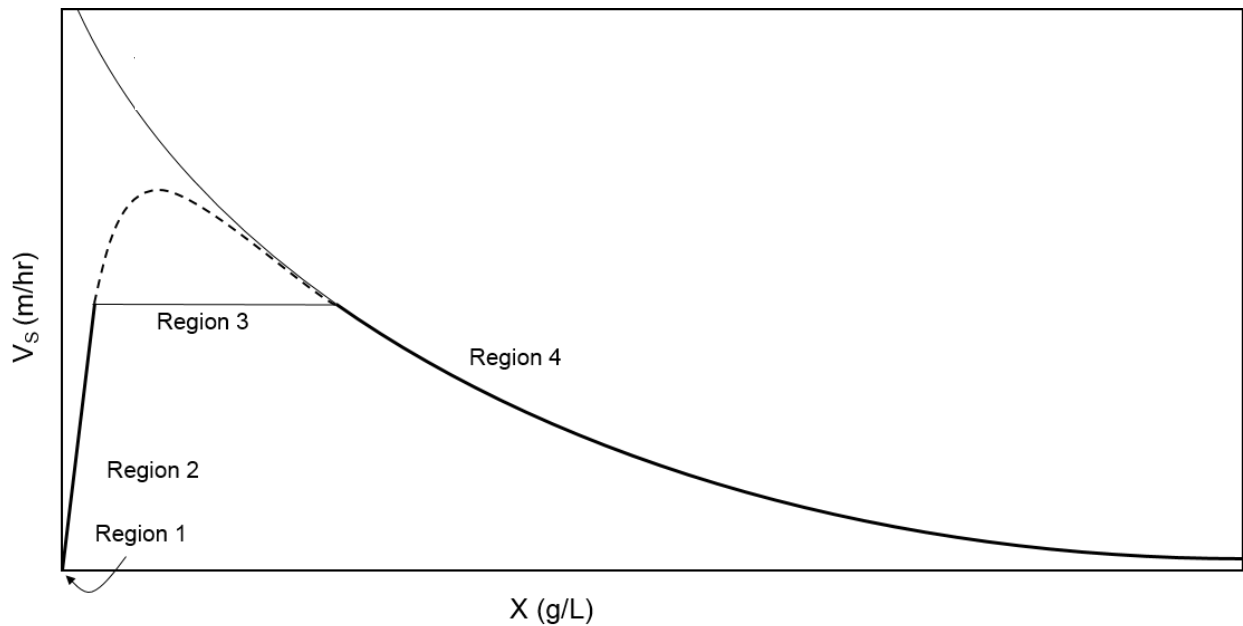


**Figure 2.6 Settling function of Takács et al. (1991) incorporating the settling characteristics of both dispersed and flocculated suspended solids. Extracted from (Mancell-Egala, In Preparation)**

#### 2.5.4 Classification of Settling Rates Tests

Granule quantification tests were developed at DCWater by Mancell-Egala to generate models for better clarifier performance by studying one-dimensional settling in secondary clarifiers. These studies accounted for the settling around the boundary layer between type 3 and type 4 settling, which may display drastic changes in settling velocity.

##### 2.5.4.1 Limit of Stokian Settling

The Limit of Stokian Settling (LOSS) is a recently developed parameter for settling characteristics developed by Abdul Mancell-Egala. This method consists of determining the TSS at which mixed liquor settling transitions from stokian (discrete or flocculent) represented by region 3 in Figure 2.6 to non-stokian (hindered/zonal) settling, represented by region 4 in Figure 2.6. (Mancell-Egala, In Preparation). The LOSS is determined by creating dilutions of ML with varying TSS ranges. The lowest concentration at which no interface is visible is the limit. The results from the LOSS test can determine how good the settleability of sludge is, with a higher TSS value representing good settling sludge, and a lower value representing poor settling sludge. A higher LOSS value increases the area under the curve in region 4 of Figure 2.6, with a higher area under the curve signifying a better settling sludge (Mancell-Egala, In Preparation).

Based on Mancell-Egala's research, it was found that the LOSS concentration for secondary system occurred from 600-700 mg/L, reaching 1000 mg/L for a good settling sludge and 500 mg/L for poor settling sludge. Sludge was also collected from Strass wastewater treatment plant which utilizes hydrocyclones to achieve aerobic granular sludge. Samples were collected from the cyclone underflow and yielded LOSS values of 1600 to 5500 mg/L for low and high values of granulation respectively (Mancell-Egala, In Preparation). Through testing, Mancell-Egala found the a high LOSS value did correlate to good settling and was a viable method in investigating settleability in clarifiers without needing mathematical models.

#### ***2.5.4.2 Surface Overflow Rate***

The SOR test was developed at DC Water to characterize sludge into granular, aggregate, and floc percentages. During this method several surface overflow rates (SOR) are applied to a sample by controlling the settling time over a certain distance (5 cm). The resulting effluent quality under those conditions is determined by measuring the solids concentration in the waste volume. In the batch experiment you simulate SOR in a clarifier by critical settling velocity (CSV). The CSV is the minimum settling velocity a particle should have to travel through a defined zone at a certain time.

When working within CSV working area the following fractions are defined:

- Granules are particles that are remaining in the system at a  $CSV \geq 10$  m/h
- Aggregates are particles that are remaining in the system at a  $CSV \geq 1.5$  m/h
- Floc are solids that need bio-flocculation to settle out at a  $CSV \geq 1.5$  m/h

#### ***2.5.4.3 Threshold of Flocculation***

The threshold of flocculation (TOF) is a measure of the concentration at which discrete settling turns into flocculant settling. This test is used to evaluate the dependence on mixed liquor concentration on the effluent quality and to select the TSS concentration range in which discrete settling is guaranteed (Mancell-Egala, 2014). At the dilution of the threshold of flocculation, the batch time is equal to the settling time when normally batch time is inclusive of flocculation and settling time. As sludge becomes more granular and settles in the discrete settling range, the TOF should decrease. An example of the curve generated by a TOF test can be seen if Figure 2.7A.

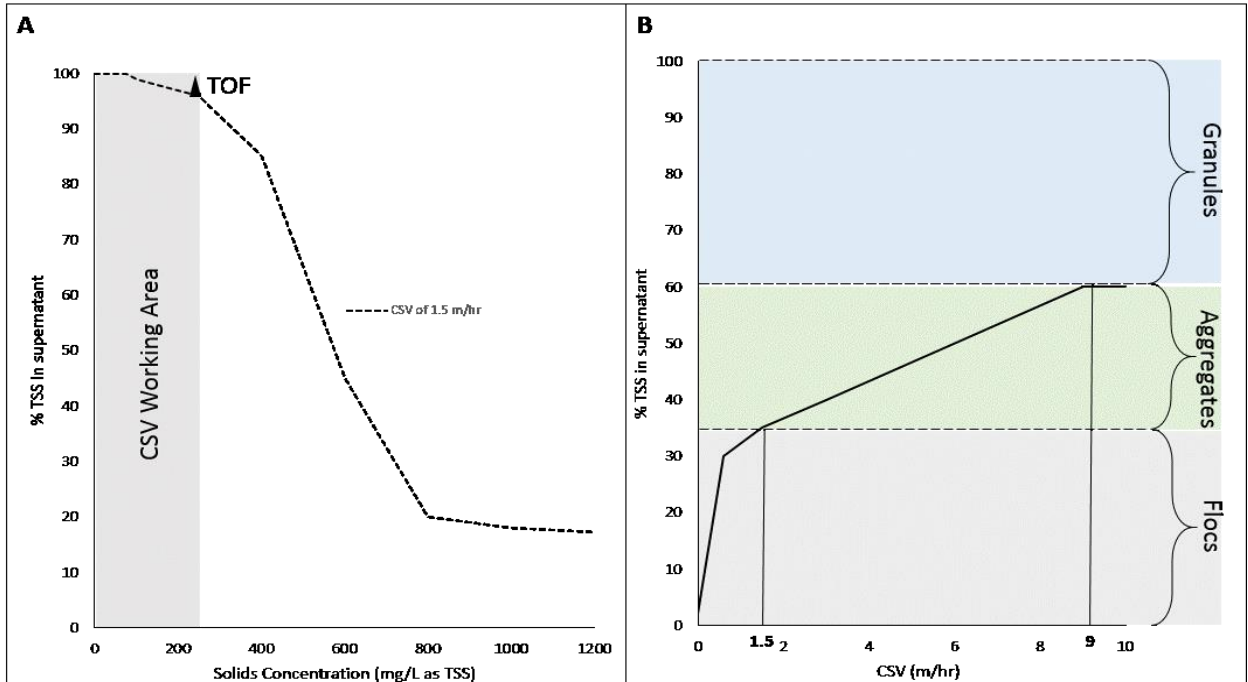


**Figure 2.7 (A) Determination of CSV working area as a region whereby no bio-flocculation occurs (No significant decrease in TSS in the supernatant) Percentage TSS in effluent versus ranging TSS of mixed liquor concentrations at an SOR of 1.5 m<sup>3</sup>/m<sup>2</sup>/h, and the grey area exhibits discrete region. Discrete settling is defined as the initial region that is independent of the MLSS, (B) Conceptual SOR curve with indication of the different solids fractions. Mancell-Egala, A. (2014). *Protocols for Settleability*. Used under fair use, 2015.**

## 3. Methods and Materials

### 3.1 Plant Setup

The entire JR process flow diagram can be seen in Figure 3.1. Influent is sent to the primary clarifier then to the integrated fixed film activated sludge (IFAS) basin composed of 9 aeration tanks which operate in parallel. The first is used for centrate equalization and the other 8 are used as IFAS reactors. Primary effluent mixed with return activated sludge (RAS) is fed into the reactors. The first three cells are anoxic, the fourth is an elongated aeration zone with IFAS plastic biofilm carriers, and the fifth is an additional anoxic zone used to increase nitrogen removal. There is a sixth cell meant for re-aeration, but it is very undersized and is not currently in use. In the aeration tank the IFAS media is filled to 45% of tank volume and coarse bubble aeration is used to keep solids and the media suspended. Media retention sieves are installed to prevent media from exiting the primary aeration zone and to prevent media from entering the nitrified recycle (NRCY) pumping chamber. 18 NRCY pumps are used, 2 in each aeration tank with one placed in the aeration zone and one in the post-anoxic zone and both fed back into the first anoxic cell. The first NRCY pump moves some DO and N into the first anoxic zone. The second anoxic zone is used as a deaeration zone with DO ranging around 2-5 mg/L. In the anoxic zone, 4 axial flow propeller-type mixers are used per each aeration tank, one per each anoxic cell. Additional carbon may be added to the anoxic zones to enhance denitrification. The suspended phase SRT is around 2 days in summer and at a minimum of 4 days in winter.

After the IFAS basin, the ML is then sent to a secondary clarifier with a RAS line which feeds the cyclones. The cyclones split the sludge into a light sludge which is then wasted to the gravity belt thickener (GBT), and then a thickened sludge will be sent through the underflow back to the beginning of the IFAS basin. The waste activated sludge (WAS) line from the secondary clarifier no longer exists and was replaced with the overflow of the cyclone. The solids from the GBT are sent to anaerobic digestion along with the gravity thickened primary sludge. This is then sent to a centrifuge where the biosolids are hauled away and the centrate is sent to the ANITA™ Mox tank and then returned to the primary clarifier. Ferric addition is used before the primary and secondary clarifiers for phosphorus polishing. The secondary clarifiers at JR are shallow, have old peripheral feeds, and have poor flow splits, exacerbating settleability issues.

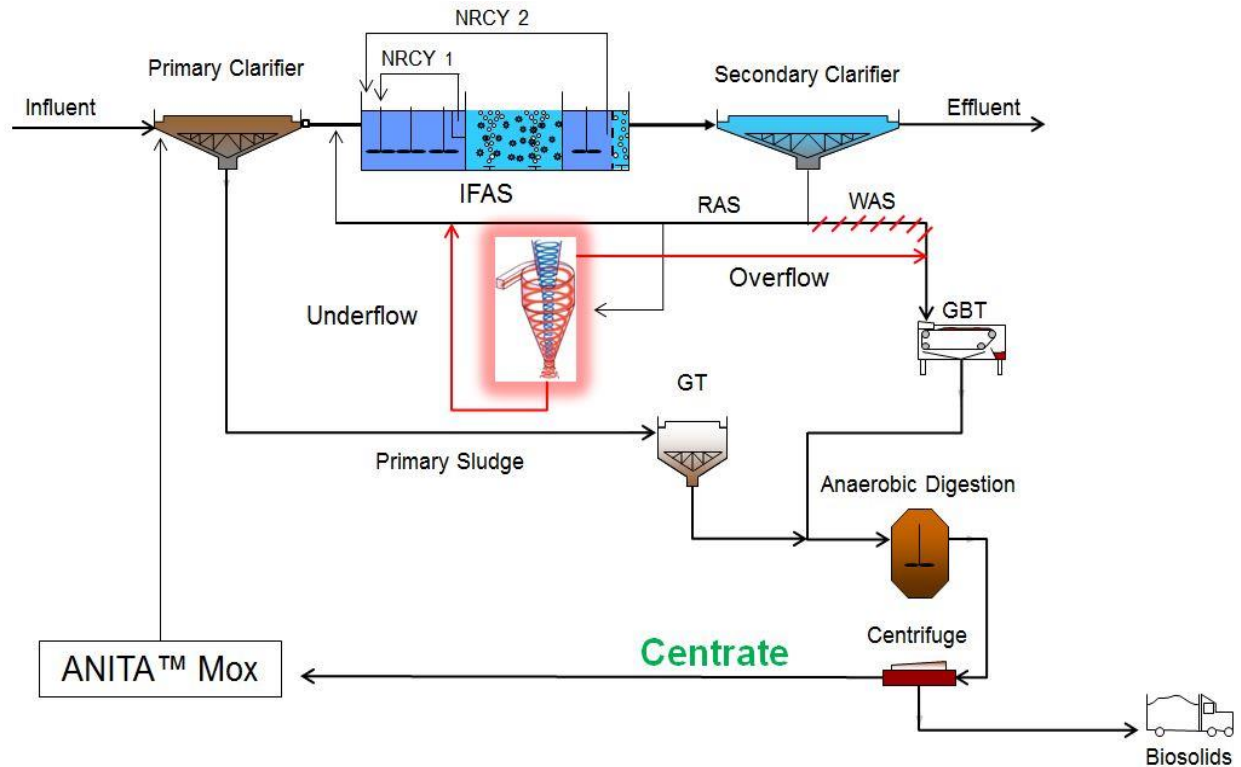


**Figure 3.1 James River IFAS Process Flow Diagram**

A tank 10 ft wide x 12 ft long x 10 ft tall was installed with 8 hydrocyclones placed on one side of the tank for which 2-8 can be operated depending on target waste rate. The tank with hydrocyclones was located in the GBT room, with the hydrocyclones pulling from the RAS line, the overflow being sent to the GBT, and then underflow being sent to the beginning of the IFAS basin. The hydrocyclones used were rated at 88 GPM. The average cyclone flow rate was 75 GPM  $\pm$  3 with either 3 or 4 running at a time to achieve a target wasting rate of 200-300 GPM. The pressure imparted to the cyclones by the pumps was around 23.2 psi, ensuring the pressure applied was maintained within a close range to achieve proper selection. The hydrocyclones received flow from the RAS line with an initial hydraulic split of 80% in the overflow and 20% in the underflow with an equal mass of TSS between the overflow and underflow.

The hydrocyclone control strategy is seen in Figure 3.2. The two pumps feeding the cyclones were controlled through variable frequency drives (VFD) to maintain a pressure of 23.2 psi, which fed into a flow meter and a pressure transmitter. Each cyclone was equipped with an isolation valve to shut the pumps off when the pressure level was too high. There was a level transmitter on the tank to shut off the pumps feeding the cyclone if it were too high and to shut

off the pumps pulling from the tank when too low. The pumps pulling from the tank were also monitored through a VFD, which then fed into flow meters and then the GBT.

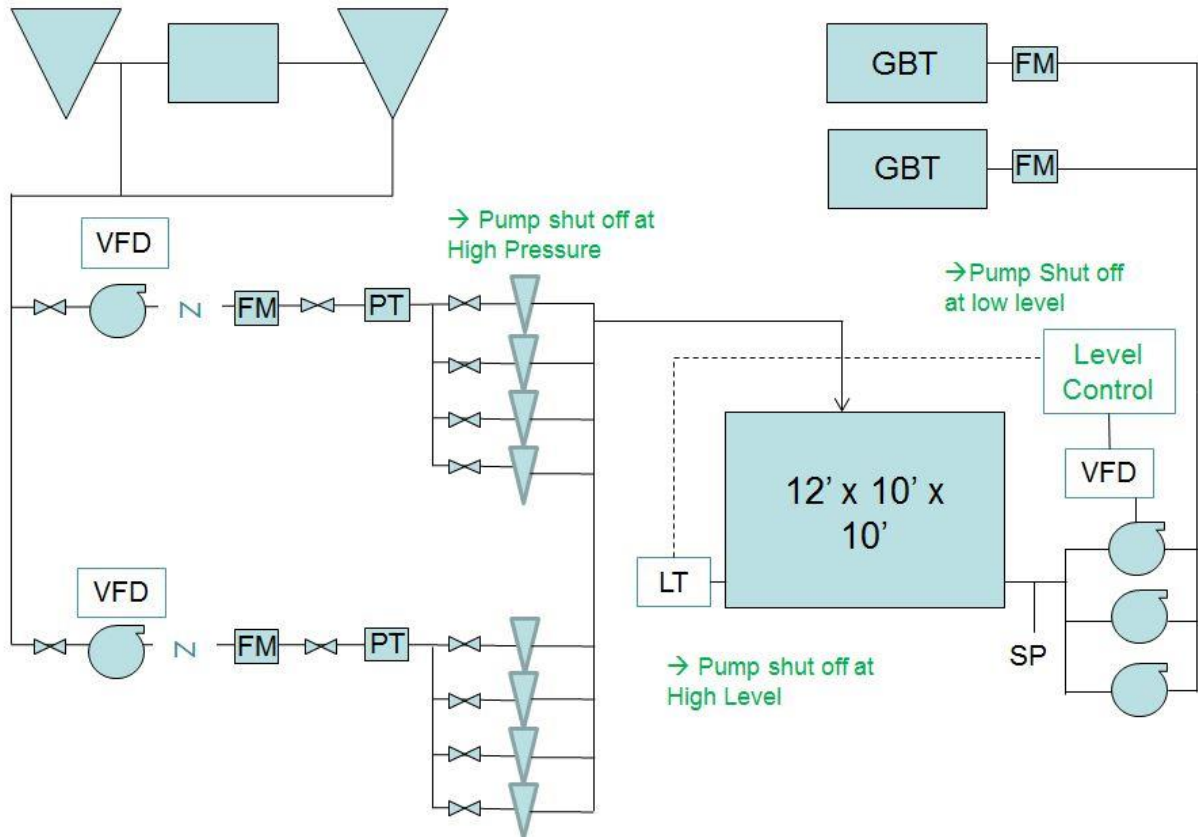


**Figure 3.2 Hydrocyclone Process and Instrumentation Diagram**

### 3.2 Cyclone Data

Samples from the cyclone feed (RAS line), the cyclone underflow, and the cyclone overflow were taken once a week, ensuring enough of each sample was collected for TSS analysis and for an ISV test in a 2 L graduated cylinder. The TSS was first analyzed and then each sample was diluted using filtered tap water to the MLSS of the plant. These diluted samples were then analyzed for their ISV, SSV5, and SSV30. Data was also collected from the Enterprise Data Server (EDS) for the GPM of each pump feeding the cyclones and for the overflow wasting rate in gallon/minute (GPM). This was used to calculate the flow split in the overflow and underflow. Using the TSS and GPM for the cyclone feed, underflow, and overflow the mass split in the overflow and underflow was calculated in two ways; as a percentage of the cyclone feed mass, and also as a percentage of the summed mass of the overflow and underflow as seen in Eq. 16 and Eq. 17.

$$\frac{lbs}{day} = TSS \left( \frac{mg}{L} \right) \times GPM \times 8.34 \times 10^{-6} \left( \frac{lbs * L}{gal * mg} \right) \times 60 \left( \frac{min}{hr} \right) \times 24 \left( \frac{hr}{day} \right) \quad \text{Eq. 15}$$

$$\text{Mass Split by feed \%} = \frac{\text{Sample} \left( \frac{lbs}{day} \right)}{\text{Feed} \left( \frac{lbs}{day} \right)} \times 100 \quad \text{Eq. 16}$$

$$\text{Mass split by summed mass \%} = \frac{\text{Sample} \left( \frac{lbs}{day} \right)}{\text{Overflow} \left( \frac{lbs}{day} \right) + \text{Underflow} \left( \frac{lbs}{day} \right)} \times 100 \quad \text{Eq. 17}$$

For continuing data collection, fresh samples will be taken after TSS analysis to prevent denitrification in samples sitting while TSS is being run, which takes 1-1.5 h. Also, SCE will be used for dilution rather than filtered tap water.

### 3.3 Plant Data

Plant data was collected from the James River plant operating reports beginning January 2011 when the IFAS reactor was fully implemented. Data was collected 3 days per week for MLTSS, RAS TSS, SRT, SVI5, SVI30, Fe dosage, influent TP, effluent OP, and effluent TP. Filament data were provided according to the filament index (FI) scale (0: none, 1: few, 2: some, 3: common, 4: very common, 5: abundant, 6: excessive).

### 3.4 Sludge Volume Index (SVI)

The SVI can be used to monitor settling characteristics of activated sludge and may be used for process control. SVI5 and SVI30 were performed according to 2710C Standard Methods.

$$SVI = \frac{\text{settled sludge volume} \left( \frac{mL}{L} \right) \times 1000}{\text{suspended solids} \left( \frac{mg}{L} \right)} \quad \text{(Rice, 2012)} \quad \text{Eq.18}$$

The SVI is determined by placing a well-mixed ML sample in a 2-L graduated cylinder with volumetric markings. Once 30 minutes has passed, the interface between the settled sludge and supernatant is measured using the volumetric markings in mL/L to obtain the settled sludge volume (SSV). The SVI is calculated as seen in Eq. 18. SVI5 and SVI30 values were obtained for the cyclone underflow, cyclone overflow, RAS, ML, ML dilutions, and ML concentrations. These values were tracked over time and compared to other parameters to characterize improvements in settleability.

### 3.5 Zone Settling Velocity

Settling is done at multiple concentrations; the original ML sample, 3 concentrations diluted below, and 3 concentrations above the MLSS concentration. Concentrated mixtures were achieved by allowing ML to settle and removing supernatant, then adding additional mixed liquor. When diluting the ML, secondary effluent was used to ensure similar ionic characteristics. The MLTSS was analyzed for only one of these concentrations. This TSS value was used to calculate the varying TSS concentrations of the dilutions and concentrations, as these were simply ratios of the raw mixed liquor. The zone settling velocity was also determined for the cyclone feed (RAS), underflow, and overflow, initially diluting the samples to 3000 mg/L to represent the MLTSS concentration of JR wastewater. The cyclone sampling points were later diluted to 2000 mg/L starting April 22<sup>nd</sup>, 2015 to better represent varying JR MLTSS values, and then on June 3<sup>rd</sup>, 2015 were again adjusted to 2500 mg/L dilutions for the most accurate result. These cyclone sampling point ISVs were plotted against ML ISV values to see how settling velocities were improving over time in the ML.

A 2 L settling column was used with a calibrating tape to represent distance in mm, while the column measurements are conventionally volumetric. The sludge sample was mixed thoroughly and poured into the cylinder while simultaneously starting a timer. The height of the solid-liquid interface was recorded for time intervals of 30 s to 1 min for 30 minutes to observe a constant zone-settling velocity. Once the rate of settling decreases, data collection ceased. Plots were generated with interface height in cm vs. time in minutes, drawing a linear line through the linear portion of the curve where settling rate is highest, corresponding to type III, or hindered settling velocity. The settling rate is recorded as the slope of this line in units of m/hr.

### 3.6 Solids Flux

The solids flux was determined by creating multiple dilutions and concentrations of JR ML ranging from 0.7-4 g TSS/L and creating ZSV curves. The dilutions were made using ML collected from the aeration effluent and diluting with filtered tap water which was assumed to have a TSS of 0 g/L. For each test, a ZSV curve was created for the original ML sample, 3 dilutions below the MLTSS value, and 3 concentrations above the ML value for a total of 7 curves.

## 3.7 Classification of Settling Rates

### 3.7.1 Limit of Stokian Settling (LOSS)

The limit of stokian settling (LOSS) must first be determined before the SOR test can be performed. A large amount of mixed liquor was collected at a point just before entering the secondary clarifier. The dilutions were produced between the ranges of 250 mg TSS/L and 1000 mg TSS/L with a maximum gap between dilutions of 100 mg TSS/L. These diluted concentrations were filled to the 2 L mark in settleometers and left to settle for less than a minute. The lowest concentration at which no interface was visible was the limit. To find the minimum ratio in which the interface was no longer visible, more dilutions between the concentrations where no interface was visible and where an interface was visible were made. After creating more dilutions between these two values, a more accurate value for the LOSS was obtained. This limit was given as a concentration in mg/L.

### 3.7.2 Threshold of Flocculation (TOF)

The threshold of flocculation (TOF) is a measure of the concentration at which discrete settling turns into flocculant settling. This test was used to evaluate the dependence of mixed liquor concentration on the effluent quality and to select the TSS concentration range in which discrete settling is guaranteed (Mancell-Egala, 2014).

At least 25 L of mixed liquor was collected at a point just before entering the secondary clarifier, ensuring it was maintained at a constant temperature. The concentration of this mixed liquor was used as the highest concentration and was then diluted multiple times with tap water to create multiple varying concentrations (~6-8) of mixed liquor, covering concentrations ranging from 200-800 mg/L. 5 L of each concentration was made; 4 L to be used for settling and the excess to be analyzed for TSS. Each concentration was then be poured into a 4 L graduated cylinder to the fill line, then poured through a funnel into a 4 L graduated cylinder with ports to provide mixing. The funnel was pulled as soon as the liquid reached the 4 L fill line, and the timer was started simultaneously. The dilution was left to settle for 2 minutes equating to a CSV of 1.5 m/hr. At the 2 minute mark the clamps were opened so that the supernatant may be decanted off the top through the tubes. The supernatant collected was then analyzed for TSS. 10-20 mL of liquid was filtered for TSS, and duplicates were run for every concentration. Once the TSS was collected for all concentrations, a graph was generated with the solids concentration on the x-axis and the % solids in supernatant (Eq. 19) on the y-axis.

$$\% \text{ Solids in Supernatant} = \text{TSS}_{\text{initial}} - \left( \text{TSS}_{\text{diluted}} / \text{TSS}_{\text{initial}} \right) * 100 \quad \text{Eq. 19}$$

The point at which line becomes linear is the minimum value of the solids concentration at which flocculation occurs, or the TOF (the line should be S-shaped). The TOF was used as the concentration in the SOR test. The SOR test uses one concentration over a period of different settling times. The TSS range for which the fraction in effluent is independent of the sludge mixture (beginning of the curve) is also the highest concentration where this is the true TOF. The latter range is the range of discrete settling and is the target TSS range for SOR tests

Using the ratio obtained from the LOSS test, dilutions should be made with one concentration being much higher than the LOSS, one at LOSS value, and then multiple concentrations at ratios lower than LOSS down to a TSS of 100 mg/L when determining the TOF.

### 3.7.3 Surface Overflow Rate (SOR)

To conduct the SOR test, a 4 L plastic graduated cylinder with ports 5 cm below the 4 L fill line must be made for decanting supernatant out of the top portion of the cylinder once the mixed liquor has settled. The ports are located on opposite sides of the cylinder 5 cm below the 4 L fill line. Each port is composed of a bulkhead fitting in which plastic tubing is attached. To prevent liquid from flowing through the tubing, tubing clamps are fitted as close to the bulkhead as possible. The tubing on both sides of the cylinder should be long enough to reach a device used for collecting the sample.

A 4L graduated cylinder with no ports is used for filling mixed liquor to the 4 L fill line. Before measuring out 4 L of liquid in the graduated cylinder, the mixed liquor must be stirred to ensure proper mixing. Once 4 L is measured, some settling may have occurred, so the liquid is poured from the initial graduated cylinder into the graduated cylinder with the port via a funnel placed on top to provide adequate mixing. The timer set for the predetermined settling time is started as soon as the liquid is filled and funnel is simultaneously removed. After it has settled for the predetermined amount of time, the clamps will be opened, allowing the supernatant to decant out of the top 5 cm of the graduated cylinder. The supernatant is then analyzed for TSS.

The concentration obtained as the TOF is used for this test. A large batch of this concentration is made using mixed liquor which is collected from a point just before the secondary clarifier and diluting it with tap water. The batch is stirred, poured into a 4 L graduated cylinder, and then funneled into a 4 L graduated cylinder with ports to provide mixing. The test is run for settling time periods of 20 s, 1 min, 2 min, 3 min, and 5 min, and then the supernatant decanted. TSS is then analyzed for the supernatant of each sample and for the original TOF mixture. A plot is then generated with the surface overflow rate on the x-axis, and the % solids in supernatant (Eq. 20) on the y-axis, creating a histogram of the flocs. This characterizes the % of the sludge that has good, medium, or poor settling based on the surface overflow rate.

The surface overflow rate is calculated as the distance of settling over the time period, the distance being 5 cm and the time periods ranging from 20 s to 5 min.

$$\% \text{ Solids in Supernatant} = \text{TSS}_{\text{initial}} - \left( \text{TSS}_{\text{diluted}} / \text{TSS}_{\text{initial}} \right) * 100 \quad \text{Eq. 20}$$

### 3.8 Floc Density

The floc density of the ML at JR was measured routinely as it was expected to increase as the sludge became more granular. Methods for the test were adapted from the 1985 GE Healthcare and Life Sciences manual on Cell Separation Media (GE Healthcare and Life Sciences, 1985). The density of the floc was measured using Percoll isopycnic centrifugation, the particles were separated based solely on differences in density, irrespective of size. A Stock Isotonic Solution (SIP) was created using 1.5 M NaCl, Percoll, and distilled water. Percoll is a high density (1.13 g/mL) solution with silica particles and a low osmotic pressure. To create the SIP, the desired osmolality was determined by measuring the osmolality of the ML at JR. The density of the SIP could be adjusted by changing the amount of NaCl in the solution. Calculations for determining the SIP can be seen in Appendix F. An SIP batch was composed of 47.15 mL Percoll, 15 mL 1.5 M NaCl, and 37.85 mL distilled water. Using a high speed centrifuge, 2 16 mL tubes, density gradient beads, and the SIP, a density gradient was made within the tubes. One tube was to show the density gradient of the beads, which composed of 6 different bead colors ranging from 1.025-1.130 g/mL. These densities were expected to bracket the density of the ML floc. The beads created a distinct line within the tube, representing increasing density moving downwards. The other tube was used for showing the floc density of the ML.

The high-speed centrifuge was set to 22°C. Initially, the 16 mL tubes were both filled with 14 mL of SIP. 2 µL of each bead type added to one tube. Both tubes were then centrifuged at 15,000 G for 30 min. Banding was not clearly defined, and beads were disturbed easily as they were pulled from the centrifuge. To increase clarity of the density gradients, the run time in the centrifuge was increased. After 3 attempts with an initial centrifuge run of 1 hour, the band formed by the beads within the tube was not as defined as would be desired, so the initial centrifuge run time was increased to 1.5 hr. The 16 mL tubes were also filled to 14.5 mL and 15.5 mL of SIP to reduce amount of air space in the tube, reducing the disturbance in the tube when being removed from the centrifuge. The tube filled with 14.5 mL SIP allowed for 1 mL of ML to be added after the density gradient was formed in the initial 1.5 hr centrifuge run. After the ML was added, the tubes were centrifuged again at 400 G for 15 min. and then removed from the centrifuge to be photo analyzed for band height and floc height within tube. The density of the floc was interpolated based on the measurements in the two tubes. Results from this test are highly precise as the solution increments are fairly narrow relative to the biomass densities.

### **3.9 Filament Quantification and Identification**

Samples of ML collected from the aeration effluent were sent periodically to Paul Pitt of Hazen and Sawyer for microscopic analysis.

### **3.10 PAO Activity Tests**

The biological phosphorus activity test is a bench-scale phosphate uptake and release test adapted from the WERF 2010 study (Neethling, 2005). This test measures the anaerobic phosphorus release rates, anaerobic COD uptake rate, anaerobic phosphorus release to COD uptake rate ratio, and aerobic phosphorus uptake rates to evaluate biological phosphorus removal. ML used for this test was collected from the aeration effluent and aerated for approximately 1 hour to remove excess ammonium. The sample was then put into a 2 L settleometer which was placed into a water bath set to the plants current temperature while being continuously mixed using stir bars and stir plates. As soon as the sample was placed in the water bath, an initial sample was collected to be analyzed for TSS and TVSS. The beaker was then covered to reduce aeration to 0 mg/L for 10 minutes to allow the sample to acclimate. Then 100 mg/L COD (10 mL NaAc per 2 L) was added to the beaker and it was stirred and mixed for 90 minutes. The preliminary phosphorus uptake period then starts by aerating the samples and monitoring the pH and DO levels. Once the DO reached 2 mg/L, an initial sample was collected to be filtered and analyzed for NH<sub>4</sub><sup>+</sup>, NO<sub>3</sub><sup>-</sup>, and NO<sub>2</sub><sup>-</sup> using HACH tubes to ensure all concentrations were <2 mg/L,

otherwise the test would provide inaccurate results. If all initial HACH tubes were  $<2$  mg/L, 4 mL Potassium Phosphate ( $K_2HPO_4$ )<sup>-</sup> was added and then the sample was aerated for 2 hours, recording pH and DO every 15 minutes. After 2 hours, a sample was taken and analyzed for OP,  $NH_4^+$ ,  $NO_3^-$ ,  $NO_2^-$  and sCOD; pH and DO. The air was then turned off for the anaerobic phosphorus release and COD uptake period. The beakers were covered and sparged with  $N_2$  gas to bring DO to 0 mg/L. The pH range of 6.8-7.5 was controlled by sparging with  $CO_2$  when pH levels were too high. As DO reached 0 mg/L the beakers were covered, the  $N_2/CO_2$  gas was turned off, and 100 mg/L COD (10 ml NaAc stock) was added to the beaker. Immediately a sample was taken and analyzed for OP,  $NH_4^+$ ,  $NO_3^-$ ,  $NO_2^-$ , sCOD, pH and DO. This was repeated every 3 minutes for 15 minutes, and then every 15 minutes for an hour. The beakers covers were then removed and air turned back on for the aerobic phosphorus uptake period. As soon as the DO reached 2 mg/L, a sample was taken every 15 minutes for an 1.15 hr and analyzed for OP,  $NH_4^+$ ,  $NO_3^-$ ,  $NO_2^-$ , pH and DO. Hach tubes were read using a DR 2800™ Spectrophotometer.

As of August 5<sup>th</sup> 2015, DPAO activity measurements were taken. DPAO activity was measured by altering the existing biological phosphorus activity test to include an anoxic phase in addition to an aerobic uptake phase. During what would usually be the aerobic phase, the system was kept unaerated and 20 mg/L of  $NO_3^-$ -N was added. The duration of the test was performed similarly; a sample was taken every 15 minutes for an 1.15 hr and analyzed for OP,  $NH_4^+$ ,  $NO_3^-$ ,  $NO_2^-$ , pH and DO. ML was measured using the original biological phosphorus activity test with the anaerobic and aerobic phases in addition to the altered DPAO activity test with anaerobic and anoxic phases. The results from this test provided data showing how much biological activity was due to PAO or DPAO, as normal PAO take up phosphorus during aerobic conditions and DPAO take up phosphorus in anoxic conditions.

### 3.11 AOB and NOB Activity Tests

In order to measure AOB and NOB activity rates a 2 L sample was collected from the cyclone feed, underflow, and overflow. The sample was aerated for 30 minutes to oxidize any excess COD in order to prevent heterotrophic competition for  $O_2$ . The 2 L container was then spiked with 20 mg/L  $NH_4^+$ -N (dissolved ammonium chloride solution) and 5 mg/L  $NO_2^-$ -N (dissolved sodium nitrite solution). The mixture was sampled continuously for 1 hour at 15 minute intervals using a 50 mL syringe. All collected samples were filtered through 0.45  $\mu$ m nylon filters and analyzed for  $NH_4^+$ -N,  $NO_2^-$ -N, and  $NO_3^-$ -N.

During the test mixing was provided by a magnetic stir bar. Temperature was controlled via submersion in a water bath. Air flow was diffused through a porous aeration stone. The dissolved oxygen was maintained between 2.5 and 4 mg O<sub>2</sub>/L. Sodium bicarbonate was added to maintain pH at approximately 7.50 and a CO<sub>2</sub> sparge was used for pH reduction. The AOB rates were calculated as the slope of the NO<sub>x</sub>-N production and NOB rates were calculated as the slope of the NO<sub>3</sub><sup>-</sup>-N production.

### 3.12 Tank Profiling

Multiple points along the IFAS reactors, the RAS line, the primary clarifier effluent, and the final effluent are sampled and filtered immediately. The samples were analyzed for NH<sub>4</sub>, NO<sub>3</sub>, NO<sub>2</sub>, PO<sub>4</sub>, using reagent kits (Hach Inc., Methods 10031, 10206, NS 10207, and 8048 respectively) as described in Standard Methods (2012). Measurements for pH, DO, and temperature were also recorded as each sample was taken. A figure of the IFAS basin can be seen in Figure 3.3.

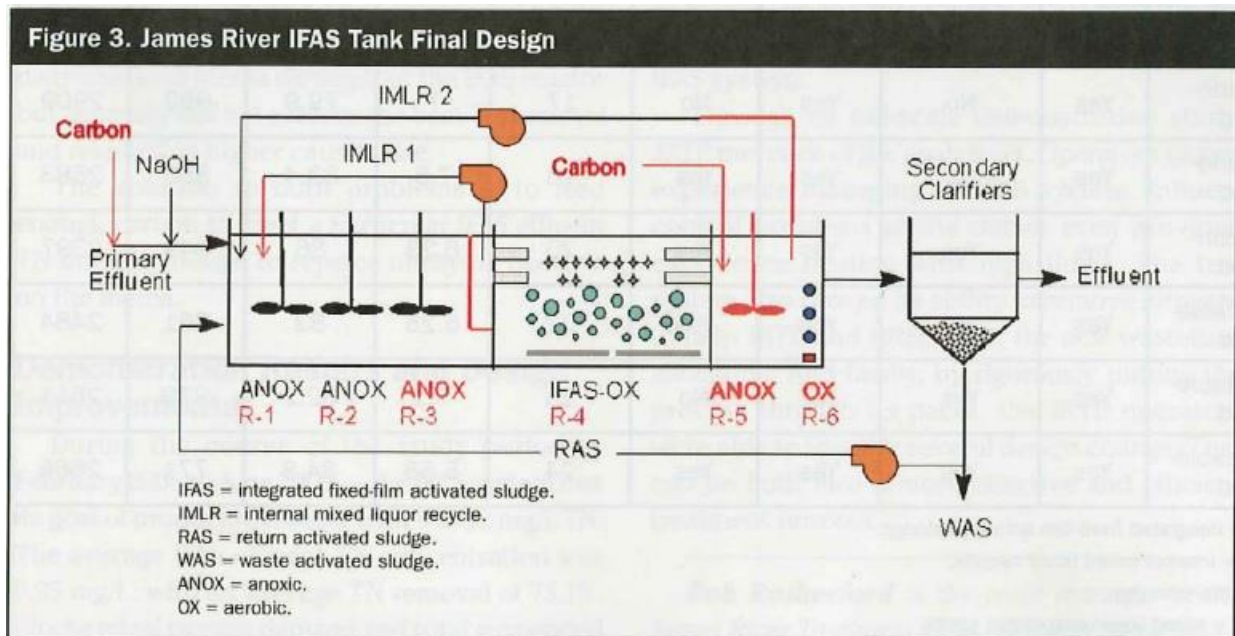


**Figure 3.3 James River IFAS Tank Design**

## 4. Results and Discussion

### 4.1 Cyclone Data

The hydrocyclones were installed on March 2<sup>nd</sup> 2015 where the smallest nozzle size was installed on the cyclone. On March 5<sup>th</sup> 2015 the 2<sup>nd</sup> largest nozzle was installed on the cyclones. Then on May 11<sup>th</sup> the largest nozzle size was put in, increasing the flow and mass split in the underflow, which can be seen in table 4.1. The nozzle size installed on the cyclones affects the percentage of flow being directed to the underflow. The desired flow split in the cyclones was 20% in the underflow and 80% in the overflow. The second largest nozzle size created an average hydraulic flow split of 94% in the overflow and 6% in the underflow. The mass split in the underflow was determined to be about 8% in the underflow. Once the largest nozzle size was installed the hydraulic flow split in the underflow increased to an average of 17.2% and achieved a mass split of about 21-22% in the underflow. Specific values for the flow split in the overflow and underflow for the two nozzle sizes can be seen in Table 4.1.

**Table 4.1 Flow and Mass Split of Cyclone Underflow and Overflow for different nozzle sizes**

Nozzle	Averages					
	Flow Split %		Mass Split by feed %		Mass Split by sum %	
	over	under	over	under	over	under
<b>2nd Largest</b>	94.0	6.1	88.3	8.0	91.6	8.4
<b>Largest</b>	82.8	17.2	84.3	22.0	79.3	20.7

### 4.2 SVI

The SVI5 and SVI30 are shown in Figure 4.9. A slight decrease in SVI5 values can be seen but SVI30 has stayed consistent over time. A decrease in SVI is desired for increased settleability. The average SVI5 was 292±28 mL/g during the pre-cyclone period in 2015 and decreased to an average of 248±21 mL/g during the cyclone optimization and cyclone operation period. The average SVI30 was 142.4±14 during the pre-cyclone period, 129.8±12 during the cyclone optimization period, and then increased to 144.1±11 during the cyclone operation period. The EMWWTP found no decrease in SVI while utilizing hydrocyclones although the Strass WWTP experienced a decrease in SVI with no seasonal upsets. Similarly to EMWWTP, JR may be experiencing stabilization in SVI as a result of the hydrocyclones. The lack of SVI improvement may also be due to the short period in which the cyclones were fully operational. Other data such

as the ISV of cyclone points and the increased granule percentage in the mixed liquor within the last 2 months of the study may suggest that the SVI would improve given more time.

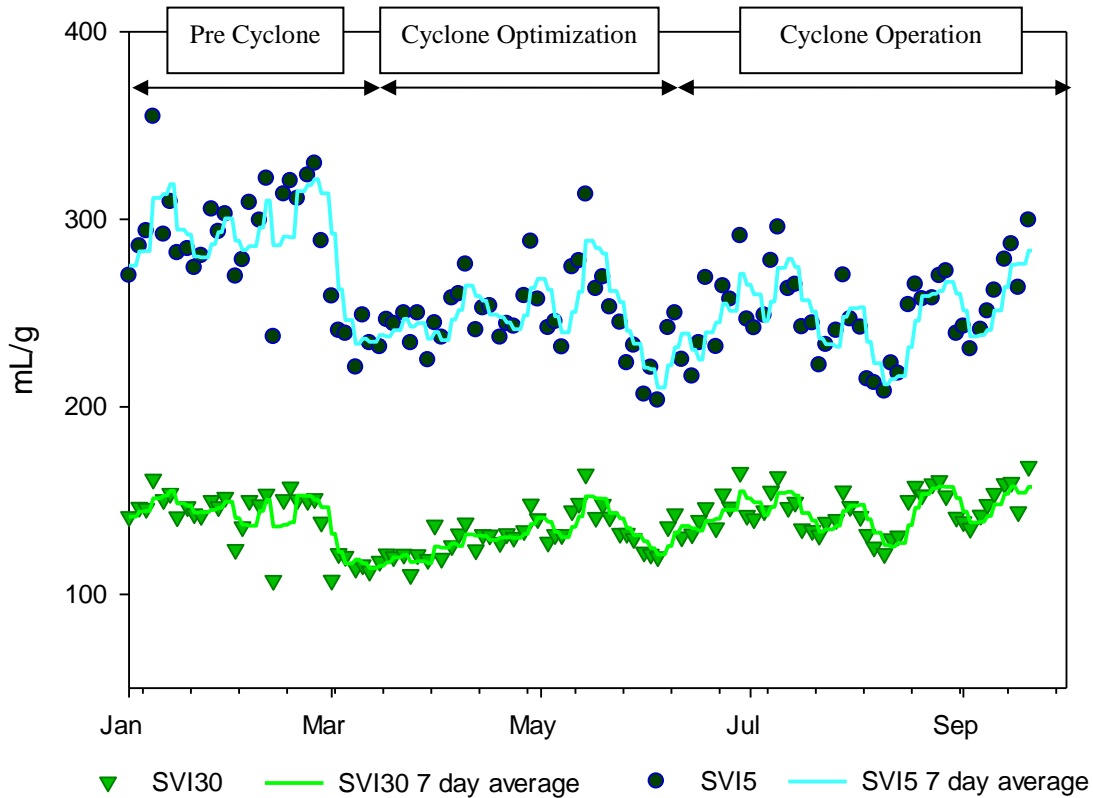


**Figure 4.1 2015 SVI5 and SVI30 of JR**

### 4.3 Solids Flux

The settling velocity curves shown in Figure 4.10 are representative of solids flux tests that were run on the aeration effluent during the pre-cyclone period, cyclone optimization period, and cyclone operation period. Actual data collected from solids flux tests is shown as points and the curves are best fit lines to this data based on the Vesilind equation. An increase in settling velocity can be seen from the pre cyclone period to the cyclone optimization period, and then again from the cyclone optimization period to the cyclone operation period. In Figure 4.11 the SFg data is shown for the pre cyclone, cyclone optimization, and cyclone operation period. Actual data is shown as points while the curves represent the calculated Vesilind velocity multiplied by the MLSS concentration to obtain SFg curves. A clear increase is seen in the SFg for a given MLSS from the pre cyclone to cyclone optimization period, and then an ever larger

increase from the cyclone optimization period to the cyclone operation period. The solids flux displays dramatic changes when there are only slight differences in the sludge settling characteristics, which is why the solids flux data shows such a sharp increase even though the SVI5 only improved slightly and the SVI30 did not improve at all.

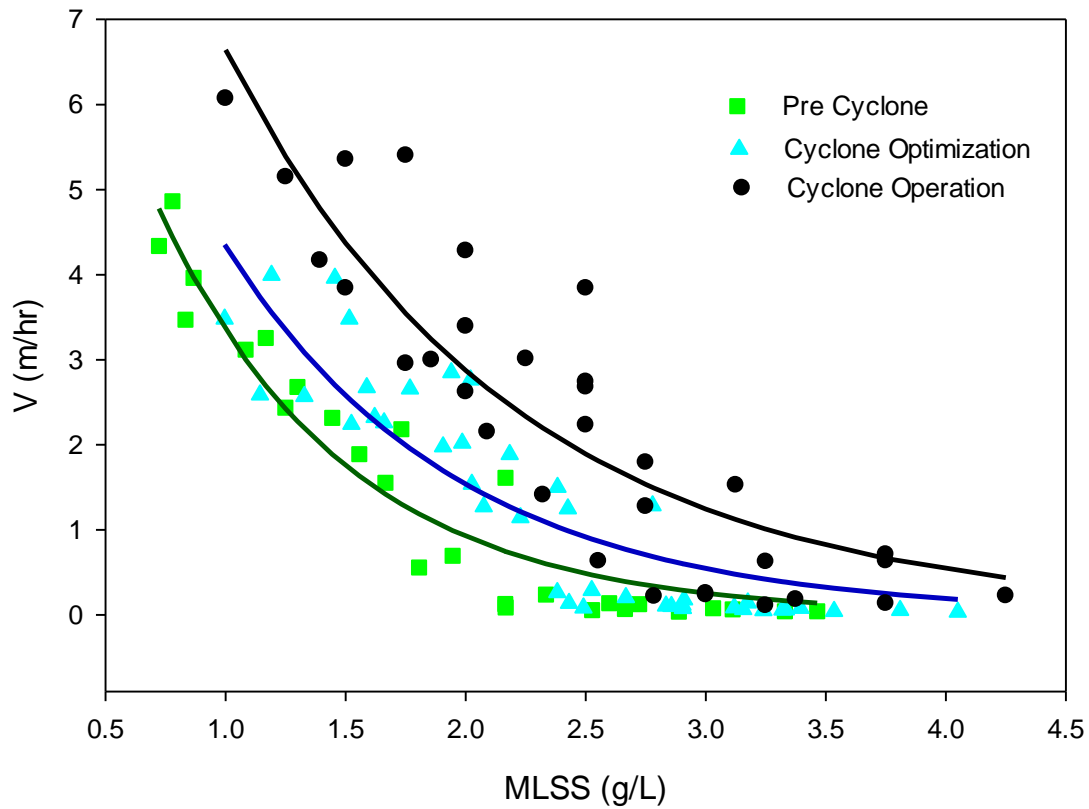


**Figure 4.2 Pre- and Post-Cyclone Settling Velocity determined by SFA and the best fit Vesilind Curve**

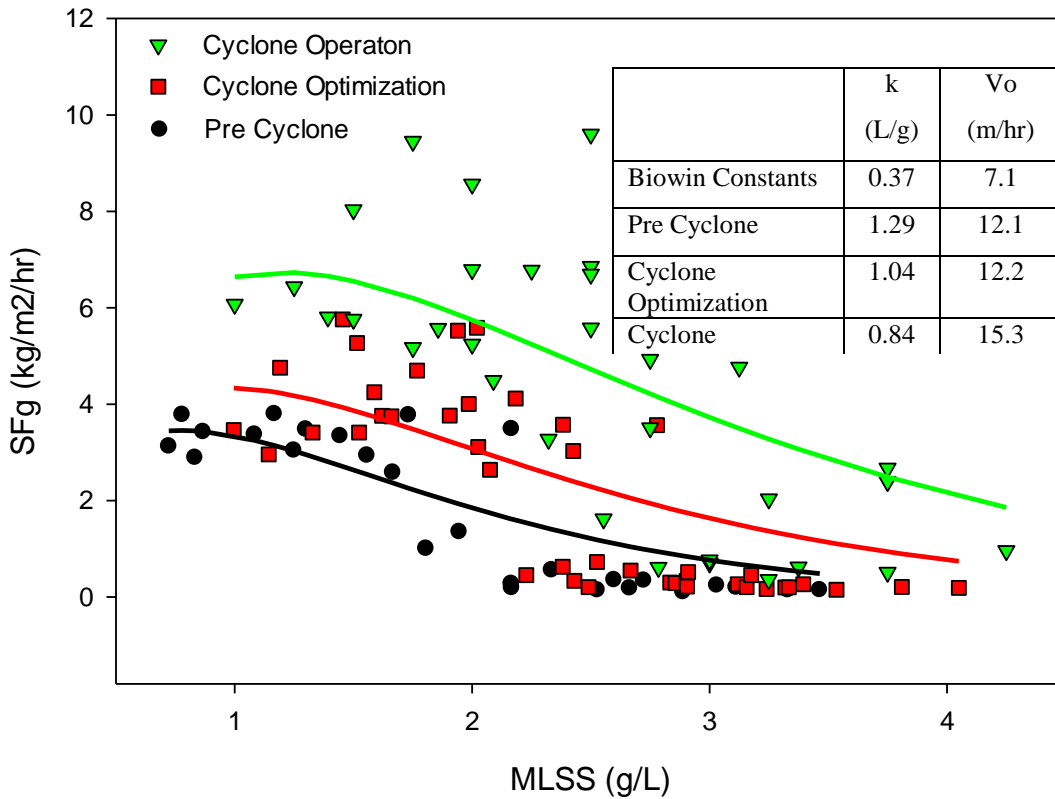


**Figure 4.3 SFg curves pre and post cyclone installation. Calculated SFg curves using the Vesilind settling velocity are shown as curves, actual data shown as points.**

The Vesilind parameters ( $k$  and  $V_0$ ) were determined for this study from the Vesilind equation. This equation is based on the solids flux theory and is a semi-logarithmic expression relating the solids MLSS concentration and the ISV.  $k$  and  $V_0$  are constants of this equation representing settling characteristics. Vesilind parameters calculated from solids flux procedures can be found in Figure 4.3. The Biowin constants for the Vesilind parameters are 0.37 L/g for  $k$  and 7.083 m/hr for  $V_0$ . A smaller  $k$  value represents a better settling sludge. A larger  $V_0$  value represents better settling sludge and a clear increase in  $V_0$  was seen in this study.  $V_0$  values during the pre-cyclone period ranged from 10.14-14.89 m/hr and during the cyclone optimization and cyclone operation periods ranged from 15.00-30.50 m/hr. The averages in the Vesilind parameters show an increase in  $V_0$  from the pre-cyclone to cyclone optimization and then again to the cyclone operation period. A decrease in the  $k$  value was also seen over these periods. This significant increase in the  $V_0$  should result in increased settling in the ML over time.

#### 4.4 Settleability

Figure 4.4 provides the ISV of the cyclone feed, underflow, and overflow all adjusted to 2500 mg/L. The data shown is only representative of the period when the cyclones were under full operation. Cyclone overflow, underflow and feed and the aeration effluent were originally adjusted to 3000 mg/L when calculating the ISV to compare all samples as this was close to the MLSS concentration of James River. Beginning April 22, 2015, all samples were adjusted to 2000 mg/L as this better matched the MLSS concentration at the time. Then on June 3<sup>rd</sup> 2015 the samples were all adjusted to 2500 mg/L, again because this better matched the MLSS concentration.

Figure 4.4 does not show an increase in the ISV in the cyclone feed which is desired as it is representative of the mixed liquor settling velocity. The important thing to note is the large difference of the underflow and overflow settling velocity, showing the system selects for solids settling at a higher rate. The cyclone feed had an average ISV of  $1.5 \pm 1.1$  m/hr, the cyclone underflow had an average ISV of  $2.5 \pm 1.3$  m/hr and the cyclone overflow had an average ISV of  $0.5 \pm 0.7$  m/hr.

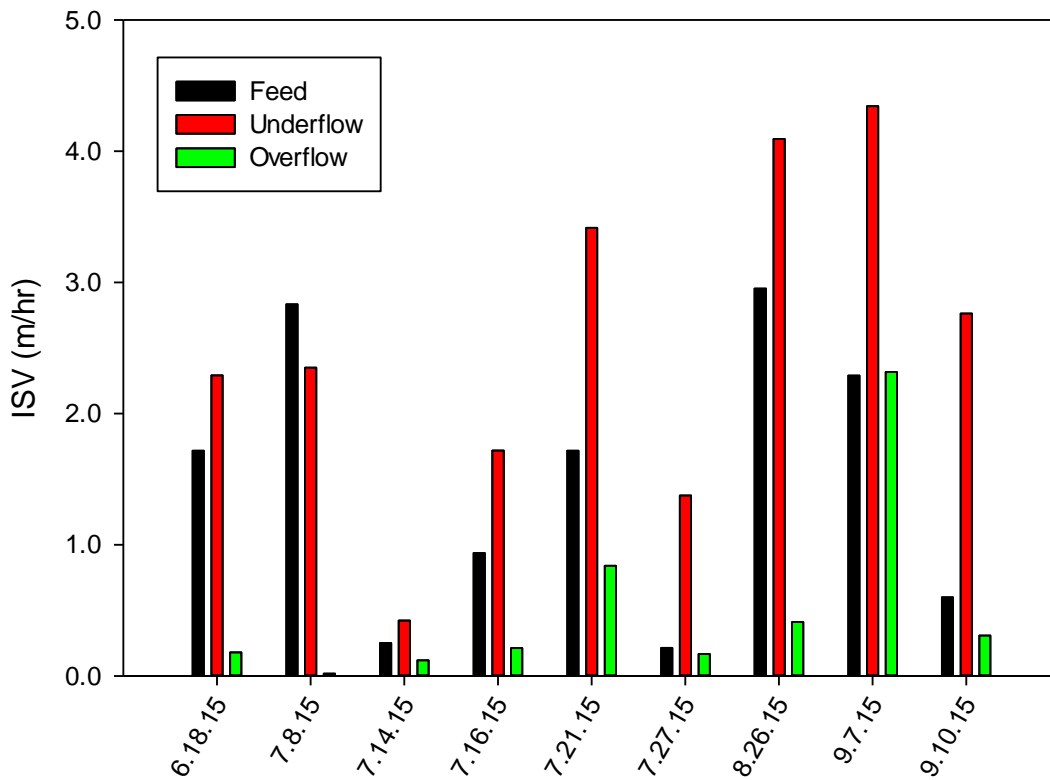
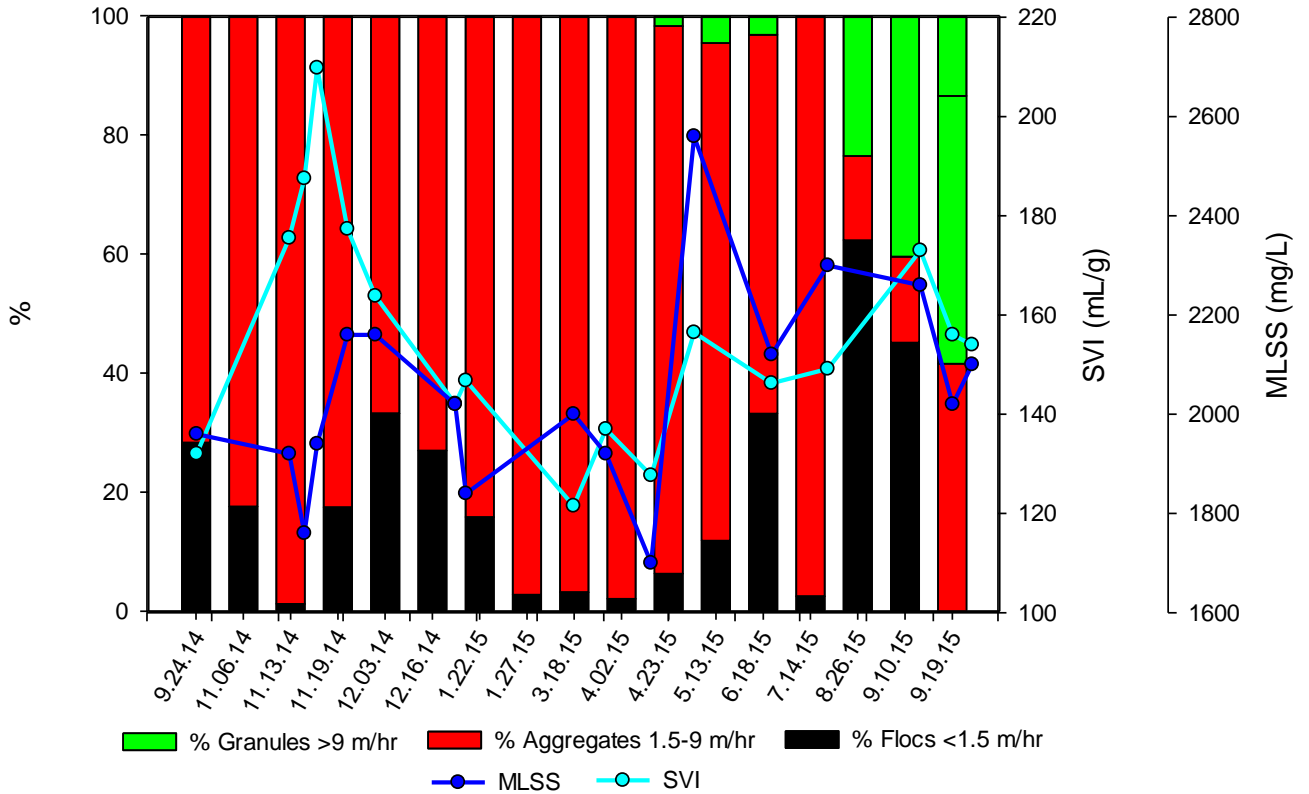


Figure 4.4 ISV of Cyclone Points adjusted to 2500 mg/L

#### 4.5 Classification of Settling Rates

In Figure 4.5 the percentages of granules, aggregates, and flocs in the mixed liquor is presented over time as determined by discrete settling. It is apparent that there is no granule percentage until April 23<sup>rd</sup>, 2015 during the cyclone optimization period where the percentage reached only 1.7%. During the cyclone operation period percentages of granules reached high values of 23.5% and 40.4%. An increased granule percentage is desired for creating a balance of flocs and granules. The aggregate percentage decreased over time while the floc percentage increased, although neither followed an exact trend. However within the last three testing periods from August 26<sup>th</sup>, 2015 to September 19<sup>th</sup> 2015 the aggregate percentage ranged from 14.1-45.0% when it had previously had an average of 84.8%. The aggregate percentage was the majority of the floc characterization during pre-cyclone and cyclone optimization periods averaging 85.6±11% and decreasing to 46.9±35%. The floc percentage within the last three testing periods increased to a range of 41.5-62.3% when previously it had an average of 14.4%. The floc fraction showed a large increase from the pre-cyclone and cyclone optimization to the cyclone operation period with averages increasing from 13.9±11% to 36.9±22%. It is unclear why the aggregate percentage decreased as the floc and granule percentages had such a high increase. The increase in granule percentage is the important takeaway from these results and should result in an increase in settling velocity and enhanced biological phosphorus removal as granules thrive within the system.



The cyclone underflow showed a consistently higher density than the underflow, which is crucial for retaining denser solids while wasting lighter solids. The cyclone underflow had a consistent density increase with a beginning value of 1.072 g/mL on July 8<sup>th</sup>, 2015 to a final value of 1.082 g/mL on September 24<sup>th</sup>, 2015. The overflow density stayed fairly constant ranging from 1.031-1.035 g/mL. The cyclone feed, or RAS line, showed fairly similar values to the aeration effluent mixed liquor values which is what would be expected, validating the accuracy of the results.

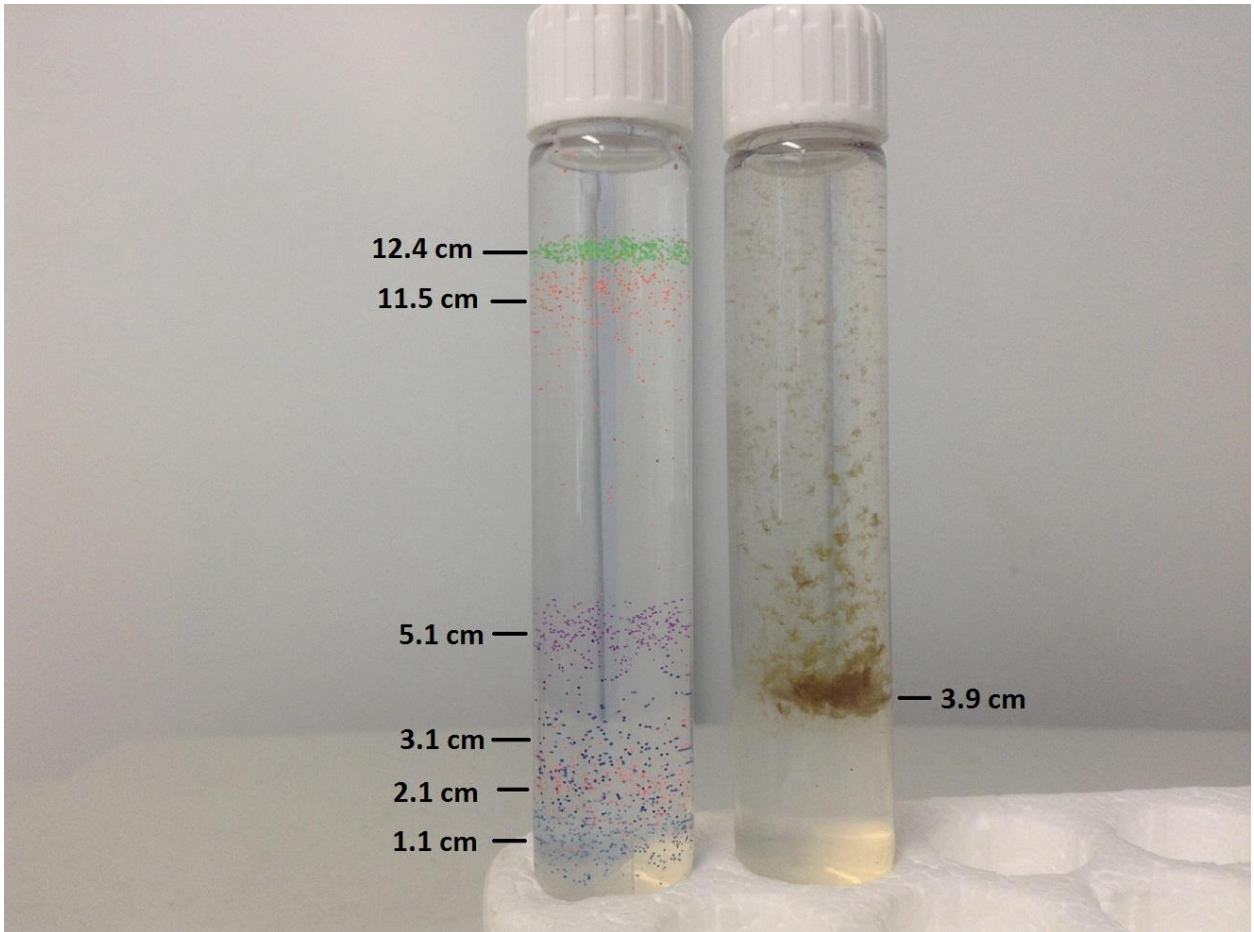


**Figure 4.6** An example of the floc density analysis using Isopycnic centrifugation from 6/22/15.

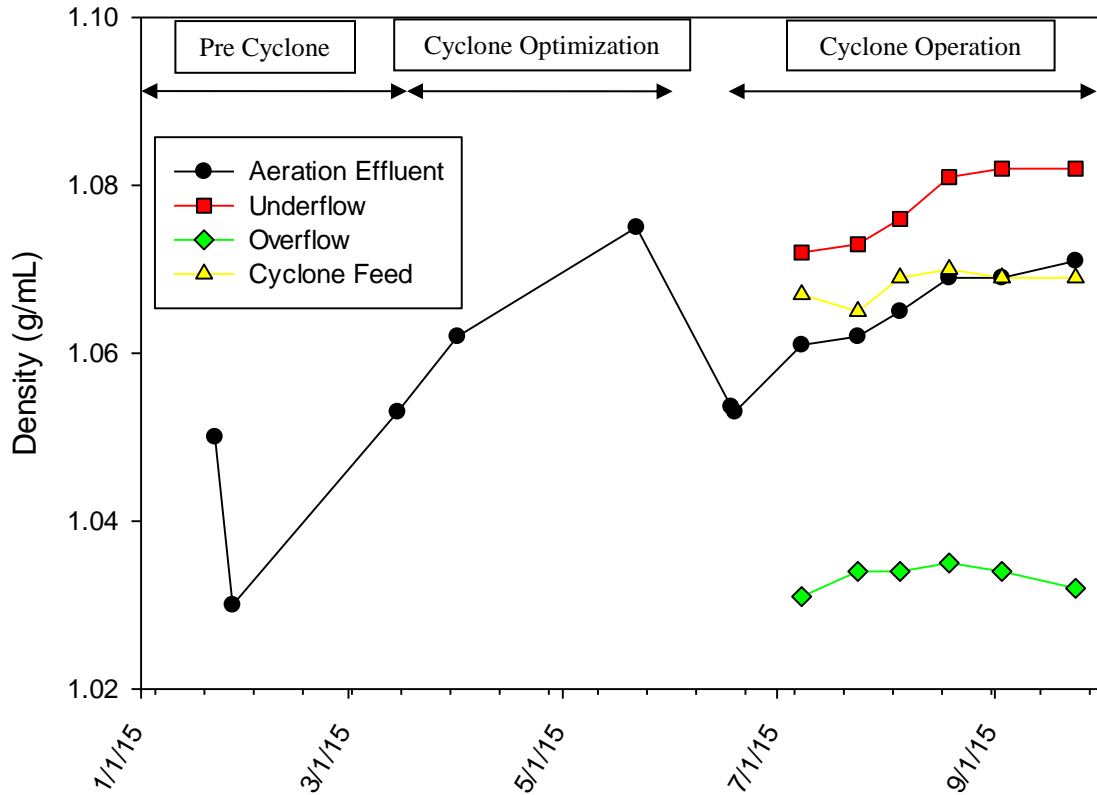


**Figure 4.7 James River ML floc density of Aeration effluent and Cyclone Sampling Points**

## 4.7 Filaments

### 4.7.1 Microscopic analysis

Observations were performed using a Leica 2500 phase contrast microscope coupled to a Leica DFC 290 camera. The Gram and Neisser staining techniques were used for identification. 50 mL samples were sent periodically for microscopic filament analysis. Complete results and photos can be found in Appendix D.

From November to May the mixed liquor contained mainly small, firm, round and irregular, compact flocs that were not penetrated by India ink. From November to April there were “few” amounts of discrete spirochetes present and beginning in March there was some free grease noted in the sample along with some iron containing solids, which ceased in April. Grease present in the ML may cause settleability issues, increasing SVI values (Jones and Schuler, 2010). In November the filamentous organism level was “few-some” but increased to “very common” in April. In November the filaments present in low levels included type 0041, type 0675, nocardioforms and

type 1701 and in March the filaments present in small amounts included type 1863, *H Hydrossis*, nocardioforms and type 1701, none of these sufficient enough to interfere with the settleability of the sludge. In April and May *nocardioform* was noticed as the main filamentous organism, present in the sludge floc and free in the solution. *Nocardioform* abundance was seen at levels that would result in foaming. In April other filaments present at levels too low to interfere with settling included type 1863, *H Hydrossis*, *Thiothrix* and type 1701. In May only minor amounts of *H Hydrossis* and type 1701 were noted. In June, when the cyclones were started up again after a 3 week shut down, the overall filamentous organism level decreased to was "some" which is not sufficient to interfere with settling. In June the filaments were all present in small amounts; they were *nocardioforms*, type 0041 and type 0675.

These results indicate the filamentous organisms are being selected against; only the ones inside the floc or slightly protruding were present in the June sample. Presence of *nocardioforms* may have been due to recycling and trapping in the activated sludge and therefore would be immune from a "selection strategy" based on dense, settling biomass.

Initial samples were sent for analysis in October 2014 and throughout the entire study the flocs contained large amounts of PAO bacteria and no GAO bacteria. However in November some GAO bacteria was present, but upon analysis of the next sample, no GAO bacteria was found. The PAO bacteria were present as large grape-like clusters of coccoid cells and clusters of small coccoid cells. It is not clear whether these are two separate types of PAO bacteria or just different morphological forms of the same organism. In April the level of small coccoid cells increased over the previous sample.

#### **4.7.2 Plant Data**

Historical data for the JR plant has not shown a correlation between seasonal variations and filament abundance. Filament abundance from 2014-2015 can be found in Appendix D with values never reaching that of nuisance levels. The primary filament type was Nocardioforms. Other filament types included 0041, 0875, and *Thiothrix* II.

#### **4.8 PAO Activity Tests**

PAO Activity tests provide results for:

- Determining amount of PAO and DPAO activity from the phosphate release rate

- The potential competition for VFA in the anaerobic zone. The ratio of phosphate released to VFA consumed indicates PAO activity. Lower ratios are indicative of competition from other VFA consuming organisms such as GAOs
- providing information on the phosphate uptake kinetics that can be used to determine the time required to remove phosphate in the aerobic or anoxic zone

Data collection for phosphorus activity tests began on August 22<sup>nd</sup> 2014 to get sufficient baseline data before the cyclones were installed. Biological phosphorus removal activity is more prevalent under warmer temperatures and during the winter months tends to be almost non-existent because of reduced biological activity rates (Brdjanovic, 1998). Results showed that reduced EBPR at low temperatures held true in this study as there is a clear correlation between temperature decrease and a decrease in phosphorus activity. In Figure 4.8b, an increase in the anoxic activity represents DPAO activity in the ML. Since startup of the hydrocyclones the anaerobic release rate, aerobic uptake rate, and anoxic uptake rate in the aeration effluent are consistent with the inconsistent biological phosphorus activity of the previous summer. Testing shows the anoxic rates are 29-56% of the aerobic uptake rates, representing the DPAO/PAO ratio. Uptake and release rates seemed to fall within similar ranges when EBPR performance was present (not in colder temperatures)(Neethling, 2005). Uptake rates are generally lower than release rates as seen in Table 2.4, meaning that a longer aerobic time is required as expected.

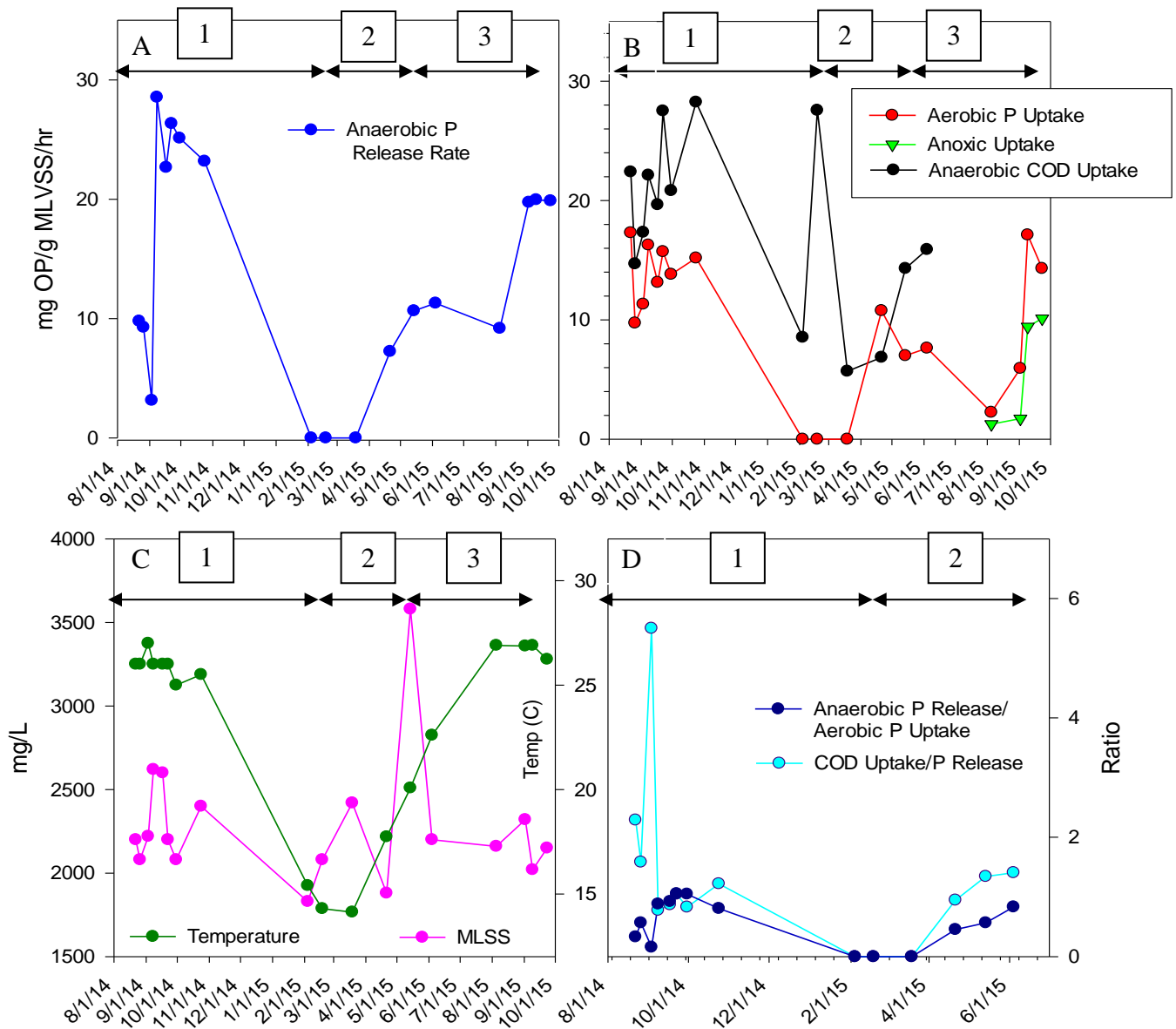


**Figure 4.8 Phosphorus Release and Uptake of Aeration Effluent**  
**A. Anaerobic Phosphorus Release Rate (mg OP/g MLVSS/hr) over time**  
**B. Aerobic Phosphorus Uptake Rate, Anoxic Phosphorus Uptake Rate, Anaerobic COD Uptake (mg OP/g MLVSS/hr) over time**  
**C. Temperature (°C) and MLSS (mg/L) of JR over time**  
**D. Ratio of Anaerobic Phosphorus Release/Aerobic Phosphorus Uptake and Ratio of COD Uptake/Phosphorus Release Rate over time**  
**Periods 1: Pre-Cyclone**  
**Period 2: Cyclone Optimization**  
**Period 3: Cyclone Operation**

In Figure 4.9 the anaerobic release rates are similar between the underflow and overflow and represent the activity of PAO and DPAO. Figure 4.9c is the anoxic activity test which represents

DPAO activity. It is clear that DPAO are being selected for in the underflow, while the aerobic activity tests representative of PAO, show slightly less activity in the underflow than overflow. This suggests that DPAO are being selectively retained within the system, which as the advantage of efficiently using COD for denitrification and phosphorus removal within the same process. The aeration effluent shows significantly higher uptake and release rates compared with the cyclone feed, although it would be expected for these samples to have similar activity. The activity in the aeration effluent is also consistently higher than activity in the underflow and overflow.

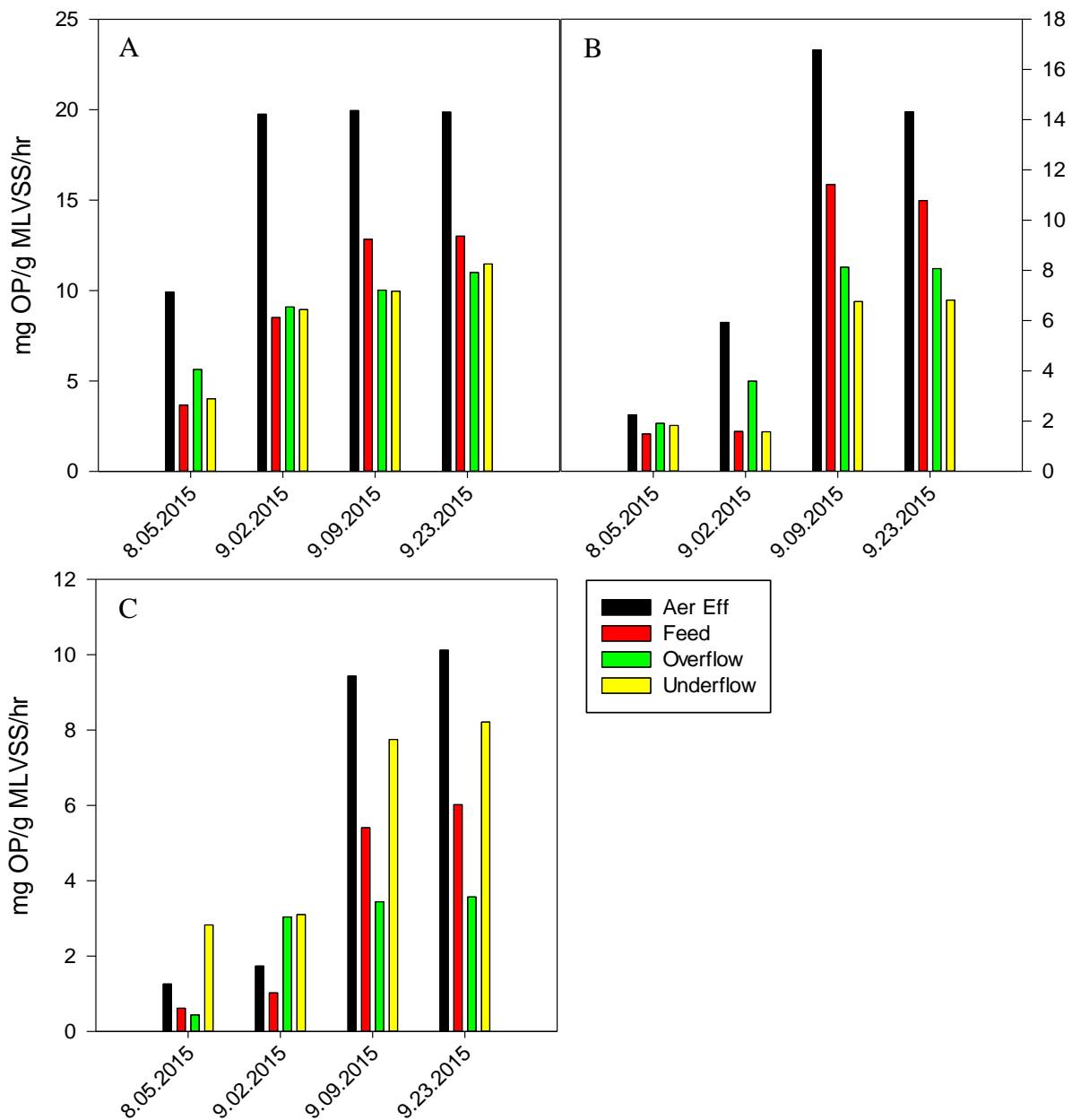


**Figure 4.9 Phosphorus Uptake and Release Rate of Cyclone Sample Points and Aeration Effluent. All data taken during cyclone operation period.**

- a. Anaerobic Release, representative of DPAO and PAO activity
- b. Aerobic Uptake, representative of PAO activity
- c. Anoxic Uptake, representative of DPAO activity

## 4.9 Phosphorus and Ferric Plant Data

Plant data was collected for Ferric addition before the primary and secondary clarifier, for the phosphorus in the raw water influent (RWI), and total phosphorus (TP) and orthophosphate (OP) in the final effluent (FNE). Values reading below the detectable range ( $<0.20$  mg/L) were recorded as 0.1 mg/L. In Figure 4.10 a clear downward trend can be observed in the Fe/influent TP and Fe/P removed ratio during the cyclone optimization period and the cyclone operation period. This suggests that less Fe was needed for phosphorus removal, and that the cyclones were effectively increasing the EBPR performance at the plant. A full list of raw data is provided in Appendix H.

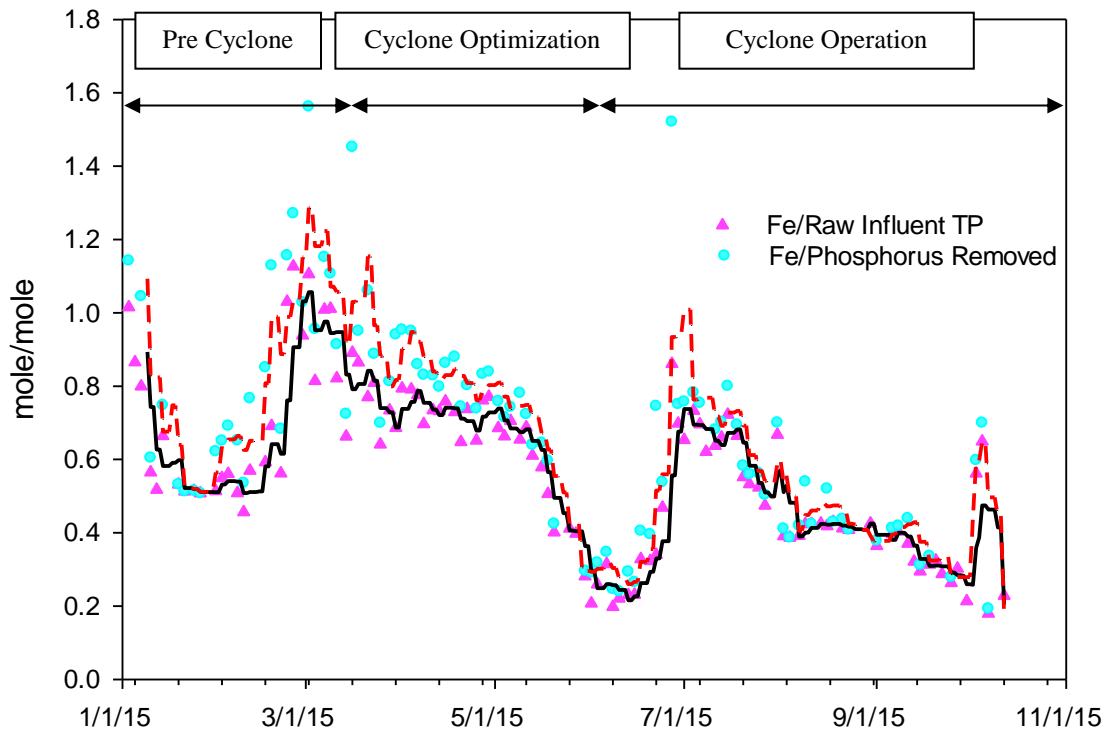


**Figure 4.10 Ratio of Ferric Addition to Raw Influent Phosphorus and Phosphorus Removed. Lines represent a 7 day moving average of each ratio.**

In Figure 4.11 the Fe added, Influent TP, effluent OP, and effluent TP are shown for 2015 with lines representing the 7 day averages. While the influent TP varies from about 3.5-6 mg/L throughout the year, the Fe addition shows steady decline from August to October, about 3 months after the cyclones had been under full operation. This indicates that about 3 months after

proper installation the cyclones had an effect on the biological phosphorus activity within the ML.

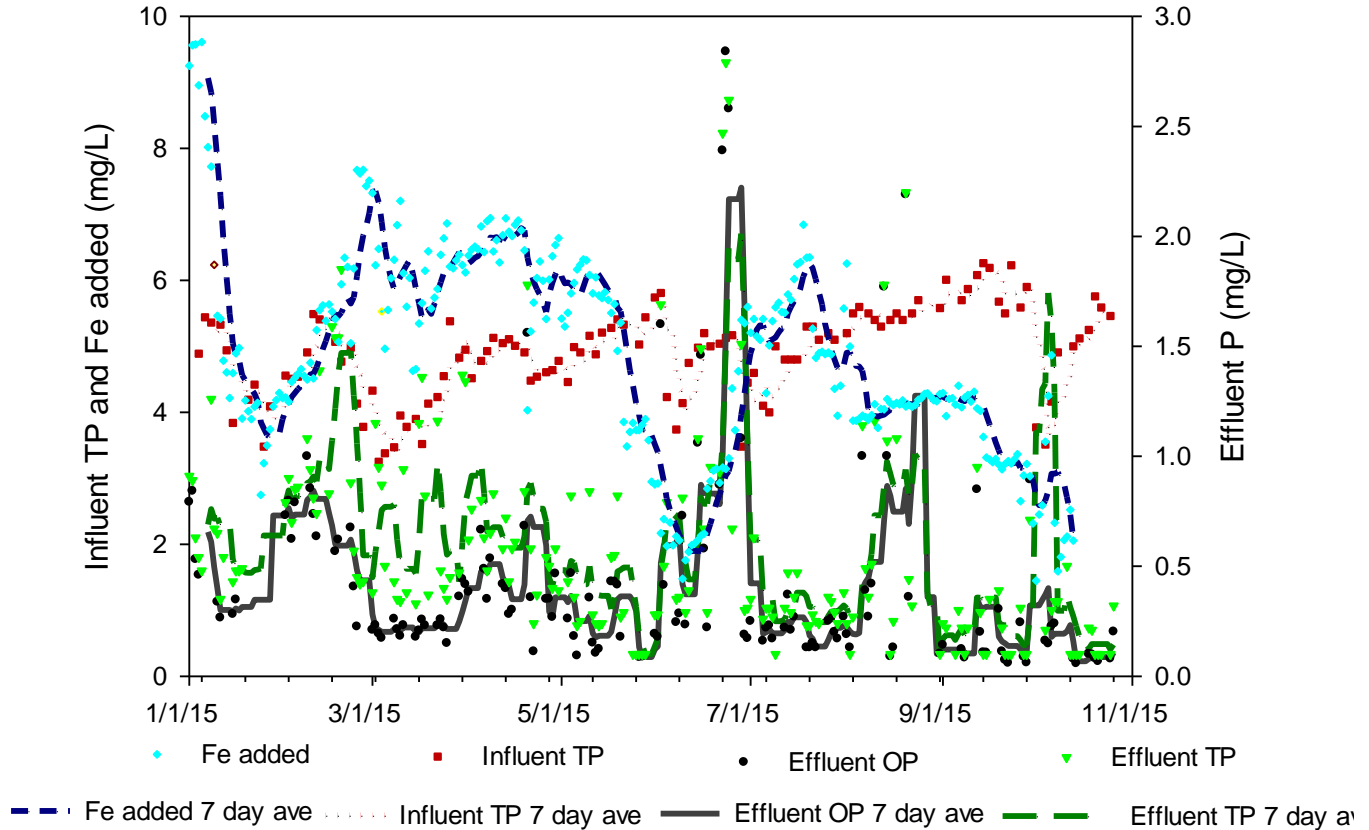


**Figure 4.11 Influent and Effluent Phosphorus concentrations**

#### 4.10 AOB and NOB Activity Tests

In Figure 4.12 the AOB and NOB activity, respectively, is provided for the cyclone feed, underflow, and overflow. It was hypothesized that the cyclones may be selectively wasting the AOB and NOB in the overflow, resulting in reduced nitrification. However, results showed that AOB activity in the underflow was similar to activity in the feed and overflow. NOB activity in the underflow was slightly larger than the activity in the overflow. These results indicate that the AOB and NOB are not being washed out in the cyclone overflow and should not result in a loss of nitrifiers.

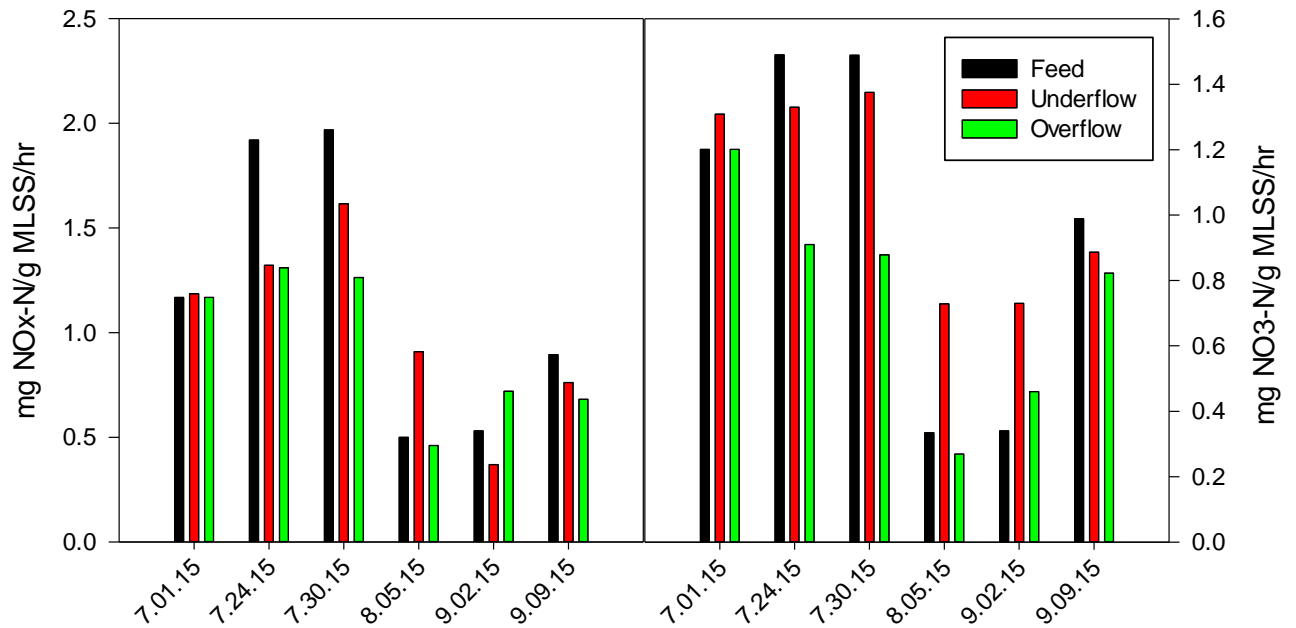


**Figure 4.12 AOB and NOB activity in cyclone sampling points. All data taken during cyclone operation period.**

- a) AOB activity
- b) NOB activity

### 4.11 Tank Profiling

In May a sharp spike in  $\text{NH}_4^+$  concentration can be seen, increasing from 1.83 mg/L at the end of March to 12.6 mg/L in early May as seen in Figure 4.13. The dramatic decrease in nitrification led to the cyclones being shut down as it was hypothesized that the cyclone were wasting the AOB and NOB in the overflow. However, AOB and NOB activity in the overflow and underflow showed no wasting in the overflow. All profiling data over the course of the project can be found in Appendix H.

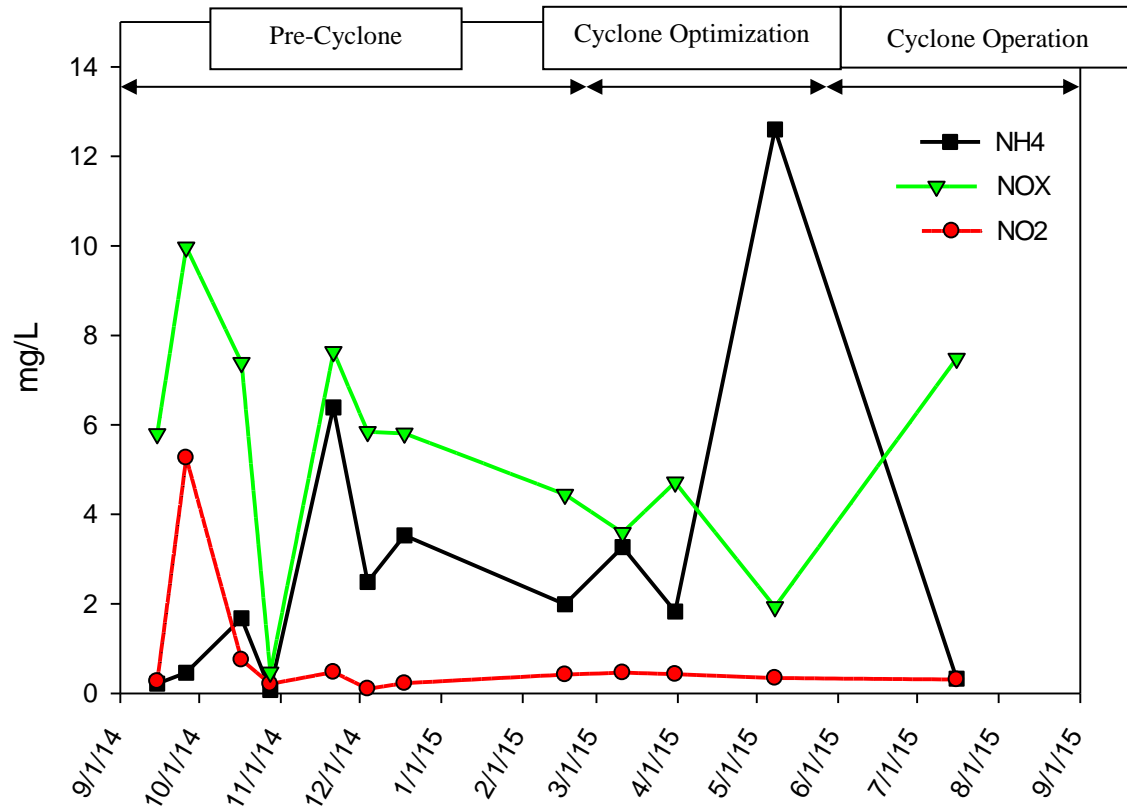


Figure 4.13 NO2, NOx, and NH4 of aeration effluent of JR ML

## 5. Conclusions and engineering significance

Preliminary conclusions can be made about the effects of hydrocyclones on the settleability and enhanced biological phosphorus removal applied to the mainstream of a wastewater treatment plant. Biological phosphorus removal activity was present in the wastewater at similar rates when comparing the period before and after hydrocyclones were installed, indicating that the hydrocyclones may not have had an effect on the biological phosphorus activity, which may have been due to the short period they were fully operational. However, it was noted that anoxic biological phosphorus activity was increasing over time indicating that DPAO were being selectively retained.

AOB and NOB activity measurements in the cyclone overflow, underflow, and feed indicated that nitrifiers were not being selectively wasted from the system, indicating that nitrification at the plant should not be affected by the hydrocyclones. Filament data taken from the plant and microscopic analysis showed that some filaments were present in the system but not at levels that would hinder settleability or cause foaming, which showed that filamentous organisms were being selected against. It was also shown through filamentous analysis that PAO were present while the GAO population was minimal. The floc density of the aeration effluent mixed liquor was shown to increase steadily over time from 1.050-1.071 g/mL. The density of the cyclone overflow and underflow showed a large difference in density, which meant that the denser sludge was being selectively retained while wasting the lighter sludge. Over time, the settleability would increase with the retention of denser sludge. Plant data collected for James River does suggest a reduction in Ferric as biological phosphorus removal remained constant during the last 2 months of data collection. A reduction in Ferric addition was noticed about 3 months after the cyclones were under full operation, indicating an increase in biological phosphorus activity. ISV tests show that the cyclone underflow has a much higher settling velocity than the cyclone overflow. The cyclone feed ISV did not increase over time but data was taken over a period slightly less than three months which may not have been enough time for a noticeable effect. 2015 SVI data shows a slight decrease in the average SVI5 decreasing from 292 mL/g to 248 mL/g after cyclones were installed, while the SVI30 value remained fairly constant. SVI is slow to change as it is more representative of the total floc structure, but as granules within the system become more stable, a decrease in SVI and increase ISV data should be observed. Solids flux data showed an increase in initial settling velocity from the pre-cyclone to cyclone optimization period and then again during the cyclone operation period. Vesilind values indicate an increase in  $V_o$  while  $k$  showed a minimal decrease, both indicating better settleability characteristics. Classification of settleability

rate data indicated that granule percentage increased from 0% during the pre-cyclone period to up to 24-40% during the cyclone operation period. Pilot scale studies demonstrated that it took about 1-3 months for full granulation so it may be that in a full-scale study it would take longer to achieve the same results due to the large volume of ML. The floc fraction showed a large increase from the pre-cyclone and cyclone optimization to the cyclone operation period with averages increasing from  $14\pm 11\%$  to  $37\pm 22\%$ . The aggregate percentage was the majority of the floc characterization during pre-cyclone and cyclone optimization periods averaging  $86\pm 11\%$  and decreasing to  $47\pm 35\%$ . It is unclear why the aggregate percentage decreased as the floc and granule percentages had such a high increase.

Wastewater treatment plants all over the world suffer from settleability issues, while also needing to meet increasingly stringent nutrient limits. Settleability is often a limiting step of the wastewater treatment process. Poor settleability may result in a high TSS effluent or a high nutrient concentration in the effluent which can lead to eutrophication in receiving water bodies. Aerobic granular sludge research has indicated the multiple benefits that it can achieve in a wastewater system by increasing settling rates through superior settling characteristics while removing nutrients in a single system through stratified layers. Using an external selector to achieve biological phosphorus or stabilize erratic biological phosphorus removal is significant in that most wastewater treatment plants cannot do this without the use of an anaerobic selector. This has the potential to apply external selectors to existing infrastructure throughout plants worldwide to achieve not only biological phosphorus removal, but also improved settleability with a very minor capital investment.

## References

- Acevedo, B., Borrás, L., Oehmen, A., & Barat, R. (2014). Modelling the metabolic shift of polyphosphate-accumulating organisms. *Water Research*, 65, 235-244. doi: <http://dx.doi.org/10.1016/j.watres.2014.07.028>
- Ahn, J.; Daidou, T.; Tsuneda, S.; Hirata, A. (2002). Characterization of denitrifying phosphate-accumulating organisms cultivated under different electron acceptor conditions using polymerase chain reaction-denaturing gradient gel electrophoresis assay. *Water Research*, 36.
- Carvalho, G.; Lemos, P.; Oehmen, A.; Reis, M. (2007). Denitrifying phosphorus removal: Linking the process performance with the microbial community structure. *Water Research*, 41.
- Carvalho, M., Oehmen, A., Carvalho, G., Eusébio, M., & Reis, M. A. M. (2014). The impact of aeration on the competition between polyphosphate accumulating organisms and glycogen accumulating organisms. *Water Research*, 66(0), 296-307. doi: <http://dx.doi.org/10.1016/j.watres.2014.08.033>
- Carvalho, M., Oehmen, A., Carvalho, G., & Reis, M. A. M. (2014). Survival strategies of polyphosphate accumulating organisms and glycogen accumulating organisms under conditions of low organic loading. *Bioresource Technology*, 172(0), 290-296. doi: <http://dx.doi.org/10.1016/j.biortech.2014.09.059>
- Cell Separation Media Methodology and Applications. (1985). In G. H. L. Sciences (Ed.): General Electric Company.
- Chudoba, J.; Cech, J. S.; Farkac, J.; Grau, P. . (1985). Control of Activated Sludge Filamentous Bulking: Experimental Verification of a Kinetic Selection Theory. *Water Research*, 191-196.
- de Kreuk, M. K. (2006). Aerobic Granular Sludge Scaling up a new technology.
- de Kreuk, M. K., de Kreuk, M., Heijnen, J. J., & van Loosdrecht, M. C. M. (2005). Simultaneous COD, nitrogen, and phosphate removal by aerobic granular sludge. *Biotechnology and bioengineering*, 90(6), 761-769.
- Denny Parker, George Ekama, Henryk Melcer, Andre van Niekirk, Dean M. Shiskowski, David J. L. Forgie, W. L. Marten, G. T. Daigger. (1998). Full-Scale Evaluation of Factors Affecting the Performance of Anoxic Selectors. *Water Environment Research*, 70(6), 1225-1231.
- Ekama, G.A.; Barnard, J. L.; Günthert, F. W.; Krebs, P.; McCorquodale, J. A.; Parker, D. S.; Wahlberg, E. J. . (2006). Secondary Settling Tanks Scientific and Technical Report (Vol. 6). London, UK: IWA.
- EnviroSim Associates, LTD. (2014). BioWin 4.0 (Version 4).
- Gao, D. W., Liu, L., Liang, H., & Wu, W. M. (2011). Aerobic granular sludge: characterization, mechanism of granulation and application to wastewater treatment. *Critical Reviews in Biotechnology*, 31(2), 137-152. doi: [10.3109/07388551.2010.497961](http://dx.doi.org/10.3109/07388551.2010.497961)
- Grady, C. P. Leslie et al. (2011). *Biological Wastewater Treatment* (Vol. 19). Boca Raton, FL: IWA Pub./CRC Press.
- Houweling, D.; Constantine, T.; Sandino, S.; Neilson, P. H.; Uri N.; Havsteen L. (2015). What the Cyclone did to my Sludge and Other Tales of Activated Sludge Granulation. *Water Environment Association of Ontario*. Toronto, Ontario, Canada.

- J. Chudoba, P. Grau, V. Ottova. (1973). Control of Activated-Sludge Filamentous Bulking- II. Selection of Microorganisms by Means of a Selector. *Water Research*, 7, 1389-1406.
- Jenkins, D.; Richard, M. G.; Daigger, G. T. (2003). *Manual on the Causes and Control of Activated Sludge Bulking, Foaming and Other Solids Separation Problems*: Lewis Publishers.
- Jones, Patricia A., & Schuler, Andrew J. (2010). Seasonal variability of biomass density and activated sludge settleability in full-scale wastewater treatment systems. *Chemical Engineering Journal*, 164(1), 16-22.
- Kim, Hyun-su, Gellner, James W., Boltz, Joshua P., Freudenberg, Robert G., Gunsch, Claudia K., & Schuler, Andrew J. (2010). Effects of integrated fixed film activated sludge media on activated sludge settling in biological nutrient removal systems. *Water Research*, 44(5), 1553-1561.
- Kuba, T., van Loosdrecht, M.C.M., Heijnen, J.J. Phosphorus and nitrogen removal with minimal COD requirement by integration of denitrifying dephosphatation and nitrification in a two-sludge system, *Water Research*, Volume 30, Issue 7, July 1996, Pages 1702-1710, ISSN 0043-1354
- Liu, Y., Wang, Z., Qin, L., Liu, T., Tay, J. (2004). Selection pressure-driven aerobic granulation in a sequencing batch reactor. *Applied Microbiology and Biotechnology*.
- Lopez-Vazquez, C. M.; Oehmen, A.; Hooijmans, C. M.; Brdjanovic, D.; Gijzen, H. J.; Yuan, Z.; van Loosdrecht, M. C. M. (2009). Modeling the PAO–GAO competition: Effects of carbon source, pH and temperature. *Water Research*, 43(2), 450-462. doi: <http://dx.doi.org/10.1016/j.watres.2008.10.032>
- Mancell-Egala, A. (2014). *Protocols for Settleability*.
- Martins, António M. P., Pagilla, Krishna, Heijnen, Joseph J., & van Loosdrecht, Mark C. M. (2004). Filamentous bulking sludge—a critical review. *Water Research*, 38(4), 793-817. doi: <http://dx.doi.org/10.1016/j.watres.2003.11.005>
- Metcalf, Eddy. (2014). *Wastewater Engineering Treatment and Resource Recovery*: McGraw-Hill Education.
- Mishima, K., & Nakamura, M. (1991). Self-Immobilization of Aerobic Activated Sludge—A Pilot Study of the Aerobic Upflow Sludge Blanket Process in Municipal Sewage Treatment. *Water Science and Technology*, 23, 981-990.
- Morgenroth E.; Sherden, T.; Van Loosdrecht, M. C. M.; Heijnen, J. J.; Wilderer, P. A. . (1997). Aerobic Granular Sludge in a Sequencing Batch Reactor. *Water Research*, 31(12), 3.
- Neethling, J. B.; Bakke, B.; Benisch, M.; Gu, A.; Stephens, H.; Stensel, H. D.; Moore, R. (2005). Factors Influencing the Reliability of Enhanced Biological Phosphorus Removal. In WERF (Ed.).
- Nyhuis, Geert. (2013). Switzerland Patent No.: U. S. P. A. Publication.
- Oehmen, A., Carvalho, G., Lopez-Vazquez, C. M., van Loosdrecht, M. C. M., & Reis, M. A. M. (2010). Incorporating microbial ecology into the metabolic modelling of polyphosphate accumulating organisms and glycogen accumulating organisms. *Water Research*, 44(17), 4992-5004. doi: <http://dx.doi.org/10.1016/j.watres.2010.06.071>

- Oehmen, A.; Carvalho, G.; Freitas, F. (2010). Assessing the abundance and activity of denitrifying polyphosphate accumulating organisms through molecular and chemical techniques. *Water Science & Technology*, 61(8), 2061-2068. doi: <http://dx.doi.org/10.2166/wst.2010.976>
- Oehmen, Adrian, Lemos, Paulo C., Carvalho, Gilda, Yuan, Zhiguo, Keller, Jürg, Blackall, Linda L., & Reis, Maria A. M. (2007). Advances in enhanced biological phosphorus removal: From micro to macro scale. *Water Research*, 41(11), 2271-2300. doi: <http://dx.doi.org/10.1016/j.watres.2007.02.030>
- Pagilla, Krishna R., Jenkins, David, & Kido, Wendell H. (1996). Nocardia Control in Activated Sludge by Classifying Selectors. *Water Environment Research*, 68(2), 235-239. doi: 10.2307/25044712
- Parker, D.; Geary, S.; Jones, G.; McIntyre, L.; Oppenheim, S.; Pedregon, V.; Pope, R.; Richards, T.; Voigt, C.; Volpe, G.; Willis, J.; Witzgall R. (2003). Making Classifying Selectors Work for Foam Elimination in the Activated-Sludge Process. *Water Environment Research*, 75(1).
- Peng Dangcong, Nicolas Bernet, Jean-Philippe Delegenes, Rene Moletta. (1998). Aerobic Granular Sludge- A Case Report. *Water Research*, 33(3), 890-893.
- Rice, E. W.; Baird, R. B.; Eaton, A. D.; Clesceri, L. S. (Ed.). (2012). *Standard Methods* (22nd ed.). Washington, DC: American Public Health Association, American Water Works Association, Water Environment Federation.
- Rutherford, Bob. (2010). Testing a Nutrient Removal Option. *Water Environment and Technology*.
- Schuler, A. J.; Jang, H. (2007). Density Effects on Activated Sludge Zone Settling Velocities. *Water Research*, 41.
- Smolders, G. J. F.; van der Meij, J.; van Loosdrecht, M. C. M.; Heijnen, J. J. (1994). Model of the anaerobic metabolism of the biological phosphorus removal process: Stoichiometry and pH influence. *Biotechnology and Bioengineering*, 43(6), 461-470. doi: 10.1002/bit.260430605
- Sriwiryarat, T., & Randall, C. W. (2005). Performance of IFAS wastewater treatment processes for biological phosphorus removal. *Water Research*, 39(16), 3873-3884.
- Stensel, H. D. (1991). Principles of Biological Phosphorous Removal. IN: *Phosphorous and Nitrogen Removal from Municipal Wastewater: Principles and Practice*. 2nd ed. Lewis Publishers, Boca Raton, Florida. 1991. p 141-166.
- WEF. (2005). Clarifier Design WEF Manual of Practice N0. FD-8 Second Edition: McGraw-Hill.
- Wett, B. (2015). [Strass SVI Update].
- Wett, B.; Bott, C.; Murthy, S.; De Clippeleir, H. (2014).
- Winkler, M. K. H., Kleerebezem, R., de Bruin, L. M. M., Verheijen, P. J. T., Abbas, B., Habermacher, J., & van Loosdrecht, M. C. M. (2013). Microbial diversity differences within aerobic granular sludge and activated sludge flocs. *Applied Microbiology and Biotechnology*, 97(16), 7447-7458. doi: 10.1007/s00253-012-4472-7
- Yuen, Weng Ah. "Empirical Equations for the Limiting Solids Flux of Final Clarifiers". *Water Environment Research* 74.2 (2002): 200-209.

## Appendices

### A. Phosphorus Activity

#### James River Phosphorus Activity Results

Date	A	B	C	D	E	F	G	H	I	J	K	L
8/22/14	26	2200	78%	1716	16.80	9.79	38.43	22.39	2.29	29.68	17.30	
8/26/14	26	2080	81%	1684.8	15.63	9.28	24.75	14.69	1.58	16.40	9.73	
9/3/14	27	2220	80%	1776	5.60	3.15	30.80	17.34	5.50	20.09	11.31	
9/8/14	26	2620	76%	1991.2	56.85	28.55	44.06	22.13	0.78	32.40	16.27	
9/17/14	26	2600	72%	1872	42.44	22.67	36.80	19.66	0.87	24.60	13.14	
9/22/14	26	2200	78%	1716	41.91	26.35	43.75	27.51	1.04	25.00	15.72	
9/30/14	25	2080	81%	1684.8	43.66	25.13	36.19	20.83	0.83	24.00	13.81	
10/24/14	25.5	2400	79%	1896	43.96	23.19	53.55	28.24	1.22	28.80	15.19	
2/4/15	15.4	1830	77%	1409.1	0.00	0.00	12.03	8.54	0.00	0.00	0.00	
2/18/15	14.3	2080	78%	1622.4	0.00	0.00	44.71	27.56	0.00	0.00	0.00	
3/19/15	14.13	2420	79%	1911.8	0.00	0.00	10.89	5.69	0.00	0.00	0.00	
4/21/15	17.73	1880	79%	1485.2	10.77	7.25	10.20	6.87	0.95	16.00	10.77	
5/14/15	20.07	3580	75%	2685	28.60	10.65	38.44	14.31	1.34	18.80	7.00	
6/4/15	22.6	2200	81%	1782	20.14	11.30	28.33	15.90	1.41	13.60	7.63	
8/5/15	26.9	2160				9.19					2.25	1.26
9/2/15	26.87	2320				19.75					5.93	1.73
9/9/15	26.9	2020				19.96					17.13	9.43
9/23/15	26.23	2060				19.87					14.31	10.12

- A. ~ Plant Temps (=Test Temp) °C  
 B. MLSS (mg/L)  
 C. MLVSS (%)  
 D. MLVSS (mg/L)  
 E. Anaerobic P release rate (mg OP/L/hr)  
 F. Anaerobic P release rate (mg OP/g MLVSS/hr)  
 G. Anaerobic COD Uptake Rate (mg COD/L/hr)  
 H. Anaerobic COD Uptake Rate (mg COD/g MLVSS /hr)

- I. COD uptake : P Release (RATIO)
- J. Aerobic P uptake rate (mg OP/L/hr)
- K. Aerobic P uptake rate (mg OP/g MLVSS /hr)
- L. Anoxic Uptake rate (mg OP/g MLVSS /hr)

## B. Phosphorus Uptake and Release Rates in Cyclone Sampling Points

Date	Anaerobic P Release (mg OP/ g MLVSS/hr)			
	Aeration Effluent	Feed	Underflow	Overflow
8/05/15	9.9189	3.6691	5.6404	4.0189
9/02/15	19.7501	8.5138	9.0924	8.9561
9/09/15	19.9555	12.8476	10.0273	9.9731
9/23/15	19.8700	13.0100	11.0000	11.4700

Date	Aerobic P Uptake (mg OP/ g MLVSS/hr)			
	Aeration Effluent	Feed	Underflow	Overflow
8/05/15	2.2531	1.4915	1.9083	1.8254
9/02/15	5.9289	1.5898	3.5882	1.5738
9/09/15	16.7762	11.4212	8.1270	6.7609
9/23/15	14.3100	10.7800	8.0700	6.8200

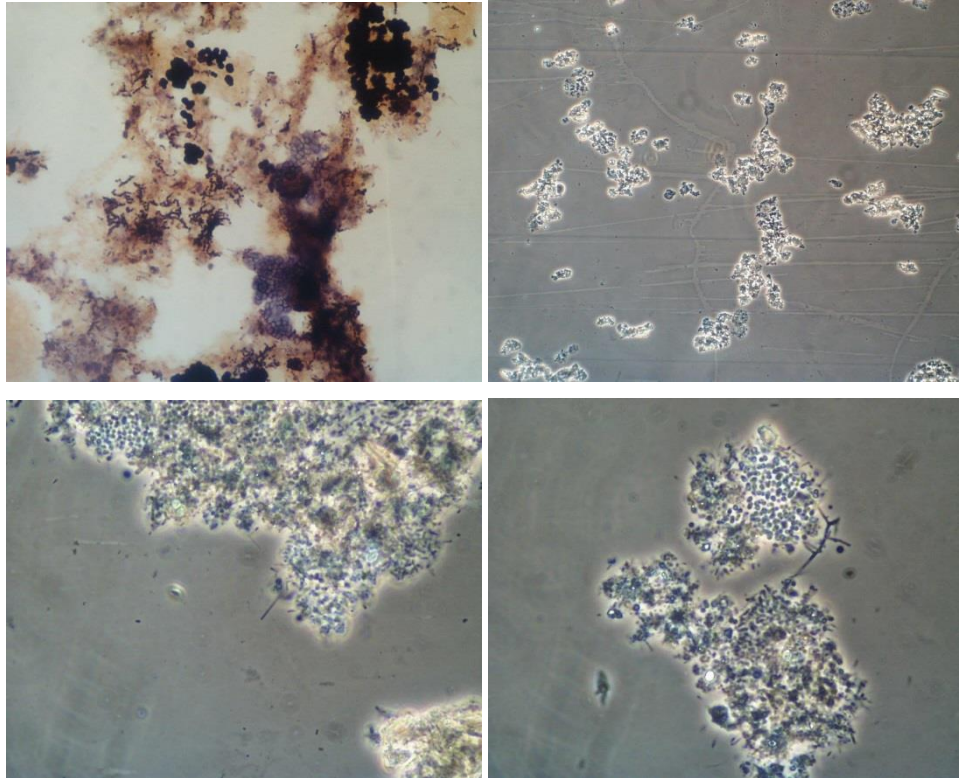
Date	Anoxic P Uptake (mg OP/ g MLVSS/hr)			
	Aeration Effluent	Feed	Underflow	Overflow
8/05/15	1.2599	0.6128	0.4394	2.8257
9/02/15	1.7346	1.0228	3.0363	3.1003
9/09/15	9.4286	5.4066	3.4431	7.7484
9/23/15	10.1200	6.0200	3.5700	8.2100

### C. AOB and NOB Activity in Cyclone Sampling Points

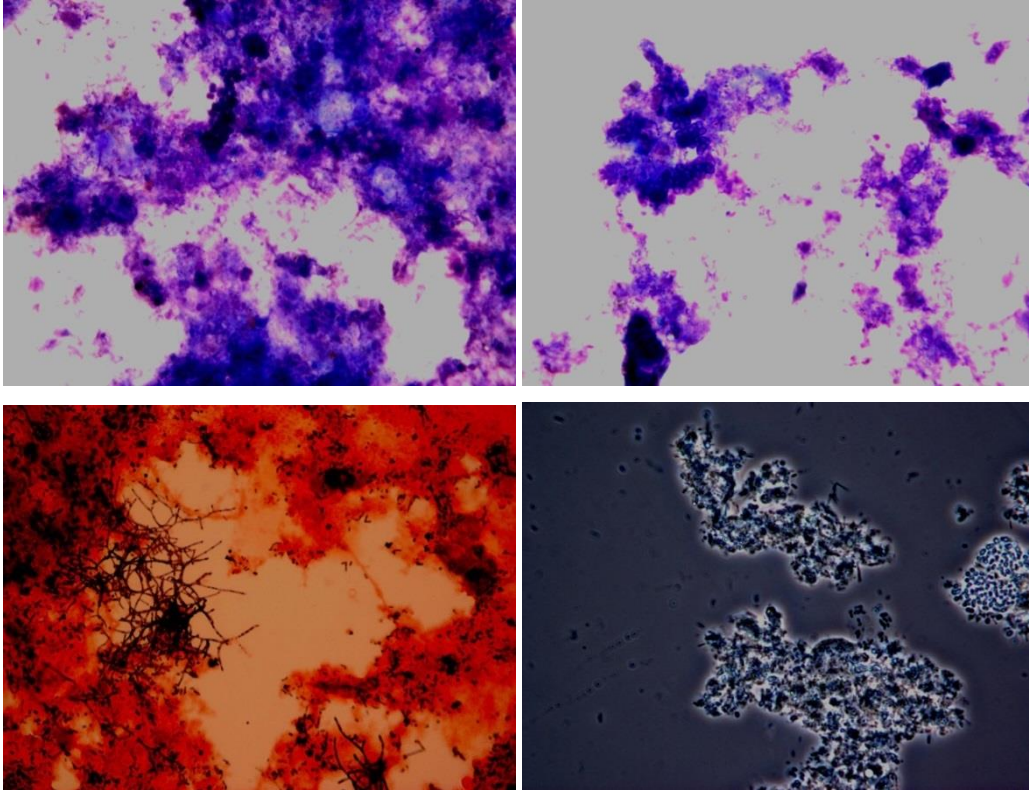
Date	AOB			NOB		
	Feed	Underflow	Overflow	Feed	Underflow	Overflow
7/14/15	1.1681	1.1851	1.1681	1.2007	1.3085	1.2007
7/24/15	1.9200	1.3221	1.3100	1.4900	1.3300	0.9100
7/30/15	1.9684	1.6166	1.2628	1.4889	1.3752	0.8787
8/05/15	0.4995	0.9084	0.4603	0.3339	0.7281	0.2689
9/02/15	0.5300	0.3695	0.7200	0.3400	0.7300	0.4600
9/09/15	0.8950	0.7616	0.6809	0.9890	0.8869	0.8222

## D. Microscopic Analysis

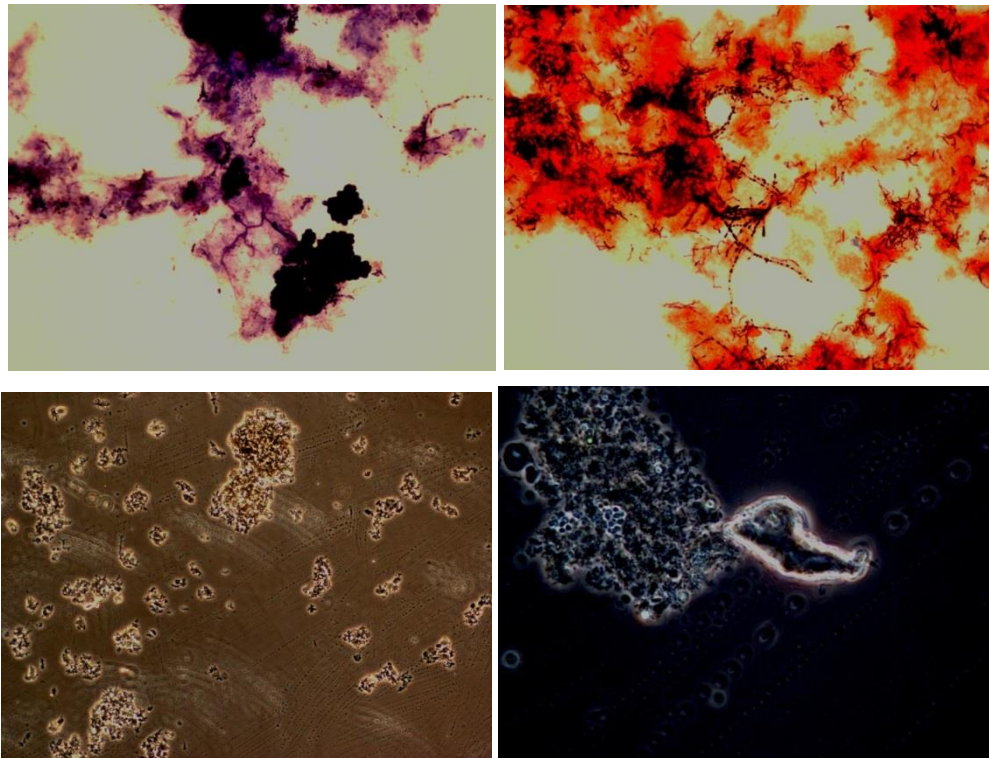
Microscope pictures and filamentous organism identification of grab samples from end of aeration basin.



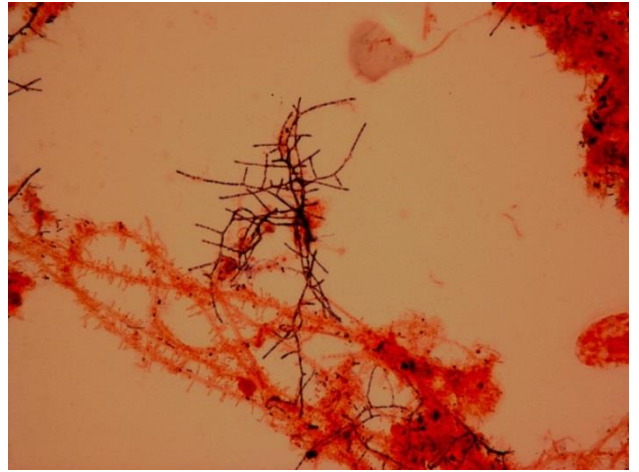
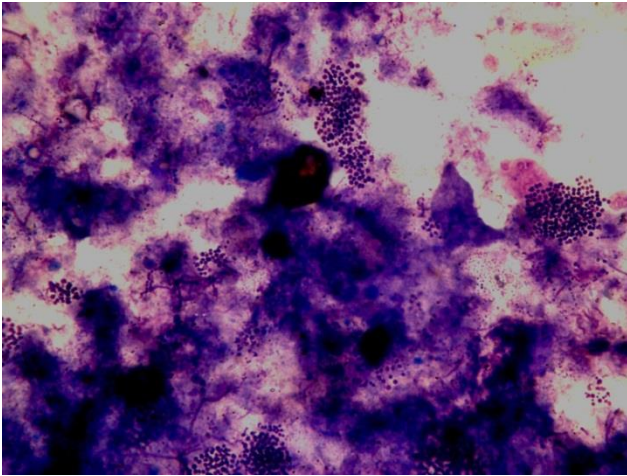
10/23/14 A) BioP Cell Clumps and G Bacteria. B) Floes. C) *Haliscomenobacter hydrossis*. D) Nocardioforms



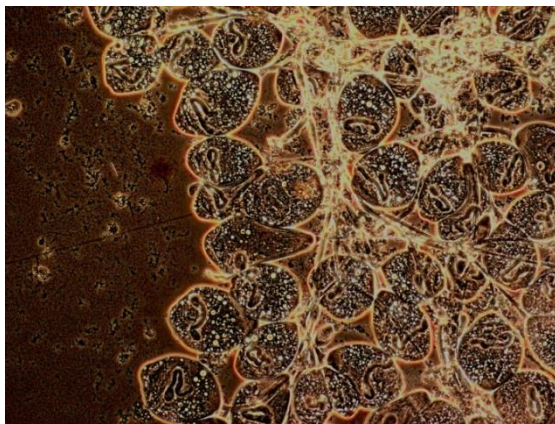
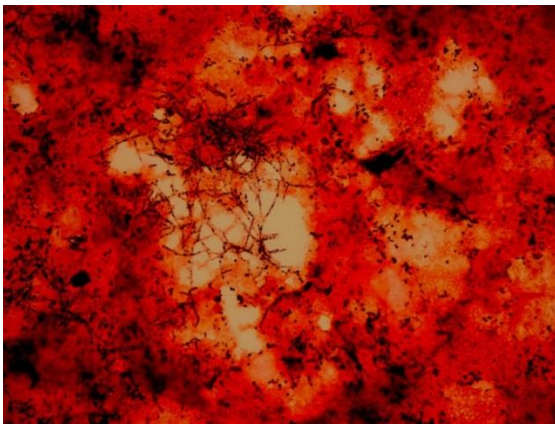
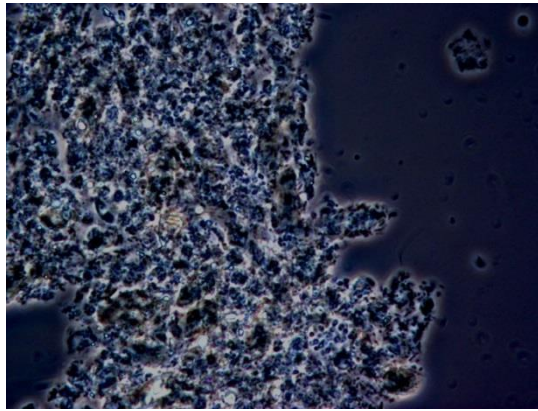
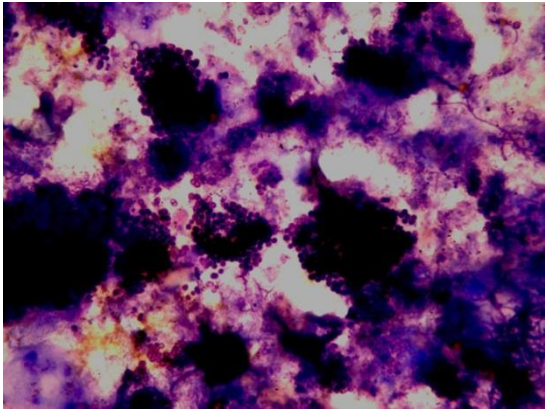
11/19/14 A) Bio P B) G Bacteria C) Nocardioforms D) Compact Floccs



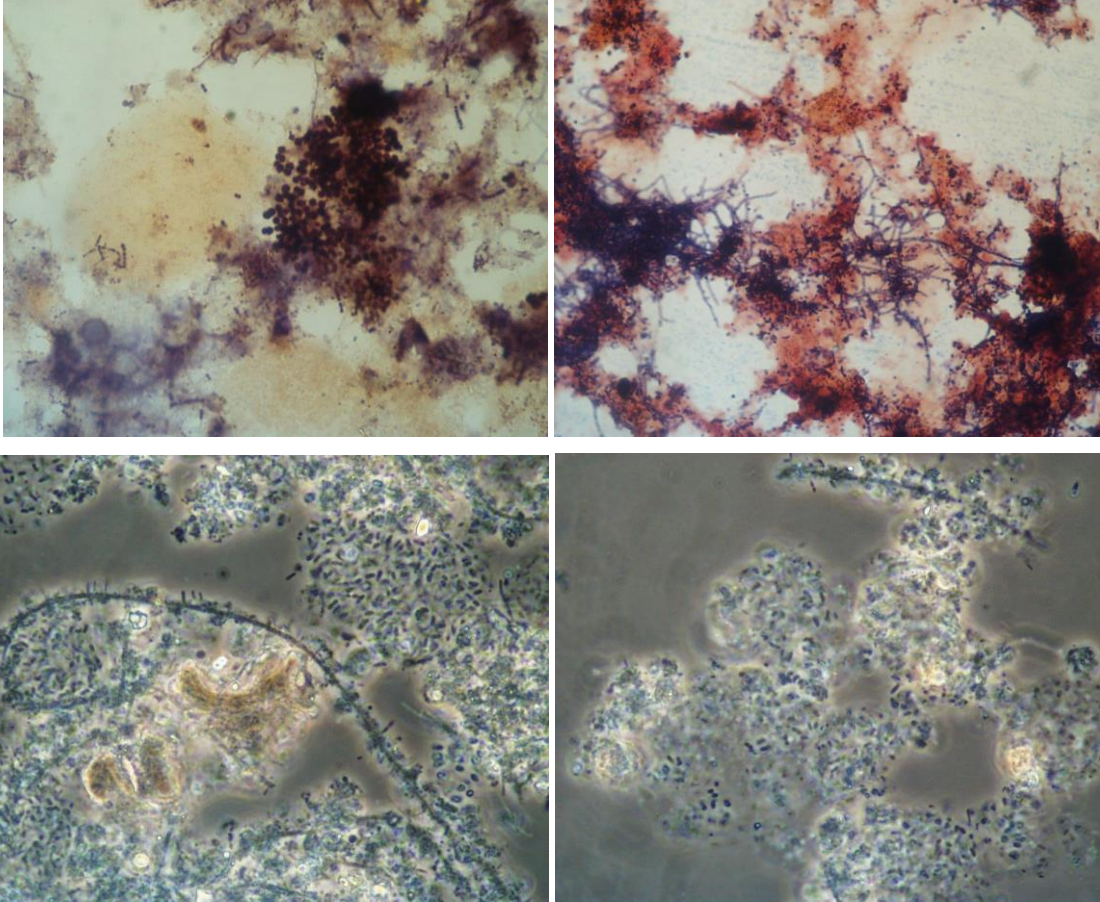
3/23/15 A) Strong BioP Clumps B) Nocardioforms Inside Flocc C) Strong Compact Floccs Mainly Small D) Grease Globule



4/23/15 A) Bio P Chains and Smaller Coccoid Clumps B) Free Nocardioforms



5/13/15 A) Strong Bio P B) Strong Compact Flocs C) Some Nocardioforms Inside Floc D) Stalked Ciliates



6/25/15 A) Bio P Bacteria B) Nocardioforms C) Type 0041, 0675 D) Amorphous Zoogeleal

### Filaments and Bacteria in JR ML

Date	Predominate		Secondary		PAO	GAO
	Type	Amount	Type	Amount	Amount	Amount
1/5/2014	NOCR	1	41	1	2	0
1/12/2014	NOCR	1	41	1	2	1
1/19/2014	NOCR	1	41	1	2	1
1/26/2014	NOCR	1	675	1	2	0
2/2/2014	NOCR	1	41	1	2	0
2/9/2014	NOCR	1	41	1	3	0
2/16/2014	NOCR	1	41	1	3	0
2/23/2014	NOCR	1	41	1	2	0
3/9/2014	41	1	675	1	2	0
3/16/2014	THI2	1	675	1	1	1
3/23/2014	NOCR	1	675	1	2	0
3/30/2014	NOCR	1	41	1	2	0
4/6/2014	NOCR	1	41	1	2	1
4/13/2014	NOCR	1	675	1	3	0
4/20/2014	NOCR	1	41	1	2	1
4/27/2014	NOCR	1	675	1	2	1
5/4/2014	NOCR	1	675	1	3	1
5/11/2014	NOCR	1	THI2	1	2	1
5/18/2014	NOCR	1	675	1	3	1
5/25/2014	NOCR	2	41	1	2	1
6/1/2014	NOCR	1	675	1	2	0
6/8/2014	NOCR	1	675	1	2	1
6/15/2014	NOCR	1	675	1	2	1
6/22/2014	NOCR	1	41	1	2	1
6/29/2014	NOCR	2	41	1	2	1
7/6/2014	NOCR	1	41	1	1	1
7/13/2014	675	1	41	1	1	2
7/20/2014	NOCR	1	675	1	2	2
7/27/2014	NOCR	1	41	1	2	2
8/3/2014	NOCR	1	675	1	2	2
8/10/2014	NOCR	1	675	1	2	3
8/17/2014	NOCR	2	675	1	2	3
8/24/2014	NOCR	1	41	1	1	2
8/31/2014	NOCR	1	41	1	3	1
9/7/2014	NOCR	1	41	1	1	2
9/14/2014	NOCR	1	41	1	2	2
9/21/2014	41	2	NOCR	1	1	3
9/28/2014	41	2	675	1	1	2
10/5/2014	NOCR	2	41	1	1	3
10/12/2014	NOCR	1	41	1	1	3
10/19/2014	NOCR	1	675	1	1	3
10/26/2014	NOCR	1	675	1	1	2
11/2/2014	NOCR	1	41	1	2	2

11/9/2014	NOCR	1	41	1	2	2
11/16/2014	NOCR	1	675	1	2	2
11/30/2014	NOCR	2	675	1	2	2
12/7/2014	NOCR	2	41	1	2	1
1/4/2015	NOCR	1	675	1	1	1
1/11/2015	NOCR	1	675	1	2	1
1/18/2015	NOCR	1	41	1	2	0
2/1/2015	NOCR	2	675	1	2	1
2/8/2015	NOCR	2	675	1	2	1
2/15/2015	NOCR	2	675	1	3	1
2/22/2015	NOCR	2	675	1	2	1
3/1/2015	NOCR	2	675	1	1	1
3/8/2015	NOCR	2	41	1	2	1
3/15/2015	NOCR	2	41	1	1	1
3/22/2015	NOCR	1	92	1	2	0
3/29/2015	NOCR	1	THI2	1	2	1
4/5/2015	NOCR	1	675	1	2	1
4/12/2015	NOCR	1	THI2	1	2	1
4/19/2015	NOCR	1	THI2	1	2	1
4/26/2015	NOCR	1	THI2	1	2	0
5/3/2015	NOCR	1	41	1	1	1
5/10/2015	NOCR	1	675	1	1	2
5/17/2015	NOCR	1	41	1	1	2
5/24/2015	NOCR	1	675	1	1	1
5/31/2015	NOCR	1	675	1	1	2
6/7/2015	NOCR	2	675	1	0	2
6/14/2015	NOCR	2	41	1	2	1
6/21/2015	NOCR	2	41	1	1	2
6/28/2015	NOCR	2	675	1	2	2
7/5/2015	NOCR	2	675	1	2	2
7/12/2015	NOCR	3	41	1	2	1

### E. Floc Density of Aeration Effluent and Cyclone Sampling Points

Floc Density (g/mL)				
Date	Aeration Effluent	Underflow	Overflow	Feed
1/22/2015	1.0500			
1/27/2015	1.0300			
3/15/2015	1.0530			
4/1/2015	1.0620			
5/22/2015	1.0750			
6/18/2015	1.0536			
6/19/2015	1.0530			
7/8/2015	1.0610	1.0720	1.0310	1.0670
7/24/2015	1.0620	1.0730	1.0340	1.0650
8/5/2015	1.0650	1.0760	1.0340	1.0690
8/19/2015	1.0690	1.0810	1.0350	1.0700
9/3/2015	1.0690	1.0820	1.0340	1.0690

## F. Floc Density SIP Calculation

Page 15 from GE document to create SIP:

Diluting Percoll to a desired Osmolality:

$$V_f = V_c \frac{O_c - O_f}{R(O_f - O_p)}$$

$V_p$  = number of parts of Percoll to be added

$V_c$  = number of parts of solute concentrate (e.g. 1.5 M NaCl) to be added

$O_c$  = osmolality of solute concentrate (e.g., 1.5 M NaCl = 2880 mOsm)

$O_f$  = desired osmolality

$R$  = ratio of aqueous volume to total volume of Percoll (typically 0.85 for NaCl)

$O_p$  = osmolality of Percoll undiluted

The average osmolality of James River ML was 525 mOsm/kg H<sub>2</sub>O. Samples were taken 3 times a day over a 3 day period, once at 7:00 am, 12:00 pm, and 4:00 pm.

$$V_p = 1 * \frac{2880 - 525}{0.85 * (525 - 20)} = 5.49 \text{ parts Percoll to 1 part 1.5 M NaCl}$$

Ratio of concentrated solute solution,  $R_x$ :

$$R_x = \frac{V_c}{V_p + V_c}$$

Desired density,  $\rho = 1.07$  g/mL, average density of beads

$$R_x = \frac{1}{5.49 + 1} = 0.15$$

Using this ratio, one can calculate the amount of Percoll (undiluted) required to make a final working solution of known density and osmolality.

$$V_0 = V \frac{R_x \rho_{10} - (1 - R_x)}{\rho_0 - 1}$$

$V_0$  = volume of percoll undiluted (mL)

$V$  = volume on final working solution (mL)

$\rho$  = desired density of final working solution (g/mL)

$R_x$  = fraction of total volume which is solute concentrate

$\rho_0$  = density of Percoll undiluted (g/mL)

$\rho_{10}$  = density of 1.5 M NaCl (1.058 g/mL)

$$V_o \text{ solution} = 100 \text{ mL} * \frac{\left(1.07 \frac{\text{g}}{\text{mL}}\right) - \left(0.15 * 1.058 \frac{\text{g}}{\text{mL}}\right) - (1 - 0.15)}{\left(1.130 \frac{\text{g}}{\text{mL}} - 1\right)} = \mathbf{47.15 \text{ mL}}$$

$$V \text{ distilled water in solution} = V - V_o = 100 \text{ mL} - 47.15 \text{ mL} = \mathbf{37.85 \text{ mL}}$$

$$\text{Volume of } 1.5 \text{ M NaCl} = R_x * \text{Working Volume} = .15 * 100 \text{ mL} = \mathbf{15 \text{ mL}}$$

Final Working SIP:

- 47.15 mL Percoll
- 37.85 mL Distilled Water
- 15 mL 1.5 M NaCl

## G. Cyclone Data

Date	MLTSS			MPOR		Flow Split %		Mass Split by Feed %		Mass Split by Sum %		GPM per Cyclone	
	Feed	Under	Over	RAS	MLS	Over	Under	Over	Under	Over	Under	Pump 1	Pump 2
3/2/2015	4240	6185	3740	4260	1980	97.8	2.2	86.3	3.2	96.4	3.6	80.0	78.5
3/5/2015	5245	6425	3750	5260	2160	92.8	7.2	66.3	8.8	88.3	11.7	75.0	75.0
3/6/2015	5760	7045	5060	4980	2020	92.9	7.1	81.6	8.6	90.4	9.6	74.5	73.0
3/9/2015	4425	5645	4225	4580	2080	92.8	7.2	88.6	9.2	90.6	9.4	75.4	75.0
3/10/2015	4420	5520	3680			92.8	7.2	77.3	9.0	89.6	10.4	75.7	75.8
3/18/2015	4775	5840	4360	5620	2100	93.5	6.5	85.4	7.9	91.5	8.5	75.1	64.8
3/25/2015	4335	5725	3940	4480	2080	93.2	6.8	84.7	9.0	90.4	9.6	75.2	72.9
3/26/2015		9620	4160	4460	1840	93.5	6.5					75.2	75.1
3/27/2015						92.7	7.3					76.3	72.5
3/28/2015						92.0	8.0					74.5	74.0
3/29/2015		10200	4220	4180	1880	92.6	7.4					74.0	74.0
3/30/2015						93.7	6.3					75.1	74.0
3/31/2015		5400	4140	4300	1920	93.3	6.7					75.0	74.8
4/1/2015						93.4	6.6					75.1	74.6
4/2/2015		5560	3760	4240	2080	93.1	6.9	82.6	9.0	90.1	9.9	74.6	74.0
4/3/2015						93.6	6.4					74.8	74.8
4/4/2015						93.3	6.7					75.4	75.4
4/5/2015		5380	4220	4360	2120	93.2	6.8	90.2	8.4	91.5	8.5	74.5	73.9
4/6/2015						93.0	7.0					75.0	74.9
4/7/2015		6060	4360	4280	2140	94.6	5.4	96.3	7.7	92.6	7.4	75.0	75.5
4/8/2015	4185	5820	3580			93.7	6.3	80.2	8.8	90.1	9.9	71.4	71.7
4/9/2015		5860	4320	4340	1920	93.6	6.4	93.2	8.6	91.6	8.4	74.1	74.2
4/10/2015						93.7	6.3					74.5	74.8
4/11/2015						94.7	5.8					75.0	75.2

15						2							
4/12/20		5460	394	404	202	94.	6.0	91.7	8.1	91.	8.1	74.6	74.7
15			0	0	0	0				9			
4/13/20						94.	5.7					74.6	74.4
15						3							
4/14/20		5060	376	382	182	94.	5.9	92.6	7.8	92.	7.8	75.0	74.9
15			0	0	0	1				2			
4/15/20						94.	5.6					75.1	74.0
15						4							
4/16/20	395	5160	319	380	180	98.	5.7	79.2	7.9	90.	9.1	75.1	74.6
15	5		5	0	0	0				9			
4/17/20						94.	6.0					75.2	75.2
15						0							
4/18/20						94.	5.9					75.4	75.7
15						1							
4/19/20		4900	350	350	170	94.	5.5	94.5	7.7	92.	7.6	75.7	75.1
15			0	0	0	5				4			
4/20/20						95.	5.0					76.0	76.3
15						0							
4/21/20		5860	380	400	176	94.	5.9	89.4	8.6	91.	8.8	76.1	76.6
15			0	0	0	1				2			
4/22/20	411		437			94.	5.4	100.	8.1	92.	7.4	76.0	76.1
15	0		5			6		7		6			
4/23/20		5720	402	410	184	94.	5.5	92.7	7.6	92.	7.6	76.1	76.1
15			0	0	0	5				4			
4/24/20						94.	5.4					75.5	76.1
15						6							
4/25/20						94.	5.7					75.7	75.9
15						3							
4/26/20		5460	454	408	162	94.	5.3	105.	7.0	93.	6.3	75.6	75.5
15			0	0	0	7		4		7			
4/27/20						94.	5.7					75.1	75.0
15						3							
4/28/20	364	5290	334	376	162	94.	5.7	86.8	8.2	91.	8.6	74.8	74.7
15	0		5	0	0	4				4			
4/29/20						94.	5.6					75.2	74.8
15						4							
4/30/20		5620	362	382	176	94.	5.5	89.5	8.2	91.	8.4	75.8	74.7
15			0	0	0	5				6			
5/1/201													
5													
5/2/201						94.	5.9					74.7	0.0
5						1							
5/3/201		5720	388	390	190	94.	5.7	93.8	8.3	91.	8.2	75.3	0.0
5			0	0	0	3				8			
5/4/201						94.	5.4					75.6	0.0
5						6							
5/5/201	599	9050	565	552	220	94.	5.6	88.8	8.5	91.	8.7	75.4	0.0
5	5		0	0	0	2				3			
5/6/201						94.	5.3					76.0	0.0
5						7							
5/7/201		7180	532	570	220	94.	5.3	88.3	6.7	92.	7.1	75.7	

5		0	0	0	7					9			
5/8/201													
5													
5/9/201													
5													
5/10/20			500	256									
15			0	0									
5/11/20					82.	17.7					77.5	78.0	
15					3								
5/12/20	6020	530	598	276	82.	17.3	73.3	17.5	80.	19.2	77.9	78.6	
15		0	0	0	7				8				
5/13/20					82.	17.7					78.3	77.8	
15					3								
5/14/20	6020	520	532	248	82.	17.4	80.7	19.7	80.	19.6	77.8	75.6	
15		0	0	0	6				4				

## H. Plant Data

Fe added/Influent TP, Fe added/P Removed, SVI5, SVI30

Date	Fe/Influent TP	Fe/Influent TP	Fe/P Removed	Fe/P removed	SVI5	SVI5	SVI30	SVI30
	mole/mole	7 day ave	mole/mole	7 day ave	mL/g	7 day ave	mL/g	7 day ave
1/1/2015					270	275	141	141
1/2/2015						275		141
1/3/2015	1.0157		1.1418			275		141
1/4/2015					286	283	146	144
1/5/2015	0.8653					283		144
1/6/2015					294	283	146	145
1/7/2015	0.7992		1.0448			283		145
1/8/2015					355	311	161	151
1/9/2015		0.8934		1.0933		311		151
1/10/2015	0.5642	0.7429	0.6038	0.8243		311		151
1/11/2015		0.7429		0.8243	292	314	151	153
1/12/2015	0.5172	0.6269		0.8243		314		153
1/13/2015		0.6269		0.8243	309	319	154	155
1/14/2015	0.6638	0.5817	0.7474	0.6756		319		155
1/15/2015		0.5817		0.6756	282	295	141	149
1/16/2015		0.5817		0.6756		295		149
1/17/2015		0.5905		0.7474		295		149
1/18/2015		0.5905		0.7474	284	292	147	147
1/19/2015	0.5315	0.5976	0.5315	0.6395		292		147
1/20/2015		0.5976		0.6395	274	280	143	144
1/21/2015	0.5124	0.5219	0.5124	0.5219		280		144
1/22/2015		0.5219		0.5219	281	280	142	144
1/23/2015		0.5219		0.5219		280		144
1/24/2015	0.5142	0.5194	0.5142	0.5194		280		144
1/25/2015		0.5194		0.5194	305	287	150	145
1/26/2015	0.5074	0.5113	0.5074	0.5113		287		145
1/27/2015		0.5113		0.5113	293	293	147	146
1/28/2015		0.5108		0.5108		293		146
1/29/2015		0.5108		0.5108	303	301	152	149
1/30/2015		0.5108		0.5108		301		149
1/31/2015	0.5138	0.5106	0.6214	0.5644		301		149
2/1/2015		0.5106		0.5644	270	289	124	141
2/2/2015	0.5492	0.5315	0.6501	0.6357		289		141
2/3/2015		0.5315		0.6357	278	284	136	137
2/4/2015	0.5601	0.5410	0.6910	0.6542		284		137
2/5/2015		0.5410		0.6542	309	286	150	137
2/6/2015		0.5410		0.6542		286		137
2/7/2015	0.5080	0.5391	0.6513	0.6641		286		137
2/8/2015		0.5391		0.6641	299	296	148	145
2/9/2015	0.4561	0.5081	0.5350	0.6258		296		145
2/10/2015		0.5081		0.6258	322	310	153	150

2/11/2015	0.5691	0.5111	0.7659	0.6507		310		150
2/12/2015		0.5111		0.6507	237	286	107	136
2/13/2015		0.5111		0.6507		286		136
2/14/2015		0.5126		0.6505		286		136
2/15/2015		0.5126		0.6505	313	291	151	137
2/16/2015	0.5924	0.5808	0.8509	0.8084		291		137
2/17/2015		0.5808		0.8084	321	290	157	138
2/18/2015	0.6910	0.6417	1.1288	0.9898		290		138
2/19/2015		0.6417		0.9898	311	315	150	153
2/20/2015		0.6417		0.9898		315		153
2/21/2015	0.5621	0.6152	0.6827	0.8874		315		153
2/22/2015		0.6152		0.8874	324	318	150	153
2/23/2015	1.0303	0.7611	1.1563	0.9893		318		153
2/24/2015		0.7611		0.9893	330	321	151	151
2/25/2015	1.1263	0.9062	1.2709	1.0366		321		151
2/26/2015		0.9062		1.0366	289	314	139	147
2/27/2015		0.9062		1.0366		314		147
2/28/2015	0.9381	1.0316	1.0284	1.1519		314		147
3/1/2015		1.0316		1.1519	259	292	108	132
3/2/2015	1.1055	1.0566	1.5621	1.2871		292		132
3/3/2015		1.0566		1.2871	241	263	122	123
3/4/2015	0.8145	0.9527	0.9559	1.1821		263		123
3/5/2015		0.9527		1.1821	239	246	120	117
3/6/2015		0.9527		1.1821		246		117
3/7/2015	1.0090	0.9763	1.1517	1.2232		246		117
3/8/2015		0.9763		1.2232	221	234	114	119
3/9/2015	1.0116	0.9450	1.1068	1.0715		234		119
3/10/2015		0.9450		1.0715	249	236	116	117
3/11/2015	0.8217	0.9474	0.9136	1.0574		236		117
3/12/2015		0.9474		1.0574	234	235	112	114
3/13/2015		0.9474		1.0574		235		114
3/14/2015	0.6621	0.8318	0.7233	0.9146		235		114
3/15/2015		0.8318		0.9146	232	238	118	115
3/16/2015	0.8910	0.7916	1.4520	1.0296		238		115
3/17/2015		0.7916		1.0296	247	238	122	117
3/18/2015	0.8650	0.8060	0.9501	1.0418		238		117
3/19/2015		0.8060		1.0418	244	241	120	120
3/20/2015		0.8060		1.0418		241		120
3/21/2015	0.7698	0.8419	1.0606	1.1542		241		120
3/22/2015		0.8419		1.1542	250	247	121	121
3/23/2015	0.8092	0.8147	0.8872	0.9660		247		121
3/24/2015		0.8147		0.9660	234	243	111	117
3/25/2015	0.6403	0.7398	0.6987	0.8822		243		117
3/26/2015		0.7398		0.8822	250	245	121	118
3/27/2015		0.7398		0.8822		245		118
3/28/2015	0.7337	0.7278	0.8128	0.7996		245		118
3/29/2015		0.7278		0.7996	225	236	119	117
3/30/2015	0.6860	0.6867	0.9406	0.8174		236		117

3/31/2015		0.6867		0.8174	245	240	137	126
4/1/2015	0.7936	0.7378	0.9540	0.9025		240		126
4/2/2015		0.7378		0.9025	237	236	119	125
4/3/2015		0.7378		0.9025		236		125
4/4/2015	0.7910	0.7569	0.9500	0.9482		236		125
4/5/2015		0.7569		0.9482	258	247	126	127
4/6/2015	0.7760	0.7869	0.8597	0.9212		247		127
4/7/2015		0.7869		0.9212	260	252	132	126
4/8/2015	0.6961	0.7544	0.8305	0.8801		252		126
4/9/2015		0.7544		0.8801	276	265	138	132
4/10/2015		0.7544		0.8801		265		132
4/11/2015	0.7342	0.7354	0.8295	0.8399		265		132
4/12/2015		0.7354		0.8399	241	259	124	131
4/13/2015	0.7313	0.7206	0.7985	0.8195		259		131
4/14/2015		0.7206		0.8195	253	257	132	131
4/15/2015	0.7576	0.7410	0.8626	0.8302		257		131
4/16/2015		0.7410		0.8302	254	249	132	129
4/17/2015		0.7410		0.8302		249		129
4/18/2015	0.7291	0.7393	0.8796	0.8469		249		129
4/19/2015		0.7393		0.8469	237	248	128	130
4/20/2015	0.6470	0.7112	0.7432	0.8285		248		130
4/21/2015		0.7112		0.8285	244	245	132	131
4/22/2015	0.7373	0.7045	0.8027	0.8085		245		131
4/23/2015		0.7045		0.8085	243	241	130	130
4/24/2015		0.7045		0.8085		241		130
4/25/2015	0.6515	0.6786	0.7379	0.7613		241		130
4/26/2015		0.6786		0.7613	259	249	134	132
4/27/2015	0.7610	0.7166	0.8328	0.7911		249		132
4/28/2015		0.7166		0.7911	288	263	148	138
4/29/2015	0.7708	0.7277	0.8392	0.8033		263		138
4/30/2015		0.7277		0.8033	257	268	140	141
5/1/2015		0.7277		0.8033		268		141
5/2/2015	0.6853	0.7390	0.7584	0.8101		268		141
5/3/2015		0.7390		0.8101	242	263	128	139
5/4/2015	0.6627	0.7062	0.7142	0.7706		263		139
5/5/2015		0.7062		0.7706	245	248	132	133
5/6/2015	0.7048	0.6842	0.7426	0.7384		248		133
5/7/2015		0.6842		0.7384	232	240	132	131
5/8/2015		0.6842		0.7384		240		131
5/9/2015	0.6538	0.6737	0.7809	0.7459		240		131
5/10/2015		0.6737		0.7459	275	251	145	136
5/11/2015	0.6874	0.6820	0.7229	0.7488		251		136
5/12/2015		0.6820		0.7488	278	261	149	142
5/13/2015	0.6103	0.6505	0.6397	0.7145		261		142
5/14/2015		0.6505		0.7145	313	289	164	152
5/15/2015		0.6505		0.7145		289		152
5/16/2015	0.5786	0.6254	0.6445	0.6690		289		152
5/17/2015		0.6254		0.6690	263	285	141	151

5/18/2015	0.5056	0.5648	0.5959	0.6267		285		151
5/19/2015		0.5648		0.6267	269	282	148	151
5/20/2015	0.4010	0.4951	0.4241	0.5548		282		151
5/21/2015		0.4951		0.5548	253	262	141	143
5/22/2015		0.4951		0.5548		262		143
5/23/2015		0.4533		0.5100		262		143
5/24/2015		0.4533		0.5100	245	256	133	141
5/25/2015	0.4112	0.4061		0.4241		256		141
5/26/2015		0.4061		0.4241	223	241	133	135
5/27/2015	0.3972	0.4042		0.4241		241		135
5/28/2015		0.4042		0.4241	233	234	130	132
5/29/2015		0.4042		0.2955		234		132
5/30/2015	0.2810	0.3631	0.2955	0.2955		234		132
5/31/2015		0.3631		0.2955	207	221	123	128
6/1/2015	0.2068	0.2950	0.2916	0.2935		221		128
6/2/2015		0.2950		0.2935	221	220	121	125
6/3/2015	0.2588	0.2489	0.3183	0.3018		220		125
6/4/2015		0.2489		0.3018	204	210	120	121
6/5/2015		0.2489		0.3018		210		121
6/6/2015	0.3143	0.2600	0.3467	0.3189		210		121
6/7/2015		0.2600		0.3189	242	222	136	126
6/8/2015	0.1978	0.2570	0.2459	0.3037		222		126
6/9/2015		0.2570		0.3037	250	232	143	133
6/10/2015	0.2201	0.2441	0.2398	0.2775		232		133
6/11/2015		0.2441		0.2775	225	239	131	137
6/12/2015		0.2441		0.2775		239		137
6/13/2015	0.2298	0.2159	0.2935	0.2597		239		137
6/14/2015		0.2159		0.2597	216	231	132	135
6/15/2015	0.2304	0.2268	0.2645	0.2659		231		135
6/16/2015		0.2268		0.2659	234	225	139	134
6/17/2015	0.3278	0.2627	0.4046	0.3209		225		134
6/18/2015		0.2627		0.3209	269	240	146	139
6/19/2015		0.2627		0.3209		240		139
6/20/2015	0.3225	0.2936	0.3955	0.3549		240		139
6/21/2015		0.2936		0.3549	232	245	135	140
6/22/2015	0.3397	0.3300	0.7448	0.5150		245		140
6/23/2015		0.3300		0.5150	264	255	154	145
6/24/2015	0.4681	0.3768	0.5378	0.5594		255		145
6/25/2015		0.3768		0.5594	257	251	147	145
6/26/2015		0.3768		0.5594		251		145
6/27/2015	0.8607	0.5562	1.5204	0.9343		251		145
6/28/2015		0.5562		0.9343	291	271	165	155
6/29/2015	0.6977	0.6755	0.7499	0.9360		271		155
6/30/2015		0.6755		0.9360	247	265	142	151
7/1/2015	0.6529	0.7371	0.7566	1.0090		265		151
7/2/2015		0.7371		1.0090	242	260	140	149
7/3/2015		0.7371		1.0090		260		149
7/4/2015	0.7326	0.6944	0.7822	0.7629		260		149

7/5/2015		0.6944		0.7629	249	246	145	142
7/6/2015	0.6954	0.6937	0.7538	0.7642		246		142
7/7/2015		0.6937		0.7642	278	256	155	147
7/8/2015	0.6203	0.6828		0.7680		256		147
7/9/2015		0.6828		0.7680	296	274	163	154
7/10/2015		0.6828		0.7680		274		154
7/11/2015	0.6367	0.6508	0.6807	0.7172		274		154
7/12/2015		0.6508		0.7172	263	279	146	155
7/13/2015	0.6594	0.6388	0.7018	0.6912		279		155
7/14/2015		0.6388		0.6912	265	275	149	153
7/15/2015	0.7216	0.6726	0.7999	0.7275		275		153
7/16/2015		0.6726		0.7275	243	257	135	143
7/17/2015		0.6726		0.7275		257		143
7/18/2015	0.6641	0.6817	0.6942	0.7320		257		143
7/19/2015		0.6817		0.7320	245	251	134	139
7/20/2015	0.5515	0.6457	0.5822	0.6921		251		139
7/21/2015		0.6457		0.6921	222	237	132	134
7/22/2015	0.5325	0.5827	0.5588	0.6117		237		134
7/23/2015		0.5827		0.6117	233	233	138	135
7/24/2015		0.5827		0.6117		233		135
7/25/2015	0.5234	0.5358	0.5623	0.5678		233		135
7/26/2015		0.5358		0.5678	241	232	140	137
7/27/2015	0.4741	0.5100	0.5027	0.5413		232		137
7/28/2015		0.5100		0.5413	270	248	155	145
7/29/2015		0.4987		0.5325		248		145
7/30/2015		0.4987		0.5325	247	253	147	147
7/31/2015	0.6672	0.5549	0.6995	0.5882		253		147
8/1/2015		0.5706		0.6011		253		147
8/2/2015	0.3905	0.5106	0.4107	0.5376	242	253	142	148
8/3/2015		0.5288		0.5551		253		148
8/4/2015	0.3865	0.4814	0.3865	0.4989	215	235	132	140
8/5/2015		0.4814		0.4989		235		140
8/6/2015		0.4814		0.4989	213	223	125	133
8/7/2015	0.3919	0.3896	0.4193	0.4055		223		133
8/8/2015		0.3896		0.4055		223		133
8/9/2015	0.4233	0.4006	0.5391	0.4483	208	212	122	126
8/10/2015		0.4006		0.4483		212		126
8/11/2015	0.4238	0.4130	0.4238	0.4607	223	215	130	126
8/12/2015		0.4130		0.4607		215		126
8/13/2015		0.4130		0.4607	218	216	131	127
8/14/2015	0.4251	0.4241		0.4814		216		127
8/15/2015		0.4241		0.4814		216		127
8/16/2015	0.4177	0.4222	0.5197	0.4717	254	232	150	137
8/17/2015		0.4222		0.4717		232		137
8/18/2015	0.4291	0.4240	0.4291	0.4744	265	246	158	146
8/19/2015		0.4240		0.4744		246		146
8/20/2015		0.4240		0.4744	258	259	153	154
8/21/2015	0.4117	0.4195	0.4371	0.4620		259		154

8/22/2015		0.4195		0.4620		259		154
8/23/2015	0.4076	0.4161	0.4076	0.4246	258	260	159	157
8/24/2015		0.4161		0.4246		260		157
8/25/2015		0.4096		0.4223	270	262	161	158
8/26/2015		0.4096		0.4223		262		158
8/27/2015		0.4096		0.4223	272	267	153	157
8/28/2015		0.4076		0.4076		267		157
8/29/2015		0.4076		0.4076		267		157
8/30/2015	0.4249	0.4249		0.3926	239	260	141	151
8/31/2015		0.4249		0.3776		260		151
9/1/2015	0.3638	0.3943	0.3776	0.3776	243	251	139	144
9/2/2015		0.3943		0.3776		251		144
9/3/2015		0.3943		0.3776	231	238	135	138
9/4/2015		0.3943		0.3776		238		138
9/5/2015		0.3943		0.3776		238		138
9/6/2015	0.3965	0.3801	0.4124	0.3950	241	238	142	139
9/7/2015		0.3801		0.3950		238		139
9/8/2015	0.4027	0.3996	0.4184	0.4154	251	241	148	142
9/9/2015		0.3996		0.4154		241		142
9/10/2015		0.3996		0.4154	262	251	154	148
9/11/2015	0.3703	0.3898	0.4388	0.4232		251		148
9/12/2015		0.3898		0.4232		251		148
9/13/2015	0.3213	0.3648		0.4286	279	264	159	154
9/14/2015		0.3648		0.4286		264		154
9/15/2015	0.2943	0.3286	0.3119	0.3754	287	276	160	158
9/16/2015		0.3286		0.3754		276		158
9/17/2015		0.3286		0.3754	264	276	144	154
9/18/2015	0.3131	0.3096	0.3362	0.3241		276		154
9/19/2015		0.3096		0.3241		276		154
9/20/2015	0.3241	0.3105		0.3241	300	283	168	157
9/21/2015		0.3105		0.3241				
9/22/2015	0.2870	0.3081		0.3362				
9/23/2015		0.3081		0.3362				
9/24/2015		0.3081		0.3362				
9/25/2015	0.2633	0.2915	0.2788	0.2788				
9/26/2015		0.2915		0.2788				
9/27/2015	0.3024	0.2842		0.2788				
9/28/2015		0.2842		0.2788				
9/29/2015		0.2828		0.2788				
9/30/2015	0.2129	0.2595		0.2788				
10/1/2015		0.2595		0.2788				
10/2/2015		0.2577		0.4380				
10/3/2015	0.5615	0.3589	0.5972	0.5972				
10/4/2015		0.3872		0.5972				
10/5/2015	0.6489	0.4744	0.6993	0.6483				
10/6/2015		0.4744		0.6483				
10/7/2015	0.1795	0.4633	0.1928	0.4965				
10/8/2015		0.4633		0.4965				
10/9/2015		0.4633		0.4965				

---

<b>10/10/2015</b>		0.4142	0.4461
<b>10/11/2015</b>		0.4142	0.4461
<b>10/12/2015</b>	0.2280	0.2037	0.1928

---

## I. Settleability

### ISV of Cyclone Sampling Points

	<b>Feed</b>	<b>Underflow</b>	<b>Overflow</b>
<b>Date</b>	m/hr	m/hr	m/hr
<b>6/18/2015</b>	1.7160	2.2903	0.1800
<b>7/8/2015</b>	2.8320	2.3486	0.0176
<b>7/14/2015</b>	0.2503	0.4217	0.1200
<b>7/16/2015</b>	0.9360	1.7177	0.2118
<b>7/21/2015</b>	1.7160	3.4149	0.8400
<b>7/27/2015</b>	0.2143	1.3749	0.1659
<b>8/26/2015</b>	2.9520	4.0920	0.4105
<b>9/7/2015</b>	2.2886	4.3418	2.3171
<b>9/10/2015</b>	0.5996	2.7620	0.3075

## J. Solids Flux Data

Date	TSS	V	SFg
	g/L	m/hr	Kg/m <sup>2</sup> *hr
<b>11/11/14</b>	3330	0.04	0.142
	2664	0.07	0.182
	2165	0.13	0.276
	1665	1.55	2.58
	1249	2.43	3.041
	832.5	3.47	2.890
<b>11/18/14</b>	2888	0.04	0.107
	2527	0.06	0.143
	2166	0.09	0.190
	1805	0.56	1.005
	1444	2.31	3.343
	1083	3.12	3.378
	722	4.34	3.131
<b>12/10/14</b>	3112	0.07	0.203
	2723	0.13	0.343
	2334	0.24	0.558
	1945	0.69	1.351
	1556	1.89	2.938
	1167	3.26	3.799
	778	4.86	3.784
<b>2/19/15</b>	3464	0.04	0.147
	3031	0.08	0.240
	2598	0.14	0.355
	2165	1.61	3.490
	1732	2.18	3.778
	1299	2.68	3.482
	866	3.96	3.431
<b>3/26/15</b>	3176	0.14	0.452
	2779	1.28	3.568
	2382	1.50	3.576
	1985	2.02	4.007
	1588	2.68	4.248
	1191	3.99	4.757
<b>4/6/15</b>	4050	0.05	0.187
	3240	0.05	0.165
	3119	0.08	0.263
	2835	0.11	0.301
	2430	0.14	0.335
	2228	0.20	0.454
	2025	1.54	3.110
	1620	2.32	3.760
<b>4/10/15</b>	3810	0.05	0.208
	3334	0.06	0.200
	2858	0.10	0.289

	2381	0.26	0.629
	1905	1.98	3.767
	1524	2.24	3.415
	1143	2.59	2.959
<b>4/29/15</b>	3535	0.04	0.149
	3156	0.06	0.206
	2904	0.11	0.334
	2525	0.29	0.727
	2020	2.76	5.586
	1768	2.66	4.699
	1515	3.48	5.272
<b>5/28/15</b>	3395	0.08	0.265
	2910	0.18	0.516
	2667.5	0.21	0.549
	2425	1.25	3.026
	2183	1.89	4.119
	1940	2.85	5.529
	1455	3.96	5.762
<b>7/14/15</b>	3249	0.11	0.358
	2785	0.22	0.610
	2553	0.63	1.615
	2321	1.41	3.273
	2089	2.15	4.493
	1857	3.00	5.570
	1393	4.17	5.806
<b>8/7/15</b>	3750	0.71	2.668
	3125	1.53	4.768
	2750	1.79	4.928
	2500	2.74	6.857
	2000	3.01	6.777
	1500	4.28	8.564
<b>8/26/15</b>	3375	0.18	0.618
	3000	0.23	0.702
	2750	1.28	3.507
	2250	2.23	5.580
	2000	0.79	1.769
	1500	2.62	5.246
<b>9/7/15</b>	4250	0.23	0.956
	3750	0.64	2.388
	3250	0.62	2.030
	2500	3.84	9.600
	1750	2.96	5.172
	1250	5.15	6.435
	1000	6.07	6.072
<b>9/10/15</b>	3750	0.14	0.510
	3000	0.26	0.766
	2500	2.68	6.696

2000	3.39	6.789
1750	5.40	9.450

### K. Classification of Settling Rates

Date	Flocs	Aggregates	Granules	SVI30	MLSS
	%	%	%	mL/g	mg/L
9/24/2014	28.3	71.7	0.0	132.0	1960
11/6/2014	17.6	82.4	0.0	175.5	1920
11/13/2014	1.2	98.8	0.0	187.5	1760
11/19/2014	17.4	82.6	0.0	209.8	1940
12/3/2014	33.2	66.8	0.0	177.3	2160
12/16/2014	27.0	73.0	0.0	163.8	2160
1/22/2015	15.8	84.2	0.0	142.1	2020
1/27/2015	2.8	97.2	0.0	146.7	1840
3/18/2015	3.2	96.8	0.0	121.5	2000
4/2/2015	2.1	97.9	0.0	137.0	1920
4/23/2015	6.3	92.0	1.7	127.6	1700
5/13/2015	11.8	83.6	4.6	156.5	2560
6/18/2015	33.2	63.6	3.2	146.2	2120
7/14/2015	2.5	97.5	0.0	149.1	2300
8/26/2015	62.3	14.1	23.5	173.0	2260
9/10/2015	45.1	14.4	40.4	156.0	2020
9/19/2015	41.6	45.0	13.5	154.0	2100

## L. James River IFAS Tank Profiles

Reactor abbreviations:

- PCE= Primary Clarifier Effluent
- ANX= Anoxic Tank
- IFAS= Aeration Tank (Integrated Fixed Film AS)
- SCE= Secondary Clarifier Effluent
- RAS= Return Activated Sludge

**9/15/2014**

Reactor	NH4	NO3	NO2	NOX	PO4	DO	pH	Temp
PCE		0.714	0.035	0.749	4.000			
ANX1	1.710	0.525	0.015	0.540	5.900			
ANX2		0.442	0.030	0.472	6.400			
ANX3		0.371	0.025	0.396	8.500			
IFAS1	0.465	3.290	0.015	3.305	1.600			
IFAS2	0.181	4.620	0.020	4.640	0.900			
IFAS3	0.088	5.470	0.020	5.490	1.100			
ANX4	0.217	5.530	0.270	5.800	0.600			
SCE	0.035	2.670	0.015	2.685	0.800			
RAS	0.821	0.513	0.015	0.528	44.500			

**9/26/2014**

Reactor	NH4	NO3	NO2	NOX	PO4	DO	pH	Temp
PCE	25.90	1.17	1.40	2.57	7.30			24.4
ANX1	5.44	0.95	1.50	2.45	3.10			24.1
ANX2	6.08	0.57	0.80	1.36	3.40			24.5
ANX3	4.98	0.63	0.67	1.30	3.10			24.3
IFAS1	2.85	3.34	3.69	7.03	1.10			24.4
IFAS2	0.20	4.35	4.64	8.99	0.60			24.6
IFAS3	0.32	4.72	5.05	9.77	0.70			23.6
ANX4	0.46	4.71	5.26	9.97	0.90			24.7
SCE	0.32	3.60	4.12	7.72	0.50			24.2
RAS	0.49	1.14	1.55	2.69	3.00			24.4

**10/17/2014**

<b>Reactor</b>	<b>NH4</b>	<b>NO3</b>	<b>NO2</b>	<b>NOX</b>	<b>PO4</b>	<b>DO</b>	<b>pH</b>	<b>Temp</b>
<b>PCE</b>		1.480	0.095	1.575	6.9	1.59	6.47	24.5
<b>ANX1</b>	9.620	1.070	1.045	2.115	3.8	0.15	6.65	24.8
<b>ANX2</b>	9.330	0.828	0.485	1.313	3.9	0.12	6.69	25.0
<b>ANX3</b>	9.550	0.373	0.045	0.418	4.8	0.13	6.68	24.9
<b>IFAS1</b>	4.910	4.590	0.340	4.930	1.5	3.63	6.54	25.1
<b>IFAS2</b>	1.770	6.890	0.475	7.365	0.7	4.41	6.44	25.1
<b>IFAS3</b>	1.180	7.280	0.455	7.735	0.5	4.62	6.40	25.1
<b>ANX4</b>	1.680	6.640	0.750	7.390	0.5	0.15	6.38	25.0
<b>SCE</b>	0.464	4.650	0.705	5.355	0.6	3.20	6.66	25.1
<b>RAS</b>	1.720	0.453	0.100	0.553	7.3	0.22	6.57	20.9

**10/28/2014**

<b>Reactor</b>	<b>NH4</b>	<b>NO3</b>	<b>NO2</b>	<b>NOX</b>	<b>PO4</b>	<b>DO</b>	<b>pH</b>	<b>Temp</b>
<b>PCE</b>	34.900	1.110	0.100	1.210	8.9	1.88	6.71	24.0
<b>ANX1</b>	7.070	0.570	0.303	0.873	6.5	0.10	6.78	23.8
<b>ANX2</b>	6.950	0.430	0.042	0.472	6.6	0.10	6.49	23.8
<b>ANX3</b>	6.880	0.429	0.015	0.444	7.6	0.06	6.75	23.9
<b>IFAS1</b>	0.552	5.260	0.434	5.694	4.1	4.31	6.53	23.9
<b>IFAS2</b>	0.898	5.610	0.273	5.883	4.1	1.91	6.51	23.9
<b>IFAS3</b>	0.548	5.830	0.267	6.097	4.1	5.86	6.52	23.6
<b>ANX4</b>	0.073	0.260	0.208	0.468	3.6	0.01	6.47	23.8
<b>SCE</b>	0.087	4.790	0.189	4.979	2.4	3.48	6.76	24.0
<b>RAS</b>	3.030	0.629	0.030	0.659	48.0	0.17	6.53	21.2

**11/21/2014**

<b>Reactor</b>	<b>NH4</b>	<b>NO3</b>	<b>NO2</b>	<b>NOX</b>	<b>PO4</b>	<b>DO</b>	<b>pH</b>	<b>Temp</b>
<b>PCE</b>	35.100	2.020	0.085	2.105	9.1	3.43	6.90	17.8
<b>ANX1</b>	12.900	1.550	1.890	3.440		0.21	6.89	16.7
<b>ANX2</b>	13.400	0.774	0.735	1.509		0.36	6.89	16.2
<b>ANX3</b>	12.600	0.541	0.390	0.931	8.1	0.09	6.90	16.6
<b>IFAS1</b>	6.850	6.030	0.540	6.570		4.43	6.89	17.3

<b>IFAS2</b>	6.720	6.260	0.375	6.635		4.24	6.90	17.3
<b>IFAS3</b>	5.570	6.720	0.390	7.110	4.1	5.08	6.90	17.3
<b>ANX4</b>	6.390	7.160	0.475	7.635	4.2	1.19	6.90	16.9
<b>SCE</b>	4.400	5.540	0.805	6.345	2.7	5.47	6.91	15.2
<b>RAS</b>	4.290	0.463	0.025	0.488	17.7	0.14	6.88	13.6

**12/04/2014**

<b>Reactor</b>	<b>NH4</b>	<b>NO3</b>	<b>NO2</b>	<b>NOX</b>	<b>PO4</b>	<b>DO</b>	<b>pH</b>	<b>Temp</b>
<b>PCE</b>	27.500	0.758	0.065	0.823	3.6	2.40	7.06	16.9
<b>ANX1</b>	7.190	0.807	0.555	1.362	1.9	0.82	7.09	16.6
<b>ANX2</b>	1.200	0.415	0.055	0.470	2.9	0.38	7.05	17.0
<b>ANX3</b>	6.900	0.339	0.025	0.364	3.3	0.19	7.02	16.9
<b>IFAS1</b>	3.360	3.600	0.160	3.760	1.6	4.47	7.02	15.4
<b>IFAS2</b>	3.670	5.190	0.180	5.370	1.4	4.67	7.01	15.8
<b>IFAS3</b>	1.200	5.620	0.195	5.815	1.1	5.31	7.03	16.2
<b>ANX4</b>	2.490	5.560	0.290	5.850	1.2	0.95	6.99	16.0
<b>SCE</b>	0.929	4.600	0.295	4.895	0.7	4.69	7.02	14.9
<b>RAS</b>	1.970	0.390	0.035	0.425	2.3	0.16	6.98	14.1

**12/18/2014**

<b>Reactor</b>	<b>NH4</b>	<b>NO3</b>	<b>NO2</b>	<b>NOX</b>	<b>PO4</b>	<b>DO</b>	<b>pH</b>	<b>Temp</b>
<b>PCE</b>	34.900	1.260	0.110	1.370	6.1	2.28	7.03	15.5
<b>ANX1</b>	8.830	0.851	0.255	1.106	1.8	0.60	7.04	14.9
<b>ANX2</b>	9.950	0.528	0.030	0.558	4.0	0.12	7.03	15.3
<b>ANX3</b>	9.100	0.304	0.035	0.339	2.9	0.10	7.08	14.7
<b>IFAS1</b>	5.220	3.490	0.140	3.630	1.2	3.92	6.95	14.6
<b>IFAS2</b>	4.440	4.690	0.125	4.815	1.2	5.33	6.96	14.5
<b>IFAS3</b>	2.990	5.090	0.165	5.255	1.0	4.94	6.94	14.5
<b>ANX4</b>	3.530	5.590	0.225	5.815	1.0	1.48	6.82	14.6
<b>SCE</b>	1.410	4.330	0.305	4.635	0.5	4.60	6.92	13.7
<b>RAS</b>	2.490	0.584	0.060	0.644	0.9	1.84	6.96	13.6

**2/17/2015**

<b>Reactor</b>	<b>NH4</b>	<b>NO3</b>	<b>NO2</b>	<b>NOX</b>	<b>PO4</b>	<b>DO</b>	<b>pH</b>	<b>Temp</b>
<b>PCE</b>	29.200	0.964	0.022	0.986	4.0	2.70	6.89	11.7
<b>ANX1</b>	10.200	0.857	0.116	0.973	2.2	0.45	6.84	12.1
<b>ANX2</b>	10.100	0.357	0.038	0.395	2.2	0.17	6.85	11.9
<b>ANX3</b>	11.600	0.189	0.014	0.203	11.8	0.12	6.87	12.1
<b>IFAS1</b>	1.950	2.800	0.204	3.004	1.5	3.98	6.84	12.0
<b>IFAS2</b>	6.160	3.250	0.238	3.488	1.7	4.42	6.85	12.2
<b>IFAS3</b>	5.880	3.680	0.264	3.944	1.8	4.28	6.85	12.3
<b>ANX4</b>	1.990	4.020	0.420	4.440	1.3	1.63	6.85	12.3
<b>SCE</b>	2.890	2.790	0.438	3.228	0.9	4.04	6.88	12.0
<b>RAS</b>	9.320	0.351	0.012	0.363	9.5	0.15	6.96	6.9

**3/11/2015**

<b>Reactor</b>	<b>NH4</b>	<b>NO3</b>	<b>NO2</b>	<b>NOX</b>	<b>PO4</b>	<b>DO</b>	<b>pH</b>	<b>Temp</b>
<b>PCE</b>	20.100	1.920	0.018	1.938	2.6	2.13	6.95	14.5
<b>ANX1</b>	6.180	0.733	0.114	0.847	7.9	0.54	6.93	14.5
<b>ANX2</b>	6.210	0.395	0.034	0.429	6.5	0.39	6.95	14.5
<b>ANX3</b>	6.130	0.356	0.014	0.370	1.0	0.27	6.93	14.8
<b>IFAS1</b>	3.050	2.540	0.280	2.820	0.6	4.09	6.94	14.5
<b>IFAS2</b>	2.270	3.070	0.328	3.398	0.6	4.37	6.93	14.7
<b>IFAS3</b>	2.330	3.160	0.330	3.490	0.5	4.91	6.94	14.6
<b>ANX4</b>	3.270	3.130	0.460	3.590	0.6	0.92	6.92	14.6
<b>SCE</b>	1.790	1.550	0.310	1.860	0.3	4.08	6.98	15.0
<b>RAS</b>	1.830	0.318	0.010	0.328	2.4	0.11	6.94	14.7

**3/31/2015**

<b>Reactor</b>	<b>NH4</b>	<b>NO3</b>	<b>NO2</b>	<b>NOX</b>	<b>PO4</b>	<b>DO</b>	<b>pH</b>	<b>Temp</b>
<b>PCE</b>	20.900	1.930	0.205	2.135	3.5	2.96	6.98	15.6
<b>ANX1</b>	5.030	1.100	0.415	1.515	1.3	0.55	6.95	15.5
<b>ANX2</b>	6.360	0.384	0.045	0.429	1.2	0.51	6.96	15.4
<b>ANX3</b>	6.550	0.376	0.025	0.401	1.8	0.13	6.94	15.3
<b>IFAS1</b>	3.460	2.500	0.315	2.815	1.3	4.35	6.92	15.4
<b>IFAS2</b>	1.620	3.950	0.305	4.255	0.8	4.68	6.90	15.4

<b>IFAS3</b>	1.380	4.370	0.320	4.690	0.9	5.01	6.91	15.4
<b>ANX4</b>	1.830	4.290	0.425	4.715	1.2	0.98	6.90	15.6
<b>SCE</b>	0.611	3.190	0.530	3.720	0.9	5.07	6.93	15.4
<b>RAS</b>	0.648	0.933	0.285	1.218	0.9	0.12	6.88	15.4

**5/08/2015**

<b>Reactor</b>	<b>NH4</b>	<b>NO3</b>	<b>NO2</b>	<b>NOX</b>	<b>PO4</b>	<b>DO</b>	<b>pH</b>	<b>Temp</b>
<b>PCE</b>	28.200	0.825	0.055	0.880	3.8	1.26	6.88	20.8
<b>ANX1</b>	10.000	0.795	0.295	1.090	2.2	0.39	6.93	20.7
<b>ANX2</b>	3.520	3.900	0.030	3.930	1.6	0.37	6.94	20.6
<b>ANX3</b>	8.900	0.406	0.030	0.436	3.6	0.18	6.94	20.5
<b>IFAS1</b>	6.080	2.980	0.200	3.180	0.7	3.82	6.94	20.7
<b>IFAS2</b>	4.180	4.580	0.245	4.825	0.4	4.47	6.93	20.6
<b>IFAS3</b>	4.900	4.510	0.195	4.705	0.5	4.15	6.94	20.6
<b>ANX4</b>	12.600	1.590	0.340	1.930	0.4	0.57	6.95	20.8
<b>SCE</b>	5.410	2.980	0.745	3.725	0.4	3.46	6.95	20.8
<b>RAS</b>	6.140	0.723	0.290	1.013	0.8	0.09	6.92	20.8

## M. Supplemental Information

### Stoke's Law

The coefficient of molecular diffusion is related to the frictional coefficient of a particle as given by the Stokes-Einstein law of diffusion. For spherical particles the coefficient of diffusion is given by the following expression (Shaw, 1996):

$$D = kT/6\pi\mu r_p = RT/6\pi\mu r_p N$$

D= coefficient of diffusion ( $m^2/s$ )

K= boltzman constant  $1.38/05 \times 10^{-23}$  (J/K)

T= temp (K)

R= universal gas law constant, 8.3145 (J/mole\*K)

$\mu$ = dynamic viscosity ( $N*s/m^2$ )

r= radius of particle (m)

N= avogadros number,  $6.02 \times 10^{23}$  (molecules/g\*mole)

The terms in the denominator correspond to the coefficient of friction for a particle as defined by Stokes law. As the particles get smaller, the coefficient of molecular diffusion increases.

Extracted from Metcalf (2014)

### Fick's Law

The transfer of mass by molecular diffusion in stationary systems can be represented by the following expression, known as Fick's first law:  $r = -D_m \frac{dC}{dx}$

Where r = rate of mass transfer per unit area per unit time ( $M/L^2T$ )

$D_m$ = coefficient of molecular diffusion in the x direction ( $M^2/T$ )

C= concentration of constituent being transferred ( $M/L^3$ )

X= distance (L)

$dC/dx$  is assumed to be constant

Extracted from Metcalf (2014)